UNIVERSIDAD DE GRANADA

ESTACIÓN EXPERIMENTAL DEL ZAIDÍN, CSIC, GRANADA
Departamento de Bioquímica, Biología Celular y Molecular de Plantas

TESIS DOCTORAL

A STUDY OF THE ROLE OF KEA1 AND KEA2 K^+/H^+ ANTIPORTERS IN CHLOROPLAST DEVELOPMENT AND DIVISION IN *ARABIDOPSIS THALIANA*

Ali Mohamed Ali Aboukila

Granada, 2016

UNIVERSIDAD DE GRANADA

Editor: Universidad de Granada. Tesis Doctorales
Autor: Ali Mohamed Ali Aboukila
ISBN: 978-84-9163-120-0
URI: http://hdl.handle.net/10481/45095

ESTACIÓN EXPERIMENTAL DEL ZAIDÍN
CSIC, GRANADA
Departamento de Bioquímica, Biología Celular y Molecular de Plantas

A STUDY OF THE ROLE OF KEA1 AND KEA2 K^+/H^+ ANTIPORTERS IN CHLOROPLAST DEVELOPMENT AND DIVISION IN *ARABIDOPSIS THALIANA*

Memoria de Tesis Doctoral presentada por el licenciado en Biología, **Ali Aboukila** para aspirar al grado de Doctor

Fdo. ALI ABOUKILA

V^{o}B^{o} Directora de la Tesis

Fdo. María Pilar Rodríguez Rosales
Doctora en Ciencias Biológicas
Científica Titular del CSIC

Submitted to the Escuela de Posgrado of
Granada University
Department of Plant Physiology
Faculty of Sciences
In partial fulfilment of the requirements for the degree of
"DOCTOR EN BIOLOGÍA"

Granada, 2016

Major Subject: Plant Physiology

The work presented in this Doctoral Thesis has been carried out in the Department of Biochemistry and Molecular and Cellular Biology of Plants, Estación Experimental del Zaidín (CSIC) in Granada, within the Research group "Ion Homeostasis and Membrane Transporters".

This work was funded by ERDF-co-financed grants from the Spanish Ministry of Economy and Competitiveness (BIO2012-33655 and BIO2015-65056-P) and Consejería de Economía, Innovación, Ciencia y Empleo, Junta de Andalucía (CVI-7558) and the Agriculture Research and Development Funds (ARDF), Ministry of Agriculture, Arab Republic of Egypt.

TO MY MOTHER WHO LEFT THIS WORLD BEFORE MAKING HER HAPPY SEEING ME A DOCTOR

Acknowledgements

In first place I like to thank work directors, Drs. Pilar Rodriguez and Kees Venema, for giving the opportunity for introducing me in the world of research, allowing me to join their group, supporting and guiding me in this way, sometimes a bit prickly but always rewarding. Thank you very much.

I also want to thank Olivier Cagnac for his support in the early beginning, he was always ready to guide me, and for being there when I needed. Also thanks to the rest of the members of my group Isabel, Elena, Fran, Andres, Kifah, Mourad and especially Noelia and Nieves, because you are much more than colleagues, because you have always been there, ready to help, to listen, support and because the work surrounded by people like you is much more enjoyable. Thank you very much to all for having always been together in good and hard times and for your friendship.

To those who paved the way for me: To my wife Marwa who always stand by me and for her self-denying and big sacrifices a very warm thanks from my deep heart, I am so grateful to you my dearest. To my children, Rukia, Abdulrahman and my little Sinai who started their life in Granada, I want to express my deepest gratitude to my family, especially my parents, who have given me everything and more, for your love, your patience, your understanding, who have always supported me, and for being always there unconditionally for everything I needed, sharing my successes and standing up when I fall. Thank you very much mom, dad and my brother, Yasser who has always exhibited his role of older brother outstandingly, taking care of me since I was little, solving my big life problems and my dear sister Sabreen who cared about me thank you all very much,

To my teachers in Egypt who taught me patiently in my early beginning, also I would like to thank Dr. Loutfy Boulos, Dr. Adel el Beltagy and Dr. Magdy Madkour for giving me the opportunity to study abroad. And a very special thanks to Dr. Ismael Abdul Galil who never hesitate supporting me when I needed.

To my friends of the whole life, Ihab, Yasser Ewiss, Yasser, Samer Mahmoud, Badry Ahmed Imam and Megahed and to all Granada friends especially Ahmed Salem.

This paragraph cannot end without a very special memory to Dr. Ali Tawfiq and his sweet family, Julia and Aida I feel very lucky to have met you in Granada and for sharing so many good and hard times, I will always remember you.

اقرأ باسم ربك الذي خلق ۩ خلق الإنسان من علق ۩ اقرأ وربك الأكرم ۩الذي علم بالقلم ۩ علم الإنسان ما لم يعلم

Recite in the name of your Lord who created۩ Created man from a clinging substance۩Recite, and your Lord is the most Generous۩Who taught by the pen ۩Taught man that which he knew not. (Surat Al-`Alaq, the Clot, the Noble Qur'an)

"كل وعاء يضيق بما جُعِل فيه, إلا وعاء العلم فإنه يتسع"

على بن ابى طالب

"Each vessel gets narrow of what it has inside except the vessel of sciences it gets wider" (Ali ibn Abe Talib)

"If we knew what it was we were doing, it would not be called research, would it?"
Albert Einstein

INDEX

List of Figures

List of Tables

I. INTRODUCTION AND OBJECTIVES

The essential mineral nutrient potassium (K^+) is the most important inorganic cation for plants and is recognized as a limiting factor for crop yield and quality. Potassium is the second most abundant mineral nutrient in plants comprising between 2 and 10 % of the plant dry weight (Leigh and Wyn Jones, 1984; Tisdale *et al.,* 1993). The essential role of potassium stems from its key role in fundamental cellular processes. As the major inorganic osmoticum it determines cell turgor and expansion, directing processes such as leaf movements, stomatal opening and closure, axial growth and tropisms (Marschner, 1995; Shabala, 2003). K^+ acts as a counter ion for the charge balance of ion transport across the plasma membrane and intracellular membranes and is fundamental for membrane potential regulation (Dreyer and Uozumi, 2011; Shabala, 2003). In chloroplasts, coupling of K^+ transport to light induced proton fluxes is fundamental for efficient photosynthesis (Carraretto *et al.,* 2013; Armbruster *et al.,* 2014; Kunz *et al.,* 2014). K^+ furthermore controls the process of photo assimilate loading into the phloem (Ache *et al.,* 2001; Gajdanowicz *et al.,* 2011), and influences the activity of more than 70 enzymes (Marschner, 1995).

Potassium uptake, transport and homeostasis play a central role in conferring tolerance to abiotic stresses like salinity, drought or heat. Under salt stress, Na^+ competes with K^+ for uptake into roots. The transcript levels of several K^+ transporter genes are either down- or up regulated by salt stress, probably reflecting the different capacities of plants to maintain K^+ uptake under salt stress (Zhu, 2003). Inhibition of photosynthesis is one of the most important parameters determining the negative effects of abiotic stresses like salinity, drought or heat on crop production, and it is well known that adequate potassium supply can alleviate the negative effects of these stresses on photosynthesis (Ashraf and Harris, 2013). The identification and study of genes that encode chloroplast K^+ ion transport proteins could thus be important to increase salt or drought tolerance and the efficiency of nutrient and water use in plants of agronomical interest by overexpression of these genes (Rodríguez-Rosales *et al.,* 2009).

Cation/Proton antiporters couple pH gradients to transport of cations thereby regulating osmotic balance, pH and intracellular cation content. These characteristics confer to them an important role in salinity or drought stress tolerance. Proteins of the CPA (Cation/Proton Antiporter) family, containing subfamilies CPA1 and CPA2 catalyze the exchange of Na^+ or K^+ against H^+ through plant cell membranes. The CPA1 family of ion transporters includes the NHX-type (K^+, Na^+)/H^+ antiporters whereas the CPA2 family of ion transporters includes genes encoding CHX and KEA proteins. While NHX

and CHX proteins have been extensively studied, there are only a few reports concerning KEA proteins. In *Arabidopsis thaliana*, AtKEA1–3 proteins show homology to bacterial K^+ efflux (Kef) transporters. AtKEA1 and AtKEA2 have acquired an extra hydrophilic domain of over 500 residues at the amino terminus (Aranda-Sicilia *et al.,* 2012; Chanroj *et al.,* 2012). In our laboratory we have determined that some *Arabidopsis thaliana* K^+/H^+ antiporters of the KEA family are localized to chloroplast membranes (Aranda-Sicilia *et al.,* 2012), which was confirmed by other studies during the course of this thesis (Armbruster *et al.,* 2014; Kunz *et al.,* 2014).

Chloroplasts from plants and algae originated from an endosymbiotic event, most likely involving an ancestral photoautotrophic prokaryote related to cyanobacteria. Both chloroplasts and cyanobacteria have thylakoid membranes, harboring pigment-protein complexes that perform the light-dependent reactions of oxygenic photosynthesis (Pfeil *et al.,* 2014). In plants, plastids have become complex organelles that are integrated into the plant host cell where they differentiate and divide in tune with plant differentiation and development (Basak and Moller, 2013). Although the genes encoding AtKEA1, 2 and 3 have a cyanobacterial origin, they have been transferred to the plant nuclear genome. Early studies suggested an important role for K^+/H^+ antiporters at the chloroplast inner envelope and thylakoid membranes. Potassium is fundamental for chloroplast electrical balance. Light induced proton pumping into the thylakoid lumen is electrically compensated by K^+ efflux from the thylakoids (Carraretto *et al.,* 2013). The resulting high stromal pH is necessary for optimal functioning of photosynthetic carbon reduction cycle enzymes. Maintenance of K^+ and H^+ homeostasis in the stroma was shown to depend on K^+/H^+ exchange at the inner envelope membrane (Peters and Berkowitz, 1991; Berkowitz and Peters, 1993; Wang *et al.,* 1993). Furthermore, photosynthesis reactions were shown to be sensitive to the chloroplast volume changes that can be induced by light, osmotic stress or water deficit, and chloroplasts rapidly regulate osmotic potential by exchange of organic solutes and K^+ (Nobel, 1968; Nobel, 1969; Robinson, 1985; Gupta and Berkowitz, 1988; Gupta *et al.,* 1989; McCain, 1995). However the molecular basis mediating the ion fluxes is not known.

In this thesis we have studied the effect of disruption of the *AtKEA1* and *AtKEA2* genes using T-DNA insertional mutants obtained from the SALK and SAIL collections. According to a recent report (Kunz *et al.,* 2014), AtKEA1 and AtKEA2 are fundamental for chloroplast osmotic balance and integrity. We have found however, that disruption of *AtKEA1* and *AtKEA2* above all compromises chloroplast development and division.

While single disruption mutants are indistinguishable from wild type plants, double *atkea1atkea2* mutants are pale yellow, show stunted growth and reduced photosynthesis in young developing leaves. This phenotype is typical of so called virescent mutants, which are in general affected in early chloroplast biogenesis (Jarvis and Lopez-Juez, 2013). In accordance double mutant plants show defective thylakoid membrane development. Furthermore AtKEA2-GFP protein is targeted specifically to the poles in young developing and dividing chloroplasts, but excluded from the division site, a localization that is dependent on the unique long N-terminal domain. Furthermore, we found that the double mutant plants have a lower amount of chloroplasts.

Apart from the obvious importance of improving photosynthesis efficiency under abiotic stress conditions for crop yield, the study of chloroplast division and development bears agricultural impact. As an example, it is thought that the ability to manipulate plastid size will result in control over starch granule dimensions. The FtsZ chloroplast division ring proteins have been shown to play a role in determining amyloplast size and in turn, starch granule size in potatoes (de Pater *et al.,* 2006). This is of commercial importance because control of starch granule size could be translated into increases in wet-milling efficiency and starch yield improvements in the order of $280 million per year (Gutierrez *et al.,* 2002).

Objectives of the study

The general objective of this work was to study the physiological function of the *Arabidopsis thaliana* AtKEA1 and AtKEA2 proteins. For this purpose we have analyzed the phenotypes of single and double T-DNA knock-out mutants, determined the subcellular location of AtKEA2 and studied the function of AtKEA2 N-terminal domain by heterologous expression in yeast and by bioinformatics approaches. This general objective was developed through the following specific objectives:

1- Phenotypic analysis of single and double mutants. T-DNA insertional mutants of *AtKEA1* (chromosome 1) and *AtKEA2* (chromosome 4) were identified from the tair website (http://Arabidopsis thaliana .org/index.jsp/) and seeds harboring T-DNA insertions in the translated regions of the genes were obtained from the NASC stock center. Double mutants were generated by crosses between the single mutants and their phenotypes analyzed under normal growth conditions or in response salt or osmotic stress or at varying light intensities. Photosynthetic parameters and thylakoid pigments and chloroplast membrane protein content were determined in collaboration with groups in USA and Germany.

2- Analysis of chloroplast number, morphology, ultrastructure. In order to determine the role of AtKEA1 and AtKEA2 in chloroplast development and division, chloroplast size and number were estimated by light microscopy in whole leaves, or in isolated and fixed mesophyll cells. A detailed study of chloroplast ultrastructure was carried out by transmission electron microscopy.

3- Analysis of AtKEA2 subcellular localization and tissue specific expression. In order to determine the subcellular localization of AtKEA2, a construct was made encoding the full length protein fused at the C-terminal end to GFP. To analyze the role of the N-terminal domain in subcellular localization, a construct of AtKEA2 without N-terminal fused to GFP was also used. The GFP fluorescence was studied by confocal microscopy in young leaf mesophyll cells, or in isolated chloroplasts. Tissue specific expression of AtKEA1 and AtKEA2 was studied by RT-PCR.

4- Study of AtKEA2 interaction with chloroplast division proteins. To determine whether AtKEA2 is associated to the chloroplast division machinery, AtKEA2-GFP was purified from chloroplast protein extracts with GFP binding protein coupled to magnetic beads. Co-purification of FtsZ1 and 2 chloroplast division proteins with AtKEA2-GFP was assayed using polyclonal antibodies.

5- Bioinformatics and biochemical analysis of the N-terminal domain. The N-terminal domain of AtKEA2 as well as several AtKEA2 deletion mutants was expressed in yeast to determine amino acid stretches involved in membrane interaction. Membrane interactions were studied in isolated yeast membranes by treatment with chaotropic agents or detergents. Phylogenetic relationships and 3D structure were predicted using available online prediction and modelling servers.

II. LITERATURE OVERVIEW

1. Importance of potassium in plants

Among the many plant nutrients, potassium (K^+) plays a particularly crucial role in a number of physiological processes vital to growth, yield, quality, and stress resistance of all crops. K^+ constitutes about 2.1–2.3 % of the earth's crust and thus is the seventh or eighth most abundant element. Therefore, soil K^+ reserves are generally large (Schroeder, 1978). K^+ concentrations in crops vary widely with site, year, crop species and fertilizer input; concentrations in the range of 0.4–4.3 % have been reported (Askegaard *et al.,* 2004). For many crops, the critical K^+ concentration is in the range 0.5 to 2 % in dry matter (Leigh and Wyn Jones, 1984). Potassium is the most abundant cation in the cytoplasm of plant cells with a concentration relatively constant at around 50–150 mM, while the concentration in the vacuole varies substantially depending on supply status. It plays a key role in the maintenance of electrostatic balance within the cell by neutralizing the net negative charges of the organic constituents produced by the metabolic pathways of the plant cell. Potassium is furthermore essential for the activity and synthesis of many enzymes, like for instance the activity of the plasma membrane proton ATPase, the synthesis of the essential photosynthetic enzyme Rubisco or synthesis of Nitrate reductase, all key enzymes in the plant metabolism (Marschner, 1995). Potassium is essential for membrane potential regulation, and therefore involved in many processes related to electrogenic transport of ions. Its role in counterbalancing electrogenic H^+ transport by membrane ATPases also confers to K^+ an important role in cellular pH homeostasis (Britto and Kronzucker, 2008). Potassium is the principal osmotically active inorganic solute in the vacuole, and its accumulation is responsible for creating osmotic potential and turgor (Marschner, 1995; Amtmann *et al.,* 2004; Britto and Kronzucker, 2008), thereby regulating processes like cell expansion, pollen tube development, and opening and closing of stomata and plant movements (Britto and Kronzucker, 2008). In addition, potassium is primarily responsible for the maintenance of a high osmotic potential in the wake of the roots, necessary for the transport of solutes driven by pressure in the xylem, and the water balance in the plant (Marschner, 1995). An overview of the transport systems involved in uptake and distribution of potassium is shown in Figure 1.1.

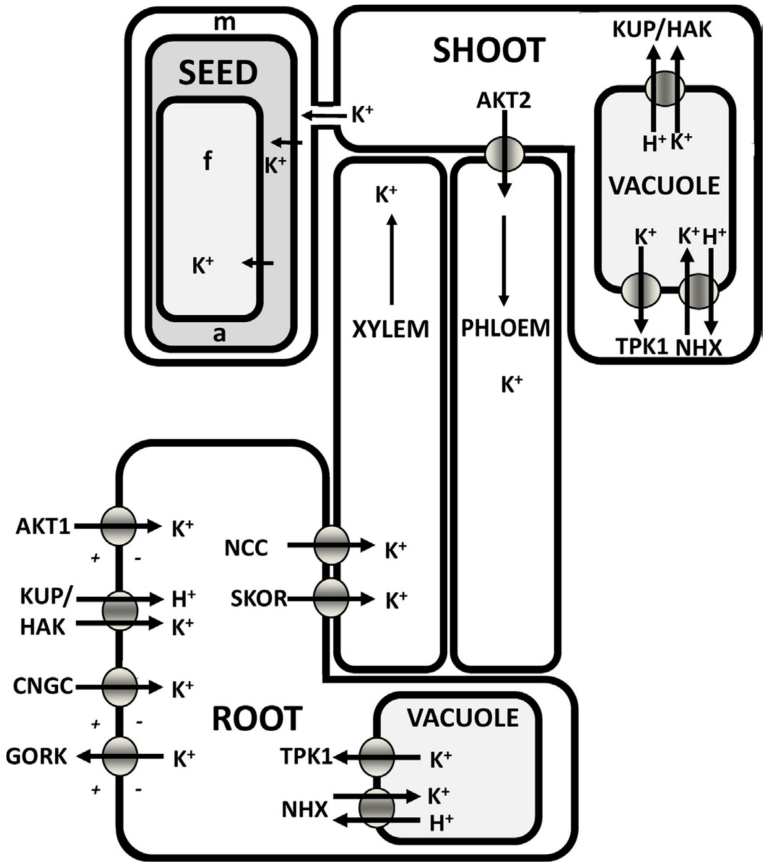

Fig. 1.1. Overview of transport processes and proteins that are involved in K^+ uptake, efflux and distribution. At the external soil: root interface transport functions are shown for passive [AKT1 and CNGC (cyclic nucleotide gated channel)] and energized (KUP/HAK) K^+ uptake and channel mediated K^+ release (guard cell outward rectifying K^+ channel; GORK); xylem loading mainly happens through K^+ selective (SKOR) and nonselective (NCC) cation channels though energized systems may also play a role; phloem loading of K^+ for recycling and/or sucrose loading may involve the AKT2 channel; K^+ flux to the seed is phloem mediated but K^+ is unloaded into the seed apoplast (a) at the junction between maternal (m) and filial (f) tissues; vacuolar K^+ accumulation is primarily driven by H^+-coupled antiporters such as NHX while vacuolar K^+ release is either passive through TPK1 type channels or, in K^+ starvation conditions, active through H^+ coupled KUP/HAK transporters (Ahmad and Maathuis, 2013).

1.1. Importance of K^+ in photosynthesis

In plants, photosynthetic complexes in the thylakoid membrane convert solar energy into a proton gradient across the thylakoid membrane. This Proton Motif Force is used to drive ATP synthesis. The electrogenic proton transport is coupled to transport of cations or anions across the thylakoid membranes, which in turn creates imbalances and ionic fluxes across the inner envelope membrane (Enz *et al.,* 1993). These transport reactions affect osmotic potential and induce chloroplast volume changes (Nobel, 1968,

1969; Robinson, 1985). It is well known that the maintenance of proper steady state ionic and pH gradients by both active and passive transport mechanisms is fundamental to chloroplast function, but knowledge about the exact molecular mechanisms involved is still limited. In that sense, well balanced pH and K^+ homeostasis have been shown to play important roles in photosynthesis efficiency, while Cl^- and Mg^{2+} fluxes also play important roles (Enz *et al.,* 1993).

1.2. K^+ and abiotic stresses

Abiotic and biotic stresses reduce crop yield to a large extent. Climate models predict that incidences and duration of drought and heat stress events will increase in some parts of the world, while other parts will suffer from heavy storms and periodic flooding. These conditions will have a dramatic impact on agricultural production and farming practices (Brouder and Volenec, 2008). Even in Europe, future climate changes are expected to be problematic, resulting more often in dry springs and rainy summers in Northern Europe and longer dry periods in the South. The effects of such climate changes could be observed in the European heat wave of 2003, which reduced crop production by around 30 % (Ciais *et al.,* 2005). On a worldwide scale, abiotic stress often leads to massive and often complete crop failures. Due to its fundamental roles in the plant, K^+ nutrition impacts on the resistance of crops to virtually all abiotic and biotic stresses, in both direct and indirect ways (Pottosin and Dobrovinskaya, 2014). Potassium availability is especially crucial for the resistance of crops to abiotic stresses like salinity, drought or high light intensity.

Inhibition of photosynthesis is one of the principal factors responsible for the negative effects of abiotic stresses like salinity, drought or K^+ deficiency on crop productivity. Salinity and drought affect photosynthesis directly, as they prevent plants from taking up water. To conserve water, they close their stomata. This simultaneously restricts the entry of CO_2 into the leaf, reducing photosynthesis (Flexas *et al.,* 2006). Further drought stress results in nonstomatal limitation, including a reduction in carboxylation efficiency and decreases in ATP synthesis and RuBP carboxylase activity. The reduction in carbon assimilation will lead to a surplus of absorbed light energy in photosystem II (PS II) and possibly to photodamage if excess energy cannot be adequately dissipated (Lawlor and Cornic, 2002; Kitao and Lei, 2007). These effects are more severe in high light intensity or high temperature conditions. Oxidative damage is further exacerbated in K^+ limiting

conditions, as K^+ directly affects stomatal conductance, and is furthermore necessary for phloem export of sucrose from source leaves. The accumulation of photoassimilates further reduces photosynthesis. The photooxidative damage results in degradation of chlorophyll and photosynthetic complexes (Cakmak, 2005)

The lowering of osmotic potential of cells as a consequence of salt or drought stress is also known to inhibit photosynthesis. This effect was shown to be related to K^+ efflux from chloroplasts and stromal acidification, and could be alleviated by adequate K^+ supply (Gupta *et al.,* 1989; Tsonev *et al.,* 2011).

More in general, chloroplasts can regulate their volume in order to retain a constant quantity of water over a range of water potentials (Robinson, 1985; MacCain, 1995). Beyond a critical limit, volume changes lead to fluctuations in the concentrations of solutes and metabolites, as well as the perturbation of ionic gradients, which directly affect photosynthesis (Kaiser *et al.,* 1981). Chloroplasts also shrink upon exposure to light. Ions are transported from the stroma to the cytosol, and water follows osmotically (Nobel *et al.,* 1969b). The molecular bases of these processes are poorly characterized.

2. Plant Cation/Proton Antiporters

2.1. The CPA1 and CPA2 families

KEA ($\underline{K}^+$ Efflux Antiporter) proteins are members of the monovalent Cation/Proton Antiporter (CPA) superfamily, found in both eukaryotes and prokaryotes (Maser *et al.,* 2001; Chanroj *et al.,* 2012). CPA proteins contain a Pfam 00999 Na^+/H^+ exchanger domain, and are involved in cation and pH homeostasis (Saier, 2000) by exchanging Na^+, Li^+ or K^+ for H^+. The members of CPA superfamily fall into two major families, CPA1 and CPA2 (Saier, 2000; Chanroj *et al.,* 2012), although it is unclear what features distinguish CPA2 from CPA1. Grouping of some proteins, like the yeast ScNha1p is indeed questionable (Chanroj *et al.,* 2012). The CPA1 family likely originated from ancestral bacterial NhaP proteins. CPA1 proteins are generally believed to catalyze electroneutral $(K^+,Na^+)/H^+$ exchange (Goswami, 2011; Vinothkumar, 2005). Members of this clade are found in all organisms, and especially the mammalian NHE family has been extensively studied. In plants, CPA1 includes the NHX ($\underline{N}a^+$-$\underline{H}^+$ e$\underline{X}$changer) proteins. The plant NHX family includes the plasma membrane-bound SOS1/AtNHX7 proteins, endosomal AtNHX5/6 proteins that are part of the eukaryote intracellular-

NHE clade and the plant-specific vacuolar clade including AtNHX1/2 (Chanroj *et al.,* 2012). These cation/H^+ antiporters are important for diverse functions, such as salt tolerance and Na^+ extrusion or accumulation, K^+ uptake into vacuoles, generation of cell turgor, cell expansion, opening of stomata, vacuolar pH regulation, and protein sorting (Pardo *et al.,* 2006; Rodriguez-Rosales *et al.,* 2009; Bassil *et al.,* 2011a; Bassil *et al.,* 2011b; Bassil and Blumwald, 2014; Reguera *et al.,* 2015).

Members of the CPA2 family are found in bacteria, algae, fungi and plants, but are relatively rare in metazoan genomes (Brett *et al.,* 2005; Chanroj *et al.,* 2012). CPA2 proteins likely originated from a NhaA-like transporter (Chanroj *et al.,* 2012). The *E. coli* NhaA protein is the best characterized Na^+/H^+ antiporter. The primary cellular function of EcNhaA is supporting growth at alkaline pH in the presence of Na^+ or Li^+ (Krulwich *et al.,* 2011). EcNhaA is electrogenic: $2H^+$ are imported into the cell as 1 Na^+ is exported (Arkin *et al.,* 2007). NhaA has been extensively studied at the biochemical and physiological level and has been the first Na^+/H^+ antiporter to be crystallized (Hunte *et al.,* 2005). The CPA2 clade can be further subdivided in a NapA-like clade, including the plant CHX proteins as well as the yeast Kha1p protein, and a KefC/B-like clade. The structure of the NapA protein from *Thermus thermophilus* was also recently resolved (Lee *et al.,* 2013). *Arabidopsis thaliana* CHX proteins are expressed in vegetative and reproductive tissues, with over half of the CHXs expressed in pollen (Sze *et al.,* 2004). Phylogenetic analysis has shown that the number of *CHX* genes has increased from 3-4 in early land plants to over 40 in eudicots. CHX proteins from early land plants, such as moss, are similar to *A. thaliana* CHX20, suggesting *CHX20* and the related *CHX16-19* genes are founding members of this superfamily. The proliferation of *CHX* genes suggests they could function in adaptation to life on dry land through roles in vegetative survival, reproductive innovations, or both (Chanroj *et al.,* 2012). The plant KEA proteins are most closely related to the KefB/C subgroup of CPA2 proteins. Among the functionally well-characterized members of the family are the *E. coli* glutathione regulated K^+ efflux transporters KefB and KefC, on which the name of the family is based. These transporters are characterized by the presence of a Na-H exchanger domain and a C-terminal KTN ($\underline{K}^+$ Transport Nucleotide) binding domain, also called TrkA-N domain (Pfam PF02254). The presence of an N or C terminal KTN domains is widespread in bacterial K^+ channels and transporters such as Kch, Trk and KefB or KefC (Choe, 2002). The minimal functional unit of the KTN domain is a dimeric molecule connected by a flexible hinge. Hinge motion can be

physically coupled to transmembrane loops to control K^+ flux, providing a mechanism of gating control (Choe, 2002). The KTN domain contains the typical Rossman fold GXGXXG…D Glycine motif involved in NAD binding, indicating metabolic control of transporter function (Jiang *et al.,* 2001; Roosild *et al.,* 2002). KefB and KefC are further activated by the ancillary proteins KefF and KefG. Electrophiles release KefC and KefB from inhibition by bound GSH, thus eliciting K^+ efflux and H^+ uptake which was suggested to serve as protective mechanism against electrophile toxicity and DNA damage (Booth *et al.,* 1996). An additional level of regulation is provided by the nucleotide binding domain. It was proposed that binding of NAD+ to the KTN domain in KefC induces an activated conformation of dimers that is further stabilized by the ancillary protein KefF, whilst NADH binding would induce an inactive conformation. Although originally proposed to function as K^+ channels, recent studies have indicated a K^+/H^+ antiporter mode of action (Fujisawa *et al.,* 2007).

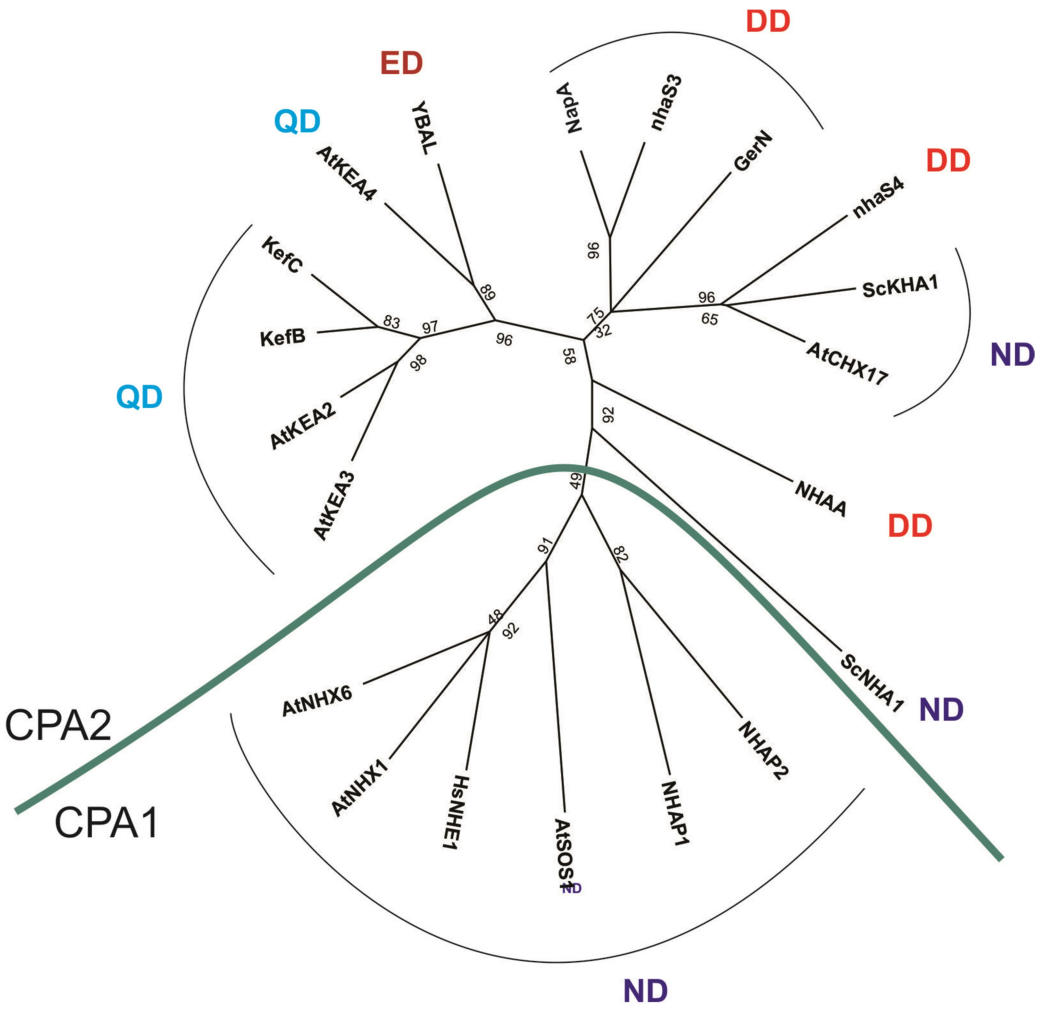

Fig. 1.2. Phylogenetic tree of representative members of CPA1 and CPA2 proteins. The conserved Pfam 00999 domains were aligned by MUSCLE and the evolutionary history of the genes were determined with MEGA6, by maximum likelihood using the Jones–Taylor–Thornton (JTT) model with a Boot strap of 100 (Tamura *et al.,* 2013). The percentage of trees in which the associated sequences clustered together is shown next to the branches. All positions containing gaps and missing data were eliminated. The amino acids that align with the conserved double Aspartate domain in NhaA (DD) are indicated for each subgroup. Presence of two charged residues (DD or ED) would indicate electrogenic transport mode, while presence of only one charged residue (ND or QD) would be indicative of an electroneutral transport mode. Sequences: *Arabidopsis thaliana* AtNHX1 (Uniprot: Q68KI4), AtNHX6 (Q8RWU6), AtSOS1 (Q9LKW9) AtKEA1 (Q9ZTZ7), AtKEA2 (O65272), AtKEA4 (Q9ZUN3) and AtCHX17 (Q9SUQ7); *Homo sapiens* HsNHE1 (P19634), *Methanocaldococcus jannaschii* NHAP1 (Q60362); *Vibrio cholerae* NHAP2 (A5F4U3); *Saccharomyces cerevisiae* ScNHA1 (Q99271) and ScKHA1 (P40309), *Escherichia coli* NHAA (P13738), KefC (P03819), KefB (P45522) and YBAL (P39830) ; *Synechocystis* nhaS4 (Q5N3F5) and nhaS3 (Q55190); *Thermus thermophilus* NapA (Q72IM4); *Bacillus cereus* GerN (Q9KI10).

It was suggested that electrogenic $2H^+/Na^+$ antiport by both NhaA and NapA is dependent on the alternative binding of $2H^+$ or $1Na^+$ to two conserved Aspartate residues (D163 and D164 in trans membrane helix 5 in NhaA), inducing a conformational switch in the protein (Goswami, 2011; Lee, 2013). In that sense it is interesting to note that, although the second Aspartate is strictly conserved in all CPA antiporters, the first Aspartate is replaced by uncharged N or Q residues in CPA1 transporters as well as in KEA/Kef proteins and most CHX proteins. The mammalian NHE antiporters of the CPA1 family are known to catalyze electroneutral Na^+/H^+ exchange, thus absence of the double Aspartate motive in both CPA1, Kef/KEA and CHX proteins might indicate that these proteins also catalyze electroneutral Cation/Proton exchange (Goswami, 2011) (Figure 1.2).

2.2. The K^+ efflux antiporters (KEA) family

Genes encoding putative KEA proteins from higher plants were first identified in *Arabidopsis thaliana* (Maser *et al.,* 2001). In *Arabidopsis thaliana* 6 KEA isoforms (AtKEA1–AtKEA6) are found (Chanroj *et al.,* 2012) (Figures 1.3 and 1.4).

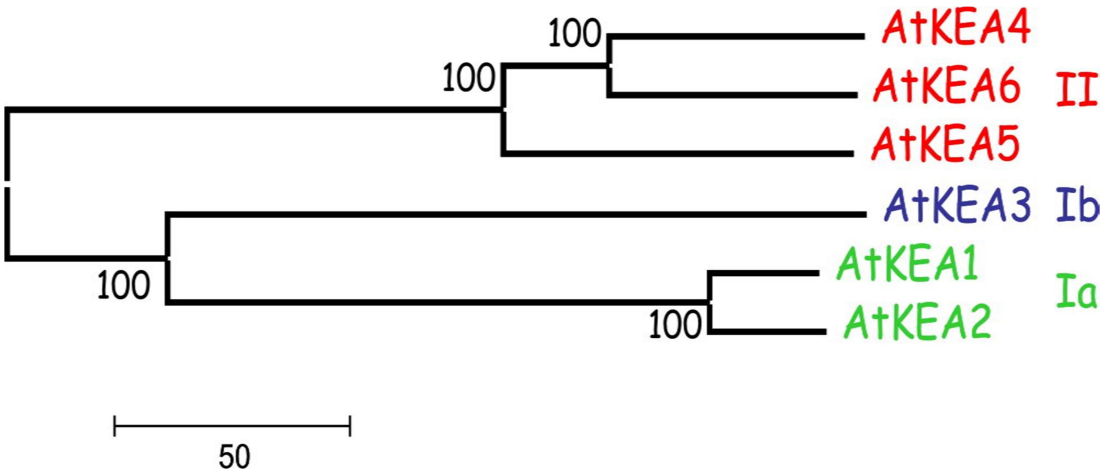

Fig. 1.3. Phylogenetic tree of *Arabidopsis thaliana* KEA proteins. Proteins were aligned by MUSCLE and the evolutionary history of the genes was determined by maximum likelihood using the Jones–Taylor–Thornton (JTT) model with a Boot strap of 100 (Tamura *et al.,* 2013). *Arabidopsis thaliana* contains 6 KEA proteins that can be divided in 3 subgroups. Group Ia and Ib proteins were shown to localize to chloroplasts. The Uniprot accession numbers for the proteins are Q9ZTZ7 (AtKEA1), O65272 (AtKEA2), Q9M0Z3 (AtKEA3), Q9ZUN3 (AtKEA4), Q8VYR9 (AtKEA5), B5X0N6 (AtKEA6).

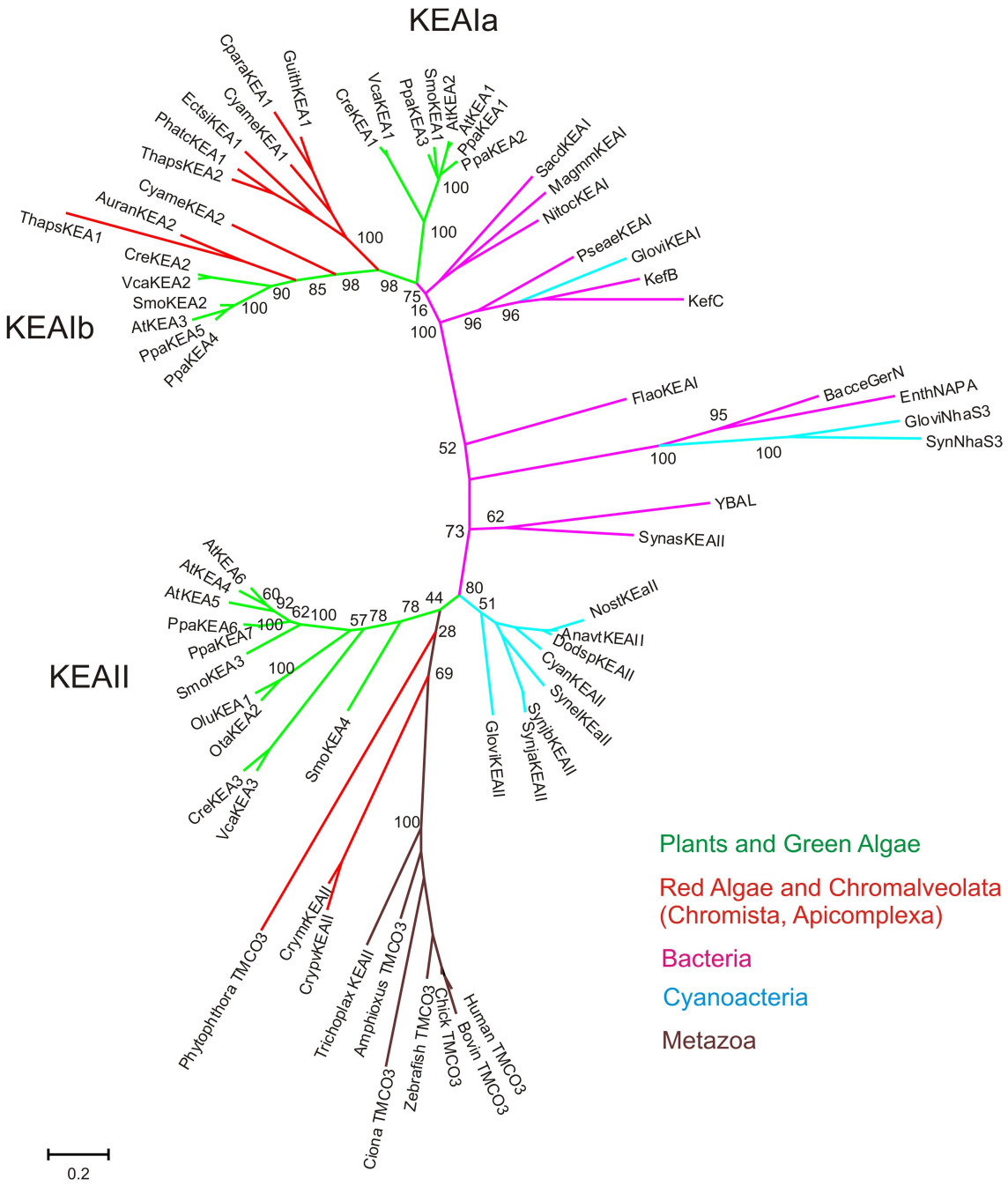

Fig. 1.4. Phylogenetic tree showing plant KEAs are found in plastid containing organisms. The conserved Pfam 00999 domains in KEA sequences from diverse organisms were aligned by MUSCLE and the evolutionary history of the genes were determined by maximum likelihood using the Jones–Taylor–Thornton (JTT) model with a Boot strap of 100 (Tamura *et al.,* 2013). The percentage of trees in which the associated sequences clustered together is shown next to the branches. The analysis involved 66 amino acid sequences. All positions containing gaps and missing data were eliminated, resulting in a total of 307 positions in the final data set (Chanroj *et al.,* 2012).

2.2.1. Evolution of KEA family

To understand the evolutionary origin of higher plant KEAs, Chanroj et al. (2012) looked for and analyzed homologs in prokaryotes, protists, metazoa, and plants (Figure 1.4). It was found that KEA genes diverged into two main branches with AtKEA1–3 in clade I and AtKEA4–6 in clade II (Figures 1.3 and 1.4). Clade I consists of the only eukaryotic proteins with a complete C-terminal KTN domain (Nagata *et al.,* 2008), and are closely related to EcKefB- and EcKefC-like proteins from bacteria, including cyanobacterium *Gloeobacter violaceus* (Figures 1.4 and 1.5). The members of the kingdom chromista such as red algae as well as secondary photosynthetic organisms contain sequences from clade I exclusively. In contrast, proteins of clade II lack a KTN domain (Figures 1.4 and 1.5), although they show homology mostly to proteins from unicellular and filamentous cyanobacteria that can contain both N-terminal and C-terminal KTN domains (Figure 1.4). Clade II genes are also present in parasitic organisms of the *phylum* Apicomplexa. These organisms contain a high number of plant and bacterial-like proteins (Abrahamsen *et al.,* 2004) due to the presence of an apicoplast (plastid), derived by secondary endosymbiosis of an ancestral green or red alga (Keeling, 2004). A clade II protein is found in the Oomycete, *Phytophthora infestans*, possibly also related to the presence of a plastid in a common photosynthetic ancestor of the chromista (Tyler *et al.,* 2006). However, AtKEA4–6 like proteins are also found in Metazoa (Placozoa; *Trichoplax adhaerens*, Basal Chordata; *Ciona intestinalis*, Higher Chordata; mammals, amphibians, fish), which does not fit with the idea that these genes were derived from a cyanobacterial ancestor by endosymbiosis.

The plant KEAIa proteins have acquired a long hydrophilic N-terminal domain of about 550 amino acids, making up almost half the size of the protein. This N-terminal domain is rich in charged amino acids, contains predicted coiled coil structures at its N-terminus, and has a C-terminal hydrophobic stretch that is predicted to form a *trans* membrane helix in some species (Figure 1.5). Nothing is known about the function of this domain (Chanroj *et al.,* 2012).

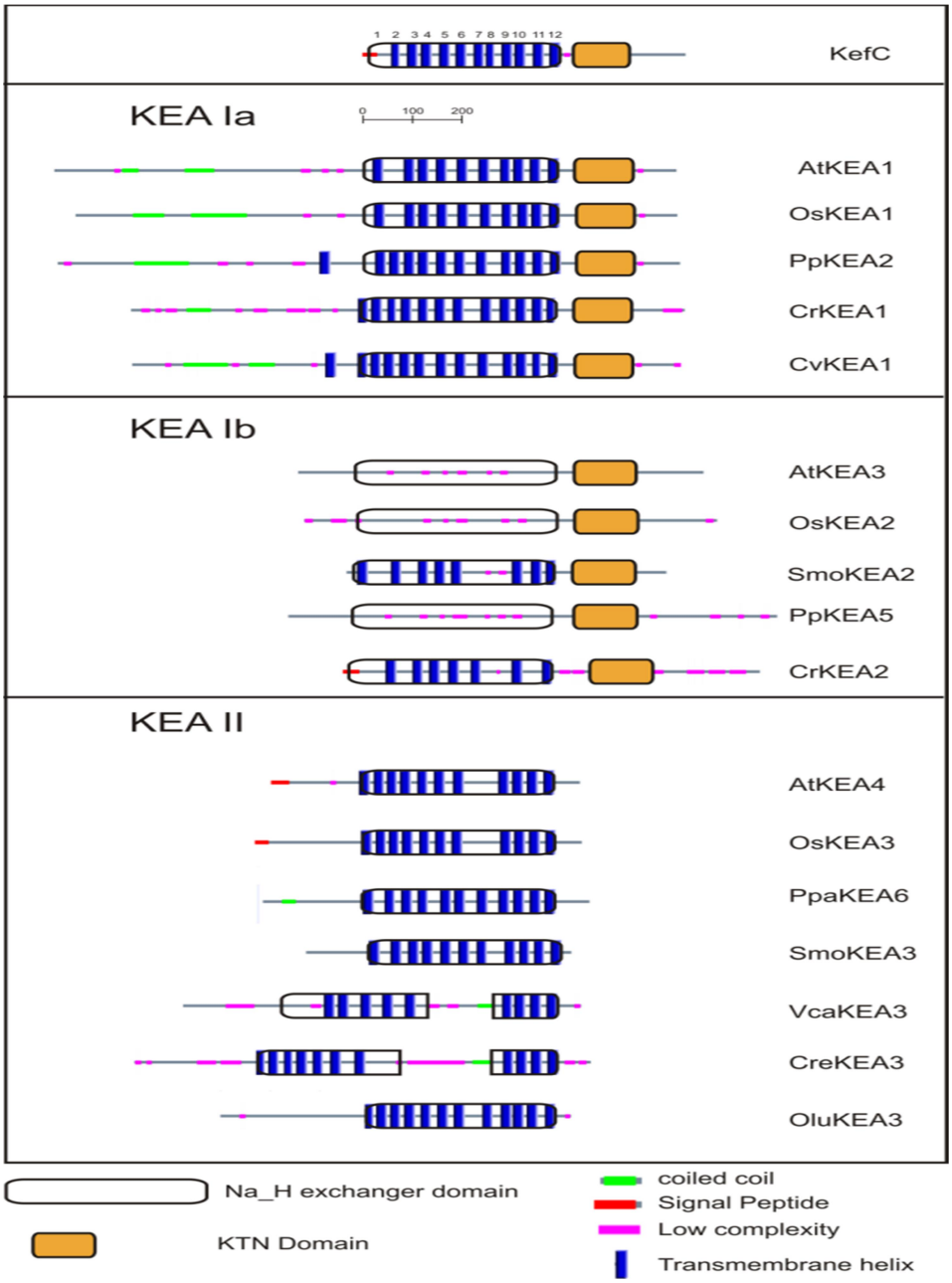

Fig. 1.5. Distinct protein domains of three KEA clades. The relative length and position of the KTN and Na_H exchanger domain in the three KEA clades is shown graphically using information obtained with the Simple Modular Architecture Research Tool (Smart, http://smart.embl-heidelberg.de/). All plant clade I proteins contain a KTN domain. In the clade II group this domain is lost, making it the shortest KEA proteins. The clade Ia proteins all have acquired a long N-terminal domain, typically containing predicted coiled coil structures. The C-terminus of the clade Ib proteins is slightly longer as compared to the other sequences. Some green algal clade II proteins have a split Na_H domain, which might be a result of erroneous gene predictions. The transmembrane helix predictions are very variable, and especially unsuccessful for the clade Ib group of proteins. The transmembrane helices are numbered from 1 to12 in KefC (Chanroj *et al.,* 2012).

2.2.2. KEA function in plants

Aranda-Sicilia et al. (2012) showed that KEA2 from *Arabidopsis thaliana* is expressed in the aerial parts of the plant and that the first 150 base pairs of the cDNA encode a chloroplast targeting peptide that is responsible for localization of the antiporter to chloroplasts. A partially purified and reconstituted short version of the antiporter, lacking the N-terminal domain was shown to mediate K^+/H^+ exchange. During the course of this PhD thesis, Kunz et al. (2014) reported that AtKEA1 and AtKEA2 are located at in the inner envelope while AtKEA3 is targeted to the thylakoid membrane. Mutants without AtKEA1 and AtKEA2 showed reduced growth and were pale green. Mutant plants also showed reduced photosynthesis efficiency and a reduced thylakoid membrane pH gradient. It was suggested that this was due to perturbation of K^+ homeostasis and osmotic balance within the chloroplasts. Double mutant plants contained enlarged or swollen chloroplasts with occasional disruptions of the envelope membrane, which could be caused by K^+ accumulation due to the inability to export K^+ from the chloroplasts in the absence of AtKEA1 and AtKEA2. These effects were exacerbated by disruption of AtKEA3 in the double mutants. The growth and photosynthesis defects could be rescued by NaCl, possibly due to induced cytoplasmic osmolyte synthesis, counteracting the swelling of the chloroplasts. Similarly, Sheng et al. (2014) showed that the disruption of the only KEAIa protein in rice (OsKEA1) also affected growth and development of the plants, and caused a phenotype called albino midrib 1 (AM1). The growth defects of the mutant plants could be partially rescued by drought stress in this case. According to these authors, OsKEA1 was involved in chloroplast development, as the mutant plants had strongly reduced thylakoid membrane development and a reduced amount of various essential chloroplast proteins. A more detailed study of the function of the AtKEA3 protein has shown that it is essential in regulating the pH of the thylakoid lumen (Armbruster *et al.,* 2014). The acidity of the lumen is an important signal to activate energy dissipation processes in conditions of excess light (Li, 2009). The rapid adjustment of the lumen pH by AtKEA3 was shown to be important for optimal photosynthesis efficiency in fluctuating light conditions (Armbruster *et al.,* 2014).

3. Chloroplast Development and Homeostasis

Chloroplasts are small (several microns in diameter) organelles that define plants, being responsible for their typical green color and photoauxotrophic lifestyle through photosynthesis. Chloroplasts are members of a family of organelles known as plastids. Small undifferentiated proplastids that are found in meristems and reproductive tissue divide and differentiate into plastids with specialized functions within different cell types (Pyke, 1997; Pyke, 2007). Depending on the developmental context, plastids fulfil a diversity of important roles besides photosynthesis. They are involved in synthesis of amino acids, fatty acids, membrane lipids, enzyme cofactors, purine and pyrimidine bases, terpenoids, pigments and hormones, and play important roles in nitrogen and sulphur assimilation. In some cases, the names of these plastids are indicative of either the types of compound they store or their functions. For example, amyloplasts store starch, chromoplasts store pigments, elaioplasts store oil and chloroplasts are the site of photosynthesis (Pyke, 2009). All plastids are bounded by an inner and outer envelope membrane that isolates the stroma from the cytosol.

When seedlings emerge from the soil, light triggers the transformation of proplastids into chloroplasts, and induces an increase in chloroplast number by fission. This transformation requires the assembly of photosynthetic complexes into thylakoid membranes, and a massive increase in total volume and solute content of the organelle. The photosynthetic pigments and thylakoid membrane lipids are synthesized at the plastid envelope and transported to the developing thylakoid membrane by so-far poorly characterized transport systems, possibly involving formation of membrane invaginations, vesicle budding or lipid binding proteins (Jarvis and López-Juez, 2013; Rast *et al.,* 2015). Proplastid to chloroplast transition occurs during differentiation of meristematic cells into photosynthetic tissue. Once chloroplasts have been established they propagate in developing (dividing) tissues. While the signal for proplastid to chloroplast transition is light, little is known about the downstream mechanisms.

Chloroplast development is regulated by nuclear genes. Chloroplast development or function in turn also regulates plant development through retrograde organelle to nucleus signalling pathways (Jarvis and López-Juez, 2013). Mutants affected in chloroplast function or development often exhibit similar leaf morphological defects, while plastid division and cell division are also linked (Tiller and Bock, 2014).

3.1 Chloroplast evolution

Chloroplasts from plants and algae originated from an endosymbiotic event, most likely involving an ancestral photoautotrophic prokaryote related to today's cyanobacteria (Douglas, 1998; Martin and Herrmann, 1998; McFadden, 1999a). In plants, plastids have become complex organelles that are well-integrated into the plant host cell where they differentiate and divide in tune with plant differentiation and development (Basak and Møller, 2013). Both chloroplasts and cyanobacteria have thylakoid membranes, harbouring pigment-protein complexes that perform the light-dependent reactions of oxygenic photosynthesis (Pfeil *et al.,* 2014). The thylakoid membrane system in chloroplasts has developed a complex structure of grana stacks connected by stroma lamella. The thylakoid membrane system appears to be separated from the inner envelope membrane. This results in the formation of two independent compartments with differing functions that require communication and transport between both membranes during thylakoid membrane development (Chigri, 2012; Vothknecht *et al.,* 2012).

Many prokaryotic features are still present in chloroplasts. For instance, the organelle retains a functional genome, but it has undergone substantial reduction during evolution and typically carries fewer than 100 protein-coding genes. Most of the 2000-3000 proteins found in plastids are encoded in the nucleus and must be imported following synthesis in the cytosol (Yarvis and López-Juez, 2013).

3.2. Protein import into the chloroplast

3.2.1. Import across the envelope membranes

As most genes have been transferred from the plastome to the nucleus after the endosymbiotic event, many nuclear encoded proteins must be transported back to the chloroplast. The majority of these proteins are directed to the chloroplast by their N-terminal sequence which functions as transit peptide. In *Arabidopsis thaliana* at least 20 different protein components in the double layer envelope membrane are involved in the translocation of the nuclear encoded chloroplast proteins (Aronsson and Jarvis, 2009). These proteins are part of the TOC or TIC (Translocation of the outer/inner envelope membrane of chloroplasts) translocon complex (Schnell *et al.,* 1997). At the arrival of preproteins (proteins having transit peptides) the import can be divided into three

different stages based on the energy requirement (Aronsson and Jarvis, 2009). At the first phase reversible contact with the receptors of the TOC complex is made by the transit peptide without consuming any energy (Perry and Keegstra, 1994; Kouranov and Schnell, 1997). In the second phase the preprotein becomes deeply inserted into the TOC complex and a contact is produced with the TIC complex that is called docking. This stage is irreversible and requires a low amount of ATP and GTP (Olsen and Keegstra, 1992; Young *et al.,* 1999; Kessler and Schnell, 2006). Finally, the preprotein is completely translocated into the stroma, and the transit peptide is removed by a stromal processing peptidase. Inner envelope membrane proteins most likely share the same transport mechanism as soluble stromal proteins. Inner envelope proteins typically possess a transport peptide and are imported via the TOC-TIC machinery. How exactly inner envelope membrane proteins are inserted into the membrane is still controversial, and could be based on a stopped-transfer signal in the protein, or processing and insertion of the protein once it is imported into the stroma (post-import pathway) (Viana and Schnell, 2010).

The recognition of the preproteins is done by TOC machinery. The TOC core complex consists of three main proteins; Toc34, Toc75 and Toc159, according to their predicted molecular weight (Schnell *et al.,* 1997). It was suggested that for every Toc159 protein there are three or four Toc75 and Toc34 proteins (Schleiff *et al.,* 2003; Kikuchi *et al.,* 2006). Both Toc159 and Toc34 are responsible for protein recognition and are called receptors. Toc75 is embedded in the outer membrane and works as a channel for preproteins. Two models were proposed regarding the TOC receptor mode of action. In the first model Toc159 is suggested to be the primary receptor subsequently associated with Toc34 and transferring the preprotein to the Toc75 channel (Keegstra and Froehlich, 1999). In the second model, Toc34 works as a preprotein primary receptor and transfers it to Toc159, which, through GTP hydrolysis, acts as a motor and transfers the preprotein to Toc75 (Becker *et al.,* 2004; Soll and Schleiff, 2004). Other TIC components, such as Tic32, Tic55 and Tic62, are suggested to work as sensors for the chloroplast redox state and may help to increase import efficiency (Aronsson and Jarvis, 2009).

3.2.2. Import across the thylakoid membrane

Proteins located in the thylakoid lumen mostly contain two targeting sequences, one for targeting across the envelope membrane to the stroma and another one for luminal targeting (Hageman *et al.,* 1986). Luminal targeting signals have a three domain structure that is composed of a positive charged amino-terminal region (N-domain), a hydrophobic core region (H-domain) and a more polar carboxy terminal region (C-domain) ending with an A-X-A consensus sequence recognized by the thylakoid processing peptidase (Dalbey and von Heijne, 1992; Brink *et al.,* 1997). According to proteomic studies approximately 100 proteins reside in the thylakoid lumen, all nuclear encoded, with about half expected to be transported through the Tat pathway and the other half through the Sec or other pathways, based on the arginine and lysine residues (Peltier *et al.,* 2002; Schubert *et al.,* 2002). The signal recognition particle (SRP) and Spontaneous pathways target *trans* membrane proteins to the thylakoid. These proteins have no target signal for the thylakoid; the targeting signal usually lies within the mature part of the protein (Jarvis and Robinson, 2004; Aldridge *et al.,* 2009; Celedon and Cline, 2013).

The Sec pathway

The Sec system transports unfolded proteins across biological membranes and consists of protein targeting components, a motor protein and a membrane integrated protein conducting channel (Wickner *et al.,* 1991). The Sec translocase is present in the cytoplasmic membrane of all bacteria, archaea, and the thylakoid membrane of plant chloroplasts and the ER of eukaryotes and is essential for the cell viability (Sargent *et al.,* 1998). It is responsible for the secretion of most extracellular proteins that fulfill diverse functions in metabolism, substrate uptake and excretion, cell envelope structure, sensing and cell communication (Stathopoulos *et al.,* 2000). The bacterial Sec translocase is composed of a membrane embedded protein conducting channel (PCC) that consists of three integral membrane proteins, SecY, SecE and SecG, and a peripheral associated ATPase, SecA, that functions as a molecular motor to drive the translocation of secretory proteins across the membrane (Wickner *et al.,* 1991) (Figure 1.6). Few is known about the mechanisms of Sec protein translocation systems in the plant cell membranes while in bacterial cells it has been extensively studied (Natale *et*

al., 2008). The channel subunits SecY and SecE and the motor SecA are essential components of the Sec translocase and are highly conserved in bacteria. SecA associates peripherally to the PCC, where it accepts secretory proteins from chaperones such as SecB (Figure 1.6) or from the ribosome (Figure 1.6), to thread the unfolded proteins through a narrow transmembrane channel formed by the PCC. ATP and the proton-motive force (PMF) provide the energy needed for this process.

The Tat pathway

In all plant and algal genomes sequenced so far genes encoding proteins that share homology to components of the Twin-arginine translocation (Tat) system are found. The Tat system is localized in cytoplasmic membranes of many bacteria and archaea, as well as in thylakoid membranes of plant plastids (Müller *et al.,* 2005) and is a general translocation system that serves to translocate unfolded and folded proteins with N-terminal signal peptides across energized membranes in prokaryotes and plant plastids (Plamer and Berks, 2012). Tat signal peptides contain a characteristic amino acid that includes two eponymous arginines (Taubert *et al.,* 2015). Initial experiments demonstrated that chloroplast Tat (cpTat) transport activity is dependent on a ΔpH threshold that is likely different for each precursor. Transport of the precursor causes counter proton flow with over 90 % of the H^+ counter flow coupled to protein transport. Further studies have demonstrated that the membrane potential Δψ can also drive the translocation of the precursor and that ion- sensitive cpTat transport occurred even after ΔpH was no longer detectable. Therefore, the Tat transport at the thylakoid requires energy in the form of the thylakoid PMF, normally generated by light induced photosynthetic electron transfer (Hou *et al.,* 2011).

The Tat systems minimally consist of the two components TatA and TatC. Often a third component, TatB, sequence-related to TatA but with a higher affinity for TatC is also found. In bacteria, TatA and TatB are known to be single-span transmembrane proteins with a short periplasmic N-terminal regions and cytosolic C-terminal domains. In *E. coli* as well as in plant plastids, TatBC-containing complexes recognize the twin-arginine motif and thereby bind the Tat substrates (Richter *et al.,* 2005).

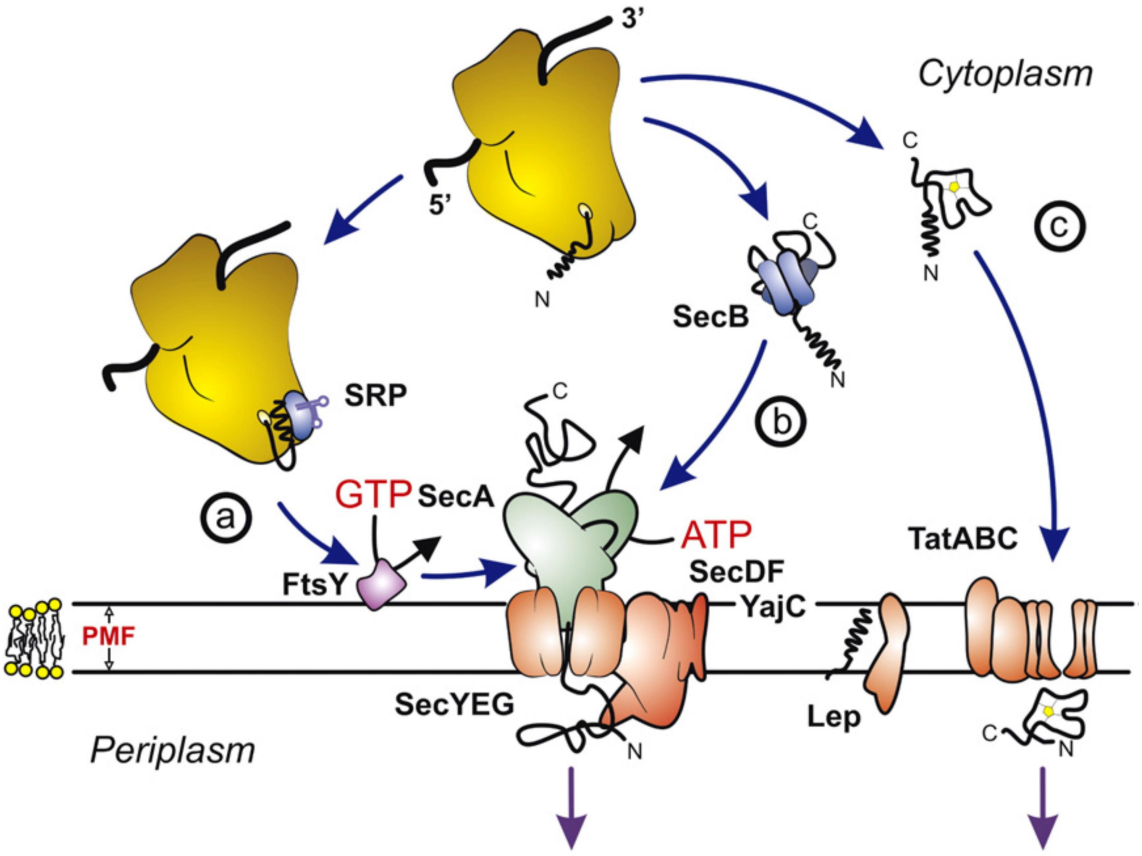

Fig. 1.6. Schematic overview of the *Escherichia coli* Sec and Tat translocases. (a) Co translational and (b) post-translational targeting routes and translocation of unfolded proteins by the Sec translocase. (c) Translocation of folded precursor proteins by the Tat translocase (Natale *et al.,* 2008).

3.3. Thylakoid membrane biogenesis

Chloroplast biogenesis requires the cytosolic synthesis of nuclear encoded photosynthetic complex components, Calvin cycle and other primary metabolic enzymes, envelope transporters and protein import complexes (Jarvis and Lopez-Juez, 2013). These nuclear encoded complex compounds assemble around plastid encoded core complexes such as the products of psaA and psaB (PSI), or psbA and psbD (PSII). It appears that this assembly takes place at specific biogenic membrane regions called biogenesis centers close to the plasma membrane in cyanobacteria, or in so called translation zones in algal cells (Nickelson and Zerges, 2013; Rast *et al.,* 2015) (Figure 1.7).

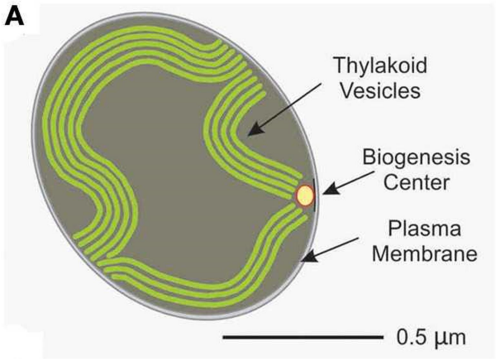

Fig. 1.7. A model showing a possible mechanism for thylakoid membrane formation in *Synechocystis* sp. At the contact points between plasma membrane and thylakoid membrane assembly of PSII and lipid insertion is suggested to take place at Biogenesis Centers (Adapted from Nickelson and Zerges, 2013).

In higher plants there is currently less evidence for the existence of a separate biogenic membrane fraction. Co-translation insertion of membrane proteins is assumed to take place at the non-stacked stroma lamellae and subsequent assembly steps are likely to occur here too (Rast *et al.,* 2015). Chlorophylls and carotenoids that are also essential for proper assembly of the photosynthetic complexes are synthesized by biosynthetic pathways inside plastids (Jarvis and López-Juez, 2013). Chlorophylls are synthesized at the plastid envelope, and final assembly with the antenna complexes takes place at the envelope or in prolamellar bodies in etioplasts. The biosynthesis of thylakoid membrane lipids requires the production and combination of fatty acids and polar head precursors. Fatty acid synthesis is completed within the chloroplast, after which lipid precursors are synthesized in the chloroplast stroma by a prokaryotic pathway or in the cytoplasm by an eukaryotic route. Lipid precursors phosphatidic acid (PA) and diacylglycerol (DAG) are conveyed to the inner envelope and further processed to form the thylakoid lipids monogalactosyldiacylglycerol (MGDG) and digalactosyldiacylglycerol (DGDG) (Jarvis and López-Juez, 2013).

One crucial but unanswered question is however how lipids and other envelope located compounds are transported from the plastid envelope to the internal thylakoid membrane system. In algal chloroplasts and proplastids of land plants, it is suggested that thylakoids arise from local invaginations of the inner envelope (Rast *et al.,* 2015). Direct contact points between the thylakoid membrane and inner envelope membranes have also been observed in mature chloroplasts in a few studies (Shimoni *et al.,* 2005), suggesting intraplastidic lipid transfer by lateral diffusion (Jarvis and López-Juez, 2013,

Rast *et al.,* 2015). On the other hand several studies have provided evidence for a vesicle based transfer system (Karim and Aronsson, 2014) (Figure 1.8). It was shown that chloroplasts accumulate small vesicles when exposed to the same drugs that inhibit vesicle transport through the cytoplasmic secretory pathway (Vothknecht and Westhoff, 2001). Furthermore, bioinformatics and proteomic studies have shown that chloroplasts contain many proteins with high sequence homology to components of the vesicle-based secretory pathway in the cytoplasm (Karim and Aronsson, 2014) (Figure 1.8). Thylakoid formation requires the action of Vesicle-Inducing Protein in Plastids 1 (VIPP1). Plants cannot survive without this protein, and reduced VIPP1 levels lead to slower growth and paler plants with reduced ability to photosynthesize (Westphal and Vothknecht, 2003; Vothknecht *et al.,* 2011). It is conserved in all organisms containing thylakoids, including cyanobacteria, green algae, and higher plants. VIPP1 interacts with Alb3 (Albino 3), a protein required for insertion of proteins into the thylakoid membrane and particularly the assembly of the light harvesting complex. Alb3 also interacts with the polypeptides of PSI and PSII reaction centers (Göhre *et al.,* 2006). While VIPP1 appears to be essential for vesicle formation, it was also suggested to be an essential part of the *Synechocystis* thylakoid biogenesis centers (Nordhues *et al.,* 2012).

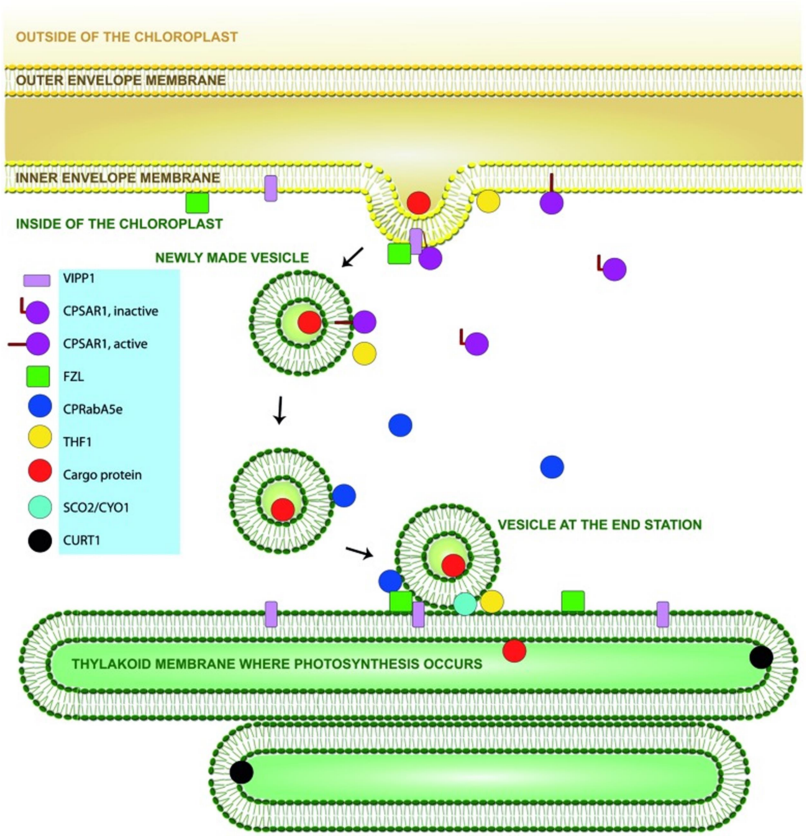

Fig. 1.8. Proposed model of vesicle formation and movement in chloroplasts. Proteins included are those with suggested involvement in chloroplast vesicle transport, and verified to be chloroplast localized (from Karim and Aronsson, 2014)

3.4. Chloroplast Division

A complex regulatory system has evolved that ensures chloroplasts divide in the middle, producing a large population of organelles of fairly uniform size and shape (Osteryoung and Pyke, 2014). Mutation of plastid-division genes results in abnormal chloroplast number, size, and shape, revealing a tight link between chloroplast division and morphology. Chloroplasts divide *via* binary fission to maintain adequate cellular levels during cell proliferation, and to produce smaller chloroplasts that are capable of phototaxis (Leech *et al.,* 1981; Possingham and Lawrence, 1983; Jeong *et al.,* 2002; Osteryoung and Nunnari, 2003).

Plastid division by binary fission implicates the coordinated assembly and constriction of four concentric rings, two internal and two external to the organelle (Figure 1.9): The FtsZ ring, inner PDring, outer PDring and ARC5/DRP5B. The two nuclear encoded and plastid targeted prokaryotic homologs of the Filamentation temperature sensitive Z

(FtsZ) proteins are responsible for chloroplast division, initiation and regulation (Osteryoung *et al.,* 1998b; Osteryoung and McAndrew, 2001; Osteryoung and Nunnari, 2003; Stokes and Osteryoung, 2003; Miyagishima *et al.,* 2004). FtsZ was the first protein of the prokaryotic cytoskeleton to be identified, and shows similarity to eukaryotic tubulin. The internal FtsZ ring and external dynamin-like ARC5/DRP5B ring are connected across the two envelopes by the membrane proteins ARC6, PARC6, PDV1 and PDV2. Assembly-stimulated GTPase activity drives constriction of the FtsZ and ARC5/DRP5B rings which pull and squeeze the envelope membranes until the two daughter plastids are formed, with the final separation requiring additional proteins. The positioning of the division machinery is controlled by the chloroplast Min system, which confines FtsZ-ring formation to the plastid midpoint.

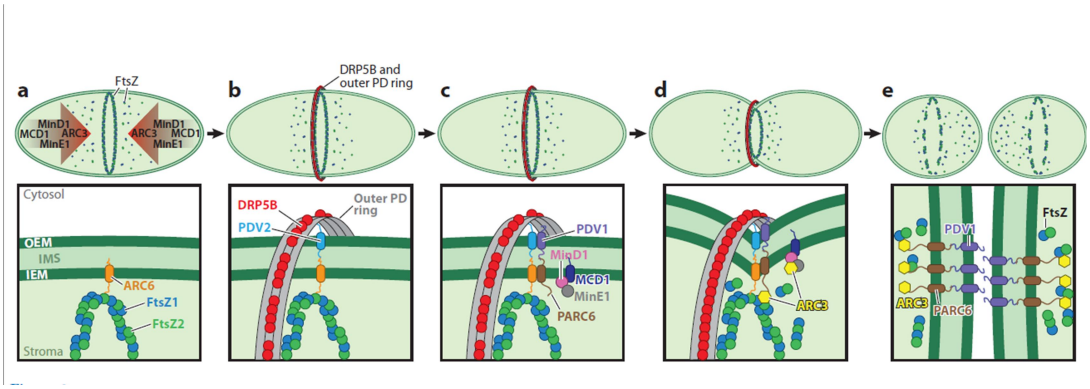

Fig. 1.9. Speculative model of the stepwise assembly and constriction of the chloroplast division complex in higher plants. Upper diagrams show chloroplasts undergoing binary fission; lower diagrams show enlarged views of the midplastid division site. Only components observed to localize at least partly at the division site are shown. FtsZ filaments are illustrated as variable FtsZ1/FtsZ2 heteropolymers. The inner plastid-dividing (PD) ring is omitted for simplicity and because its composition is unknown. Figure partly adapted from Osteryoung and Pyke (2014).

FtsZ polymers self-assemble at the midplastid and are restricted to that position by the chloroplast Min system, which consists of ARC3, MinD1, MinE1, and MCD1. FtsZ2 interaction with ARC6 probably stabilizes ARC6 at the division and tethers heteropolymers to the inner envelope membrane (IEM), resulting in Z-ring formation (Figure 1.9a). PDV2 in the outer envelope membrane (OEM) is positioned at the division site through direct interaction with ARC6 in the intermembrane space (IMS). PDV2 recruits the dynamin-related protein ARC5/DRP5B from the cytosol to the chloroplast surface. PARC6 positions PDV1 at the division site downstream of ARC6.

PDV1 also recruits ARC5/DRP5B to the division site independently of PDV2. Inside the chloroplast, MCD1, MinD1, and MinE1 are all detected at the division site prior to constriction (Figure 1.9c), though their functions there are unclear. PDV1 and PDV2 together promote constriction of the ARC5/DRP5B ring, probably through direct interaction (Figure 1.9d). It is likely that ARC3 is recruited to the division site during constriction by direct interaction with PARC6. ARC3, as a direct Z-ring assembly inhibitor, may enhance remodeling and constriction of the Z ring, possibly aided by FtsZ1, which promotes recycling of FtsZ subunits into heteropolymers.

3.5. Ion channels and transporters in chloroplast membranes

Channels and transporters are required for the movement of molecules across the two chloroplast envelope membranes. The outer envelope does not play any part in selective transport of metabolites (Fuks and Homble, 1999); this membrane is permeable to macromolecules up to molecular masses of about 10 kDa and contains nonspecific large pores which permit the flux of ions and molecules and acts as a barrier to large solutes only (Heiber et al., 1995). The inner envelope membrane of chloroplasts acts as the main osmotic barrier that delimits the chloroplast stroma from the cytoplasm of the plant cell. It is permeable to small neutral molecules only and controls the passage of solutes and ions into and out of the stroma via several metabolite translocators and ion transport systems (Finazzi et al., 2015).

3.5.1. K^+/H^+ exchange at the thylakoid membrane

Light induced electron transport across the thylakoid membrane gives rise to proton pumping into the thylakoid lumen. The resulting Proton electrochemical potential difference (pmf) is used for ATP synthesis by the thylakoid ATP synthase. Early reports indicated that the proton accumulation is electrically compensated by K^+ or Mg^{2+} efflux, or Cl^- influx (Enz *et al.,* 1993). Recently, it was demonstrated that the thylakoid membrane potassium channel TPK3 plays a fundamental role in thylakoid charge compensation (Carraretto *et al.,* 2013). On the other hand, although light induced release of Mg^{2+} into the stroma has been demonstrated, to date no Mg^{2+} transporter was identified at the thylakoid membrane. T-DNA disruption of the thylakoid Cl^- channel AtCLCe has subtle effects on photosynthesis activity and a role in charge equilibration

has not yet been demonstrated (Marmagne *et al.,* 2007). K^+ thus appears to be the fundamental coupling ion.

Recently another K^+ transport system, the K^+/H^+ antiporter KEA3, was also found to be localized at the thylakoid membrane (Armbruster *et al.,* 2014). It is generally assumed that the pH gradient (ΔpH) and the electric field (ΔΨ) generated by the electron transport chain are equally capable of driving ATP synthesis (Kramer *et al.,* 2003). An increase in conductivity to counter ions, for instance by opening of the TPK3 channel, will promote the development of the ΔpH component, but short-circuit the membrane potential, while activity of KEA3 would only dissipate the ΔpH component, leaving the ΔΨ intact. Acidification of the thylakoid lumen specifically activates energy-dependent Quenching (qE) by triggering an intrathylakoid signal transduction pathway involving protonation of key regulatory proteins like PsbS. Energy-dependent quenching dissipates excess absorbed light energy as heat in the antenna of Photosystem II (PSII) acting on the time-scale of seconds to minutes. It was shown that KEA3 accelerates the downregulation of energy-dependent quenching (qE) by dissipation of the thylakoid ΔpH (Armbruster *et al.,* 2014) which helps plants to rapidly adjust photosynthetic quantum yield in fluctuating light conditions. At the same time, reduced luminal acidification in plants with impaired TPK3 function causes increased sensitivity to high light intensities, as the mechanisms to dissipate excess light energy are not activated. It thus appears that the coordinated activation and deactivation of TPK3 and KEA3 enables the interconversion of ΔΨ and ΔpH in response to environmental stimuli, in order to optimize photosynthesis (Kramer *et al.,* 2003)

3.5.2. Electrogenic K^+/H^+ exchange at the envelope membrane

In the dark the cytoplasmic and stromal pH are close to 7, but upon illumination the stroma becomes alkaline, as a consequence of proton pumping across the thylakoid membrane. An alkaline stroma pH is a prerequisite for the full activation of pH-dependent Calvin Cycle enzymes (Demmig and Gimmler, 1983). This implies that, in light, a pH gradient exists between the cytosol (pH 7) and the stroma (pH 8). This gradient is important for exchange of metabolites and reducing equivalents between stroma and cytosol, and uptake of a variety of solutes by proton symporters (Hohner *et al.,* 2016).

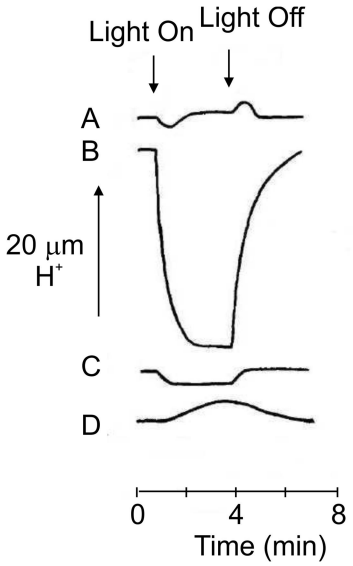

Fig. 1.10. Recording of light-dependent pH changes in the medium of a chloroplast suspension. pH changes were measured with a pH electrode. In A a trace for a suspension of chloroplasts is shown. The measurement is an underestimation of the real changes, as a fraction of the chloroplasts in the preparation is broken. Ferricyanide-dependent oxygen evolution indicated that 5 % of the chloroplasts in this preparation had lost the inner membrane. In broken chloroplasts the medium will alkalinize, due to proton transport into the thylakoid lumen, as shown in B, where chloroplasts were broken prior to the measurement by dilution in H_2O. C shows an extrapolation of B for the percentage (5 %) of broken chloroplasts in A. In D finally the signal in A is corrected for the signal from broken chloroplasts by subtracting C from A. The result is an estimated small transitory acidification (Adapted from Heldt *et al.,* 1973).

It is generally assumed, that in order to maintain this pH gradient, an active proton extrusion mechanism exists at the envelope membrane to compensate passive diffusion of protons from cytosol to the stroma. Evidence for such active proton extrusion is based on the observation that illumination of isolated chloroplasts induces a small transitory acidification in slightly buffered solutions (Figure 1.10) (Heber *et al.,* 1971; Heldt *et al.,* 1973; Heber and Heldt, 1981). Experiments on equilibration of lipophilic cations and tracer studies in isolated chloroplasts indicate that a considerable membrane potential of around -100 mV exists across the envelope membrane due to Gibbs Donan equilibrium, in low salt solutions. At higher KCl concentrations more similar to the situation inside the cell, this membrane potential becomes very small (Demmig and Gimmler, 1983). In illuminated chloroplasts the membrane potential further increases by about 10 mV, concomitant with light induced proton extrusion and coupled K^+ uptake (Wu *et al.,* 1991). It thus appears that light induces electrogenic proton extrusion. Alternatively increased membrane potential could be caused by increased

fixed negative charges at the inner leaflet of the envelope membrane at the more alkaline stromal side (due to proton pumping into the thylakoid lumen), but this does not explain the proton efflux observed (Demmig and Gimmler, 1983). K^+/H^+ exchange is not abolished by the K^+ ionophore valinomycin, leading to the idea that K^+ and H^+ fluxes are electrically and indirectly coupled (Wu *et al.,* 1992; Wang *et al.,* 1993). Several mechanisms have been proposed to explain this H^+ efflux, but the molecular identity of the transporters involved is lacking. Proton extrusion was suggested to depend on a K^+ stimulated vanadate sensitive envelope P-type H^+-ATPase (Scherer *et al.,* 1986; Berkowitz and Peters, 1993; Shingles and McCarty, 1994; Peters and Berkowitz, 1998), but no P-type proton pumps predicted to be targeted to the chloroplast envelope membrane can be found in the *Arabidopsis thaliana* genome (Axelsen and Palmgren, 2001). Alternatively, an electron-transfer chain could be responsible for active proton extrusion. Although proteins that could fulfil such functions are found in the envelope membrane, their function in H^+ extrusion has never been demonstrated (Jäger-Vottero *et al.,* 1997; Murata and Takahashi, 1999; Kovacs-Bogdan *et al.,* 2010). In algae, the plastome-encoded, putative heme-binding, inner envelope protein YCF10 from *Chlamydomonas* is essential for enhancing carbon fixation and inorganic carbon uptake (Rolland *et al.,* 1997). The YCF10 protein was suggested to be involved in plastid pH regulation and to be part of a redox chain in the envelope membrane (Jäger-Vottero *et al.,* 1997; Rolland *et al.,* 1997). In *ycf10* deficient mutants of *Chlamydomonas* the CO_2 or HCO_3^- uptake was compromised and cells failed to grow photoautotrophically (Rolland *et al.,* 1997). It was hypothesized that YCF10 is crucial for acidification of the intermembrane space by H^+-translocation to allow for the conversion of HCO_3^- to CO_2, which in turn could diffuse into the chloroplast (Rolland *et al.,* 1997). A similar observation was made for the cyanobacterial homologue PcxA (CotA) that was shown to be involved in light-induced Na^+-dependent H^+ -extrusion. The *cotA* insertion mutant MA29 of the cyanobacterium *Synechocystis* sp. shows no H^+ export leading to a diminished CO_2 uptake. However, to date no proof is available that a protein with similar function exists in higher plants. Finally, the alkaline stromal pH could be maintained by direct export of protons from the thylakoid lumen to the cytosol by some not well defined temporary or spatial connection (Heber and Heldt, 1981).

The envelope membrane potential drives uptake of cations or efflux of anions (Demmig and Gimmler, 1983). In illuminated chloroplasts the reported *in vivo* stromal ion

concentration is 100 to 150 mM K^+ and about 50 mM Cl^-, while in the dark K^+ and Cl^- ion concentrations are similar to cytoplasmic concentrations (Demmig and Gimmler, 1983; Neuhaus and Wagner, 2000). K^+ loss from chloroplasts, or reduced uptake by chloroplasts in low salt media was shown to cause stromal acidification which in turn inhibits carbon fixation. The acidification can be prevented by addition of K^+ but also Na^+, Rb^+ or even Mg^{2+} to the medium, indicating that the cation transport pathway involved is not very specific. The K^+ induced alkalinization is accompanied by K^+ accumulation, showing it does require K^+/H^+ antiport and is not caused by some other physicochemical process. The presence of a variety of cation and anion channels in chloroplasts inner envelope membranes has been inferred from biochemical and electrophysiological studies (Pottosin, 1992; Wang *et al.,* 1993; Heibert *et al.,* 1995). The presence of a K^+ channel in the envelope membrane was inferred from biochemical studies with membrane vesicles as well as patch clamp studies (Heibert *et al.,* 1995). Non selective cation channels activities were also detected in chloroplasts inner envelopes (Pottosin, 1992) as well as several anion conductive pathways (Wijngaard and Vandenberg 1997; Fuks and Homble, 1999). Surprisingly however, to date the molecular identity of none of the proteins involved in this electrogenic cation or anion exchange is known. The envelope inner membrane was shown to contain two proteins MSL2 and MSL3, with homology to mechanosensitive channels of small conductance (MscS) (Haswell and Meyerowitz, 2006). In bacteria MscS are thought to act as a safety valve, regulating the release of ions and small solutes when gated by membrane tension under challenging osmotic conditions (Sotomayor *et al.,* 2007). In *Arabidopsis thaliana* these proteins play an important role in chloroplast division and are important for plastid volume regulation in response to hypoosmotic stress (Wilson and Haswell, 2012).

3.5.3. Inner envelope membrane (Na^+, K^+)/H^+ antiporters

While the expected electrogenic H^+ and K^+ uniport transport systems at the chloroplast inner envelope membrane are up to today not identified, several most likely electroneutral Na^+/H^+ or K^+/H^+ exchangers were identified recently (Aranda-Sicilia *et al.,* 2012; Kunz *et al.,* 2014; Muller *et al.,* 2014). For thermodynamic reasons it is however difficult to explain how such electroneutral antiporters could be involved in the development and sustaining of these H^+ or K^+ gradients. Antiporters are more likely

involved in chloroplast volume regulation, or coupling of secondary transport to the H^+, Na^+ or K^+ gradient. The first cation/proton antiporter that was suggested to be localized at the inner envelope membrane of chloroplasts was AtCHX23 (Song *et al.,* 2004), but later studies localized this protein to endosomal membranes (Lu *et al.,* 2011). The NHD1 or NhaD1 protein is a genuine envelope Na^+/H^+ antiporter, involved salt tolerance by export or accumulation of Na^+ in chloroplasts in *Arabidopsis thaliana* and *Mesembry anthemum* (Cosentino *et al.,* 2010; Muller *et al.,* 2014). In C4 plants it was suggested to operate as a two-translocator system together with the sodium: pyruvate cotransporter BASS22 (Furumoto *et al.,* 2011). Most recently, the *Arabidopsis thaliana* KEA1 and KEA2 proteins were identified as K^+/H^+ antiporters and shown to be localized to the chloroplast inner envelope membrane (Aranda Scicilia *et al.,* 2012; Kunz *et al.,* 2014). A model for AtKEA1 and AtKEA2 function in chloroplast is shown in Figure 1.11.

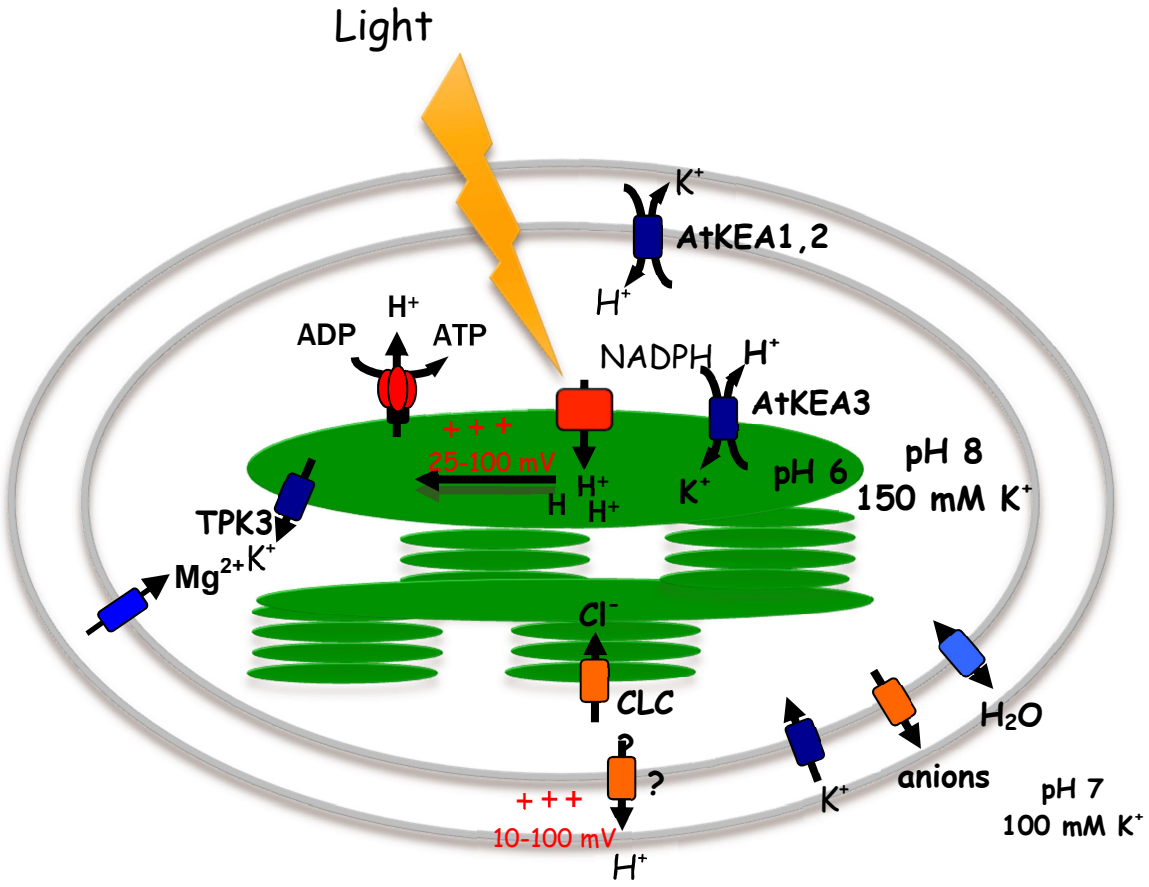

Fig. 1.11. Model of K^+ and H^+ fluxes across chloroplast membranes. In the light, thylakoid membranes accumulate protons, and the stroma becomes alkaline. The thylakoid pH gradient is regulated by K^+/H^+ exchange via the antiporter AtKEA3 and channel TPK3. An unidentified mechanism is responsible for H^+ extrusion across the envelope membrane, creating an outside positive membrane potential that drives uptake of K^+ and Mg^{2+}, or efflux of anions through unidentified channels. Antiporters AtKEA1 and AtKEA2 were suggested to be involved in K^+ efflux and osmoregulation.

3.5.4. Chloroplast volume regulation

In analogy with the situation in mitochondria, active electrogenic proton extrusion would pose a problem for chloroplast volume regulation (Bernardi, 1999). With a cytoplasmic K^+ concentration of 100 mM, a membrane potential of 100 mV would potentially lead to the accumulation of 10 M potassium, which obviously is not happening. *In vivo*, potassium concentration was estimated to be about 150 mM inside the chloroplasts, more in line with a modest membrane potential of around 10 mV, as also estimated in isolated chloroplasts in high salt solutions (Demmig and Gimmler, 1983). Such a weak membrane potential could be caused by a relatively weak proton extrusion activity combined with a high conductance to K^+ or other ions. Like in

mitochondria, electroneutral K^+/H^+ exchange can avoid excessive K^+ accumulation and concomitant swelling of chloroplasts. In accordance, it was shown that disruption of envelope antiporters AtKEA1 and AtKEA2 results in bigger and rounder chloroplasts with occasionally disrupted envelope membranes, as judged by electron microscopy images (Kunz *et al.,* 2014). The effect of AtKEA1 and AtKEA2 disruption on chloroplast ion concentrations is not yet determined. More than 40 years ago it was already shown that chloroplasts shrink upon illumination (Nobel, 1968), which could thus be due to light activation of KEA1/2. Other players are the mechanosensitive channels MSL2 and MSL3 (Velly *et al.,* 2012), especially as shrinkage is accompanied by a reduction of ion content per mg chlorophyll for Cl^-, K^+, Na^+ Ca^{2+} and Mg^{2+} (Nobel, 1969). The largest decrease is observed for the Cl^- content, which was reported also to carry most of the ionic current through bacterial MscS channels (Sotomayor *et al.,* 2007). *In vivo* the volume decrease is observed as a flattening which can be inhibited by CCCP or Nigericin, clearly indicating the involvement of K^+ and H^+ fluxes (Nobel *et al.,* 1969). Such flattening that was proposed to be important for photosynthetic efficiency, also suggests structural constraints on chloroplast shape and localized ionic gradients. Clearly, it would be very illustrative to repeat some of the old measurements to determine ion content, ion flux and chloroplast size using the T-DNA disruption mutants for the now identified antiporters and channels. The combined action of active H^+ extrusion, Cl^- channel activity and a K^+/H^+ antiporter would result in net K^+ and Cl^- efflux, which can be fine-tuned by regulation of individual transport activities (Figure 1.12).

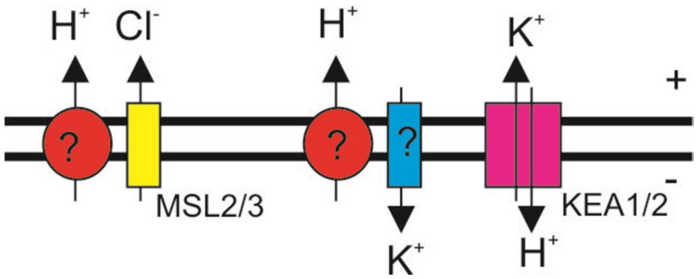

Fig. 1.12. Possible mechanism for volume regulation in chloroplast envelopes. Proton extrusion by an uncharacterized mechanism drives electrogenic K^+ uptake and anion efflux by unidentified potassium channels and possibly MSL2/3. The pH gradient drives K^+ efflux via KEA1/2. Fine tuning of these activities would allow for volume regulation.

3.5.5. Effect of osmotic homeostasis on chloroplast division

An unsuspected link between osmotic homeostasis and chloroplast division was found by Haswell and Meyerowitz (2007). These authors observed that the two mechanosensitive channel homologs MSL2 and MSL3 affect chloroplast division and chloroplast osmotic balance. The *msl2msl3* double mutant plants had less chloroplast that are enlarged and contain multiple FtsZ rings that are responsible for fission at the midcell by constriction. It was suggested that MSL2 and MSL3 control plastid size, shape and division by altering ion flux in response to changes in membrane tension. Genetic analyses indicate that these two genes and components of the Min system function in the same pathway to regulate chloroplast size and FtsZ ring formation, but no direct interactions between the channels and FtsZ or Min system components could be shown (Wilson *et al.,* 2011, 2012). MSL2 and MSL3 are likely required to maintain ion homeostasis in the chloroplast stroma and changes in ion concentration could affect the function of chloroplast division proteins. For example, MinD is a Ca^{2+} stimulated Mg^{2+}-dependent ATPase and its function could be altered by abnormal stromal Ca^{2+} or Mg^{2+} levels. Alternatively, MSL2 and MSL3 could regulate membrane tension. Tension induced changes in lipid spacing and membrane bilayer thickness could interfere with the ability of MinD or other components to interact with membrane phospholipids (Wilson *et al.,* 2012).

4. Forward and reverse genetics

4.1. T-DNA Mutagenesis as a tool to study gene function

The complete sequencing of the genome of *Arabidopsis thaliana* (AGI, 2000) is a major milestone in plant biology research. The determination and analysis of the genome sequence of *Arabidopsis thaliana* has provided the first detailed description of the genetic blueprint of a higher plant (Lin *et al.,* 1999) and revealed several novel processes involved in plant growth and development. With the availability of complete genome sequences, the focus of research worldwide is now on functional genomics. One of the most challenging tasks for plant scientists is assigning functions to a large number of uncharacterized plant genes. The functions of ~69 % of the genes were classified according to sequence similarity to proteins of known function in other

organisms (AGI, 2000). Definitive functions for individual genes have been thoroughly established for less than 10 % (Ostergaard and Yanofsky, 2004). Out of the ~25000 genes identified in *Arabidopsis thaliana*, the functions of only a few thousand have been defined with great confidence (Bouche and Bouchez, 2001). According to the Annual Report 2010 of The Multinational Coordinated *Arabidopsis thaliana* Functional Genomics Project (http://www.Arabidopsis thaliana .org/ portals/masc/masc_docs/masc_reports.jsp), the experimentally verified functions of just over 9000 of the ~27,000 *Arabidopsis thaliana* genes had been annotated as of March 2010.

To determine the function of these new genes, two approaches are classically used; forward genetics and reverse genetics. Forward genetics begins with a phenotype and asks the question what is the sequence of the gene causing the altered phenotype. Reverse genetics begins with a mutant genome sequence and asks the question what is the resulting change in phenotype. These two approaches are fundamentally different, and whereas forward genetics has been in operation for more than a century, the recent avalanche of complete genome sequences has only now created the opportunity for pursuing reverse genetics in an exhaustive and complete manner (Krysan *et al.,* 1999). Gene function is most frequently determined by disruption of the gene. In yeast and *Escherichia coli* homologous recombination is the best methodology to disrupt genes, but, although there has been a report of homologous recombination with intact *Arabidopsis thaliana* plants (Kempin *et al.,* 1997), the frequency of this event may be so low as to preclude its use for generating knockout mutations in each of the 25000 genes that comprise the 120-Mb genome.

Therefore, the insertion of foreign DNA into the gene of interest is the most commonly used way to disrupt gene function. In *Arabidopsis thaliana*, insertional mutagenesis involves the use of either transposable elements (Parinov *et al.,* 1999) or T-DNA. The foreign DNA not only disrupts the expression of the gene into which it is inserted but also acts as a marker for subsequent identification of the mutation. Because *Arabidopsis thaliana* introns are small, and because there is very little intergenic material, the insertion of a piece of T-DNA on the order of 5 to 25 kb in length generally produces a dramatic disruption of gene function. If a large enough population of T-DNA transformed lines is available, one has a very good chance of finding a plant carrying a T-DNA insert within any gene of interest. Mutations that are homozygous lethal can be maintained in the population in the form of heterozygous plants.

Polymerase chain reaction (PCR) methods have been developed to allow one to easily detect plants that carry a particular mutation of interest (McKinney *et al.,* 1995; Krysan *et al.,* 1996). An advantage of using T-DNAs as the insertional mutagen, as opposed to transposons (Martienssen, 1998; Wisman *et al.,* 1998), is that T-DNA insertions will not transpose subsequent to integration within the genome and are therefore chemically and physically stable through multiple generations. The mobility of transposons is not necessarily a disadvantage. In situations in which multiple members of a gene family are arranged in tandem along a chromosome, the ability of transposons to "hop" to nearby locations provides a convenient method for creating mutations within all of the members of the gene family within a single plant.

Saturation of the *Arabidopsis thaliana* genome with T-DNA insertions has been an experimental goal during the first decade of the 21st century. As a first step in determining the function of all *Arabidopsis thaliana* genes, a consortium of *Arabidopsis thaliana* researchers generated a large collection of T-DNA insertion mutants (Alonso *et al.,* 2003). The Salk Institute Genome Analysis Laboratory (SIGnAL) used high-throughput sequencing methods to identify the sites of the T-DNA insertions within the *Arabidopsis thaliana* genome. Following identification of the mutant locus in a line, the lines were made publicly available through the *Arabidopsis thaliana* Biological Resource Center (ABRC, https://abrc.osu.edu/) at Ohio State University (The SALK collection). The ABRC is also distributing approximately 54,000 lines from the Syngenta *Arabidopsis thaliana* Insertion Library (SAIL) collection. SAIL is an insertion collection which was generated from approximately 100,000 individual T-DNA mutagenized *Arabidopsis thaliana* plants. Several other resources of mutant lines generated by different consortia are also available from ABRC (WiscDsLox, GABI-Kat) (Berardini *et al.,* 2015). All information relative to the available T-DNA mutants, as well as a wealth of other information relative to *Arabidopsis thaliana* and the *Arabidopsis thaliana* genome is available through the The *Arabidopsis thaliana* Information Resource (TAIR) (Berardini et al. 2015). In Europe, up to now (27-6-2016), the T-DNA seeds are distributed by The Nottingham *Arabidopsis thaliana* Stock Centre (NASC, http://Arabidopsis thaliana .info/).

The consequences of inserting a T-DNA element into the *Arabidopsis thaliana* genome depend on the nature of the T-DNA as well as the precise site of insertion. Figure 1.13 diagrams several of the possible outcomes of T-DNA insertion and proposes a standard nomenclature for describing them. The "knockon" mutations are a special case

in which the T-DNA construct carries a constitutive promoter, such as the cauliflower mosaic virus 35S promoter, capable of driving expression of genes adjacent to the site of insertion (Wilson *et al.,* 1996). The "knockworst" category includes those T-DNA insertion events that lead to large-scale chromosomal rearrangements. Such T-DNA induced rearrangements have been documented in *Arabidopsis thaliana* (Figure 1.13) (Krysan *et al.,* 1999; Nacry *et al.,* 1998; Laufs *et al.,* 1999).

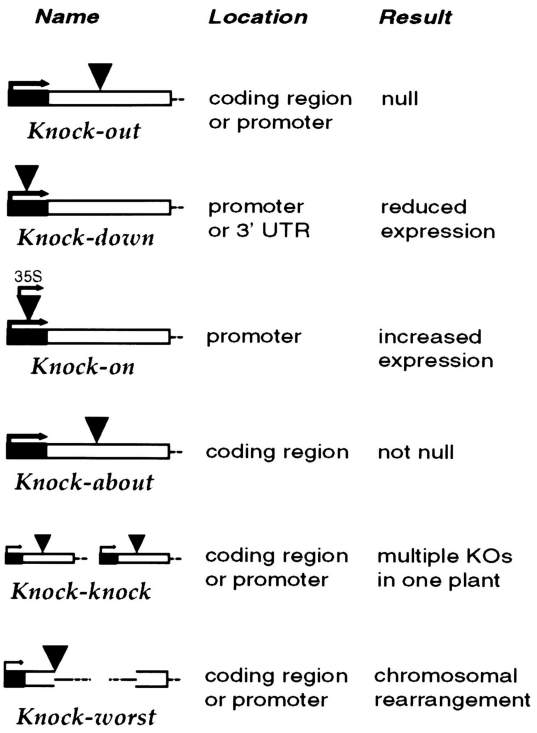

Fig. 1.13. Knockology, the insertion of a T-DNA element into an *Arabidopsis thaliana* chromosome can lead to many different outcomes. This figure shows several of these possibilities and proposes a standard nomenclature to describe them. The coding region of the gene is shown as a white box, the promoter is the black region with the arrow, and the T-DNA element is represented by a black triangle. KOs, knockouts; UTR, untranslated region (Krysan *et al.,* 1999).

Gene knockouts, or null mutations, are important because they provide a direct route to determining the function of a gene product. Most other approaches to gene function are correlative and do not necessarily prove a causal relationship between gene sequence and function. For example, DNA chips provide an exciting means to discover conditions under which gene expression is regulated on a genome wide scale (De Risi *et al.,* 1997; Wodicka *et al.,* 1997; Singh-Gasson *et al.,* 1999). However, because factors other than mRNA level alone determine the activity of a gene product *in situ*,

expression studies, even when done on a genome wide scale, cannot prove a causal relationship. By contrast, the availability of a null mutation for the gene of interest allows one to directly monitor the effect that this deficiency has on the organism's ability to function.

The phenotypes of double or higher order mutants can be used to determine whether genes act in different pathways or in the same pathway, the order in which genes act in a pathway, and whether they have redundant functions.

Double mutants are obtained by crossing homozygous single mutants. Because *Arabidopsis thaliana* is naturally self-pollinated, the generation of cross-progeny requires some human intervention. It is preferable to design crosses such that the F1 progeny is easily distinguishable from self-progeny of the female parent. An easy way to do this is to use a female parent that carries a recessive mutation and a male parent that lacks the mutation (i.e., is wild type for this trait). For example, a female parent that is homozygous for gll (i.e., lacking trichomes) can be crossed to a wild-type male parent (i.e., with trichomes), resulting in F1 progeny with trichomes. Any plants that arise from self-fertilization of the female parent will exhibit the mutant phenotype (i.e., lacking trichomes) and can be easily eliminated (Zhu *et al.,* 1998). Once suitable parent plants have been chosen, it is important to select the best flowers to use in the cross. To reduce the possibility of self-fertilization, flowers from the female parents must be used before the anthers begin to shed pollen onto the stigma. For the male parent, choosing an open flower that is visibly shedding pollen is important (Krysan *et al.,* 1999). The appearance of flowers at the appropriate developmental stage varies among ecotypes and developmental mutants; for Columbia, flowers in which the tips of the petals are just visible are the best choice for the female parent. The first two or three flowers on the first inflorescence shoot are often infertile, and these should be avoided. The next few flowers are the best. As the plants get older, the flowers tend to become smaller, and the failure rate for crosses increases.

4.2. Mutant phenotypic analysis

The phenotypes of knock-out mutants are difficult to predict, and it is also quite common for mutants, first isolated because of a specific phenotype, to have other, pleiotropic defects, i.e., multiple defects in addition to that of primary interest. Thus, it is often necessary to characterize a variety of phenotypic parameters. This is particularly important as the field of molecular genetics expands. If a number of

groups, each looking for a different phenotype, independently identify different mutations in the same gene, an awareness of additional defects will often show that the new mutation is allelic to existing mutants (Zhu *et al.,* 1998). It is important to confirm that the various phenotypes of an individual are genetically linked. Phenotype mapping becomes more important, however, when dealing with a mutant that has been isolated by site-selected mutagenesis. In this case, it must be shown that any phenotype co-segregates with the induced mutation. Definitive proof that a phenotype is indeed due to the disrupted gene can only come from complementing the mutant with a wild-type copy of the disrupted gene or by constructing trans-heterozygotes carrying two independently isolated mutations (Krysan *et al.,* 1999).

III. MATERIALS AND METHODS

1. Materials

1.1. Bacteria

1.1.1. Bacterial strains

Two strains of *Escherichia coli*, Mach1™T and ccdB Survival™, were used for the amplification and the multiplication of plasmids; while the *Agrobacterium tumefaciens* strain GV3101was used for transformation of *Arabidopsis thaliana* plants (Table 2.1).

Table 2.1. Strains of *Echerichia coli* and *Agrobacterium tumefaciens* used

Strain	GENOTYPE	SOURCE
Mach1™T1^{R}	*F- φ80(lacZ)ΔM15 ΔlacX74 hsdR(rK-mK+) ΔrecA1398 endA1 tonA*	Invitrogen™
ccdB Survival™ 2	*F- mcrA Δ(mrr-hsdRMS-mcrBC) Φ80lacZΔM15 ΔlacX74 recA1 araΔ139 Δ(ara-leu)7697 galU galK rpsL (StrR) endA1 nupG fhuA::IS2*	Invitrogen™
GV3101	Rif' derivative of *Agrobacterium tumefaciens* cured of its pTiC58 plasmid. Resistance to Rifampicin (10 mg/l) (in genome), Gentamicin (30 mg/l) (in helper plasmid). Binary vector confers Kanamycin resistance (25 mg/l)	Van Larebeke et al. 1974

1.1.2 Bacterial cultures

Different liquid and solid media were used for bacterial cultivation (Table 2.2). Solid media were prepared by adding 10 g/l of bactoagar to the liquid media. Sterilization was performed by autoclaving (Autoclave Selecta mod. Presoclave 75 l) at 120 ^{o}C and 1 atm for 20 minutes. For selection of transformants, the culture media were supplemented with the appropriate antibiotics. Antibiotics were prepared as concentrated stock solutions (10 mg/ml) in MilliQ ® water and filter sterilized through 0.45 μm filters (Pall Corporation, Ann Arbor, Michigan, USA). The antibiotics were added to autoclaved media at the following final concentrations: Ampicillin, 100 μg/ml, kanamycin 50 μg/ml, rifampicin 30 μg/ml, spectinomycin 50 μg/ml, gentamycin 25 μg/ml.

Manipulation of the bacterial cultures was performed in a horizontal laminar flow cabinet (ESCO model LHC-4B1) to prevent contamination. For the bacterial cultivation in liquid medium, a colony from a previous culture was inoculated into 3 ml of fresh medium (dilution 1/250 of a saturated mother culture). The *E. coli* culture was incubated in growth tubes for 16 hours at 37 ^{o}C and 40 rpm.

Table 2.2. Media used for growing bacteria

MEDIUM	COMPOSITION	PURPOSE
LB	Bacto-triptone 1% (w/v) NaCl 1% (w/v) Yeast extract 0.5% (w/v) pH 7.0 with NaOH	Standard cultivation of *E. coli*
SOB	Bacto-triptone 2% (w/v) Yeast extract 0.5% (w/v) NaCl 10 mM KCl 25 mM $MgCl_2$ 10 mM $MgSO_4$ 10 mM pH 6.7-7.0 with NaOH	Cultivation of *E. coli* competent cells
SOC	Bacto-triptone 2% (w/v) Yeast extract 0.5 % (w/v) NaCl 10 mM KCl 2.5 mM $MgCl_2$ 10 mM $MgSO_4$ 20 mM Glucose 2% (w/v)	Cultivation of *E. coli* after transformation
YEP	Bacto-tryptone 1% (w/v) Yeast extract 1%(w/v) NaCl 0.5% (w/v)	Cultivation of *A. tumefaciens*
Infiltration Medium	Sucrose 5% (w/v) Silwet L-77 0.05% (v/v) ½ x Murashigue and Skoog (MS) salts	Transformation of *A.thaliana*

1.1.3. Preparation of competent *E. coli* cells

Competent cells of *E. coli* were prepared according to the method described by Inoue et al. (1990). 125 µl of a saturated culture of *E. coli* was inoculated in 250 ml of SOB medium (Table 2.2) and incubated at 20-25 ^{o}C and 250 rpm, until an optical density of 0.6 at 600 nm was reached. The culture was chilled on ice and centrifuged at 2500 g for 10 minutes at 4 ^{o}C. The pellet was resuspended in 80 ml of ice-cold transformation buffer composed of 100 mM PIPES (Piperazine-N, N'-bis 2-ethanesulfonic acid), 250

mM KCl, 15 mM $CaCl_2$, 55 mM $MnCl_2$, pH 6.7 with KOH, and incubated on ice for 10 minutes. After centrifugation at 2500 g for 10 min, the resulting pellet was resuspended in 20 ml of ice-cold buffer containing DMSO (dimethyl sulfoxide) to a final concentration of 7 %. 200 µl aliquots were frozen in liquid nitrogen and stored at -80 ^{o}C.

1.1.4. Preparation of competent *A. tumefaciens* cells

A 5 ml culture of *A. tumefaciens* (GV3101 strain) in LB medium (Table 2.2) without antibiotics was inoculated from a frozen stock and grown overnight in a cell culture roller drum at 28 ^{o}C and 40 rpm. The next day 2 ml of the culture was diluted into 50 ml LB medium in a 250 ml flask and incubated with vigorous shaking at 28 ^{o}C in an orbital shaker at 250 rpm until an optical density at 600 nm of 0.5 to 0.6 was reached. The culture was chilled on ice for 10 minutes, and centrifuged at 4000 g for 15 minutes at 4 °C. The supernatant was removed and the pellet was resuspended in 20 ml of 20 mM $CaCl_2$. The cells were kept in ice for 20 to 90 minutes and then centrifuged at 4000 g for 15 min. The pellet was resuspended in 1 ml of 20 mM $CaCl_2$, 20 % glycerol. Aliquots of 100 µl in 1.5 ml Eppendorf tubes were frozen in liquid nitrogen and stored at -80 °C.

1.1.5. Transformation of *E. coli*

One to ten ng plasmid or ligation mixture was added to an aliquot of 200 µl of frozen competent cells. The cells were incubated on ice for 30 minutes and then subjected to a heat shock at 42 ^{o}C for 2 minutes. After cooling on ice for 2 minutes 1 ml of LB or SOC medium (Table 2.2) was added. Then cells were incubated at 37 ^{o}C in an orbital shaker for at least one hour. Afterwards, the cells were pelleted by a short centrifugation at 15000 g and suspended in 200 µl of SOC. Aliquots of 50 and 200 µl were plated on LB medium supplemented with appropriate antibiotics for selection of plasmid-containing cells.

1.1.6. Transformation of *A. tumefaciens*

One µg of plasmid DNA was added to a frozen aliquot of competent cells. Cells were thawed slowly and kept on ice for 15 to 30 minutes. Next, cells were heated at 42 ^{o}C for 2 minutes and cooled on ice for 5 minutes. 1 ml of LB (without antibiotics) was added and cells were kept for 3 hours at 28 ^{o}C in a cell culture roller drum at 40 rpm. Cells were directly plated on LB plates with the required antibiotics to select for the used

plasmid. For strain GV3101 100 μg/ml gentamycin was also included to assure maintenance of the helper plasmid.

1.2 Yeast

1.2.1 Yeast strains

The yeast *Saccharomyces cerevisiae* is a suitable system for heterologous eukaryotic gene expression, as it constitutes a genetically well characterized eukaryotic system in which most mechanisms for post translational modification of proteins are conserved and because cells multiply rapidly. Yeast is especially well suited for expression of plant membrane proteins, since many of them are toxic in bacteria (Haro *et al.,* 1993; Darley *et al.,* 2000). In this study we used yeast to clone *AtKEA2* gene constructs by *in vivo* recombination, as they were highly toxic in bacteria. Moreover, the existence of mutants with disruptions in genes coding for membrane transporters makes yeast an ideal tool for the molecular study of transporters of higher eukaryotes (Maresova and Sychrová, 2005). The *Saccharomyces cerevisiae* strain used in this study is BYa (Table 2.3).

Table 2.3. Yeast strain used

Strain	Genotype	Reference
BYa	*(Mat a; his3Δ1; leu2Δ0; met15Δ0; ura3Δ0)*	Euroscraf web site

1.2.2. Yeast culture

All media used were sterilized by autoclaving at 15 Psi and 120 °C, for 20 minutes. Components such as vitamins, nitrogen bases and antibiotics were filter sterilized through 0.45 μm filters, before being added to the previously autoclaved media. Solid media were prepared by adding 20 g/l bactoagar to the corresponding liquid medium prior to autoclaving. To select or cultivate yeast transformed with plasmids conferring auxotrophy, yeast cells were grown in SD minimal medium (Table 2.4), to which the compounds required were added at the following concentrations: adenine, 20 mg/l; histidine, 20 mg/l; leucine, 30 mg/l; uracil, 20 mg/l and tryptophan, 20 mg/l. Yeast cultures were also grown in SC-Ura medium (Table 2.4).

Table 2.4. Media used for growing yeast

Medium	Compound	Concentration
SD / SG	Glucose/Galactose	20 g/l
	YNB[1]	6.7 g/l
	MES	3.9 g/l
SC-Ura	Glucose	20 g/l
	YNB	6.7 g/l
	Mix Drop-out[2]	1,92 g/l
	MES	3,9 g/l
APD / APG	H_3PO_4	8 mM
	$MgSO_4$	2 mM
	$CaCl_2$	0.2 mM
	KCl	1 mM
	L-Arginine	10 mM
	Glucose/Galactose	20 g/l
	Trace elements*	1 ml/l
	Vitamines*	1ml/l
*Trace elements	BO_3H_3	0.8 mM
	$CuSO_4.5\ H_2O$	0.016 mM
	KI	0.06 mM
	$Fe_3Cl.6\ H_2O$	0.07 mM
	$MnSO_4$	0.26 mM
	$Na_2Mo\ O_4$	0.08 mM
	$ZnSO_4.7\ H_2O$	0.14 mM
*Vitamins	Biotin	0.80 µM
	Niacin	0.32 µM
	Pyridoxine HCl	0.19 µM
	Thiamine HCl	0.12 µM
	CalciumPantothenate	0.08 µM
YPD / YPG	Peptone	20 g/l
	Glucose/Galactose	20 g/l
	Yeast extract	10 g/l

[1]Yeast Nitrogen Base (Difco™), pH 5. 7, adjusted with Arginine
[2]Yeast Synthetic Drop-out Medium Supplement without Uracil (Sigma-Aldrich ®), pH 5. 7, adjusted with Arginine

Yeast cultures were grown at 28 °C. Liquid cultures were started by inoculating a fresh colony from an agar plate or by inoculating a 1/1000 dilution of a fresh saturated yeast culture. The culture was incubated for 1 day (rich medium) or 2 days (minimal medium) in a rotary shaker at 40 rpm. To avoid contaminations yeast cultures were manipulated in a horizontal laminar flow cabinet (Microflow Horizontal model 480).

1.2.3. Yeast transformation

Yeast transformation was performed according to the protocol of Gietz and Woods (2002). A liquid culture of 3 ml YPD was grown overnight at 30 °C, rotating at 40 rpm. The culture was centrifuged for 30 seconds at 15000 g, the supernatant removed and the pellet resuspended in 1 ml of 100 mM lithium acetate (LiAc). The resulting suspension was incubated 5 minutes at 30 °C, and centrifuged as described above. To the resulting pellet was added in the following order: 240 µl of 50 % (w/v) PEG3350 (polyethylene glycol), 36 µl of 1 M LiAc, 50 µl of 2 mg/ml salmon sperm DNA (ssDNA), 5 to 10 µl of plasmid (0,1-1 µg) and mili Q H_2O up to a final volume of 360 µl (Table 2.5). The pellet was resuspended by stirring for 1 minute and kept at 28 ^oC for one hour, then incubated at 42 °C for 60 to 120 minutes. Thereafter the mixture was centrifuged for 15 sec at 7000 g, and the pellet resuspended in 300 µl of sterile distilled H_2O. The transformation mixture was plated on SD solid medium supplemented with the appropriate amino acids and nitrogen base or SC-Ura medium, and incubated at 28 ^oC until colonies appeared (3 days approximately).

Table 2.5. Yeast Transformation mix

Compound	Volume (360 µl)
PEG 3500 50% w/v	240 µl
LiAc 1,0 M	36 µl
Salmon Sperm DNA (2 mg/ml)	50 µl
Plasmid DNA (0,1-1 µg)	5-10 µl

1.2.4. Yeast vectors used

For most studies we used vector pYES-DEST52 or derivatives thereof. pYES-DEST52 is a 7.6 kb high copy number shuttle vector derived from pYES2/CT (Invitrogen) and adapted for use with the Gateway® Cloning Technology. It is designed for high-level, galactose-inducible expression in *Saccharomyces cerevisiae* using the yeast GAL1 promoter, while it can also be maintained and propagated in bacteria. Two recombination sites, *att*R1 and *att*R2, downstream of the *GAL1* promoter permit recombinational cloning of the gene of interest from an entry clone. The *ccd*B gene is located between the two *att*R sites for negative selection. The vector further harbors a

V5 epitope and 6xHis tag for detection and purification of recombinant proteins. The vector contains an *URA3* selectable marker for selection in yeast and an ampicillin resistance gene for selection in *E. coli* (Figure 2.1).

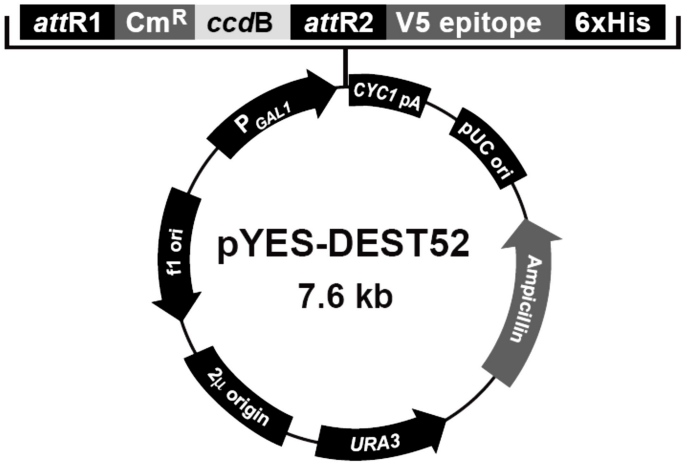

Fig. 2.1. The pYES-DEST52 vector.

1.3. Plant Materials

In this study *Arabidopsis thaliana* wild type plants and T-DNA transgenic lines from SALK and SAIL collections were used (Table 2.6). All lines used were Columbia 0 ecotype.

Table 2.6. T-DNA transgenic lines used in this study

NASC Code	Name	Gene	T-DNA insertions	Selective Marker
N859459	SALK-045324	AtKEA2	in Exon (Homozygous line)	Kanamycin
N509732	SALK-009732	AtKEA2	in Exon (Homozygous line)	Kanamycin
N861469	SAIL- 1156-H07	AtKEA1	in Intron (Homozygous line)	BASTA
N875131	SAIL- 586-D02	AtKEA1	in Exon (Heterozygous line)	BASTA

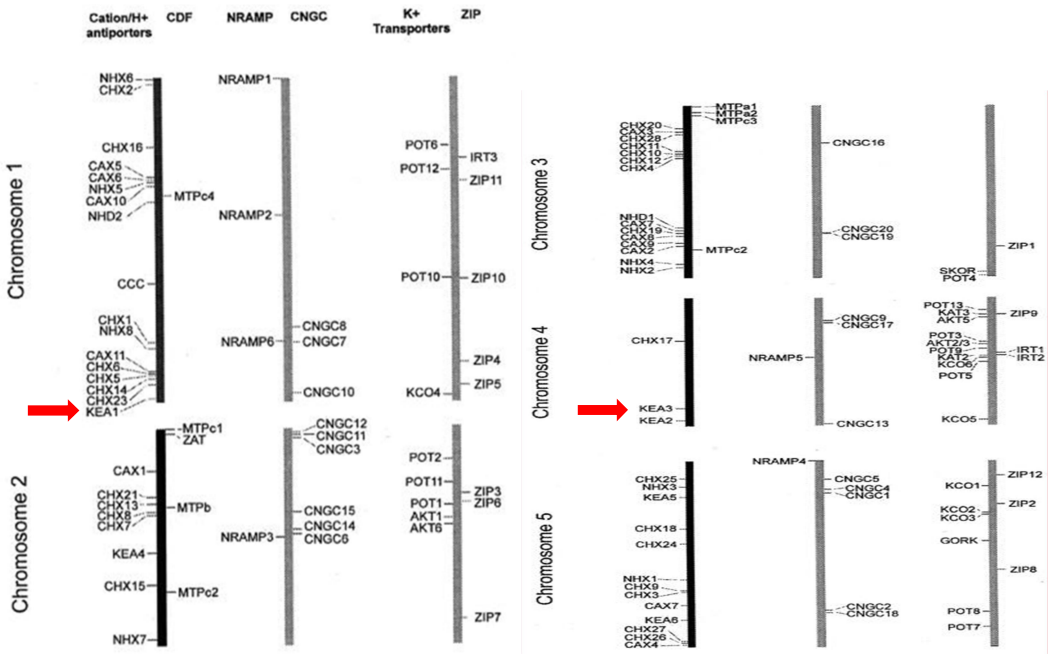

Fig. 2.2. Location of *KEA* genes in *Arabidopsis thaliana* genome

1.3.1. Characterization of plant material

Insertional mutants in *AtKEA1* (chromosome 1) and *AtKEA2* (chromosome 4) (Fig 2.2) were identified from the TAIR (The *Arabidopsis thaliana* Information Resource) website (http://Arabidopsis thaliana .org/index.jsp/) and seeds harbouring T-DNA insertions in the translated regions of the genes were obtained from the NASC (Nottingham *Arabidopsis thaliana* Stock Centre). We obtained two homozygous lines for AtKEA2 with insertions in exons from the SALK collection. For AtKEA1 we obtained one homozygous T-DNA insertional mutant with a T-DNA insertion in an intron and one heterozygous line with an insertion in an exon both from the SAIL collection. A second homozygous line for AtKEA1 was obtained by self-crossing of the heterozygous line SAIL_586_D02. By PCR analysis using primers designed at the I-Sect website (http://signal.salk.edu/cgi-bin/tdnaexpress) we checked the location of the T-DNA and confirmed two homozygous AtKEA2 T-DNA mutants and one homozygous AtKEA1 T-DNA mutant. From the heterozygous line, we produced homozygous ones by self-crossing. Absence of expression of the disrupted genes was checked by RNA extraction and subsequent RT-PCR.

1.3.2. Genotyping of AtKEA1 and AtKEA2 T-DNA insertional mutants

We determined whether the lines were homozygous or heterozygous by PCR using specific primers of the disrupted gene and one T-DNA border primer:

Gene specific forward primer + T-DNA reverse primer

Gene specific reverse primer + T-DNA reverse primer

Gene specific forward + reverse primer (control reaction)

The exact insertion site of the T-DNA in *AtKEA1* and *AtKEA2* was assessed by sequencing of PCR products separated in a 1 % agarose gel.

The various alleles were checked by PCR, using the primers shown in the Table 2.7.

Table 2.7. Primers used for genotyping *Arabidopsis thaliana KEA1* and *KEA2* T-DNA insertional mutants

For CTTCTCCAAAAGCAACAAACG Rev TGAAGCTCTTGGACTAGCTGC	Salk_045234 (kea2-1)
For ATCTAGGGAACGACCAATTGC Rev AACTTCTTCTCGCCAACTTCC	Salk_009732 (kea2-2)
For TTTGCAGGCTGAAACTTTCTG Rev CCTAATTCATCGAAAGGAGGG	Sail_586_D02 (kea1-1)
For ATTATGTTGCTGGTCAGGCTG Rev GCTCCATATCGTGGTCTTCTG	Sail_1156_H07 (kea1-2)
Rev ATTTTGCCGATTTCGGAAC	Salk Lbp1.3
Rev TAGCATCTGAATTTCATAACC AATCTCGATACAC	Sail Lb3

A PCR product will only be obtained using the T-DNA reverse primer and gene specific forward primer if the T-DNA is present and orientated with T-DNA left border at the left. Using two gene specific primers will only result in a PCR product if the T-DNA is not inserted, as the fragment will be too big to be amplified. In this way homozygous T-DNA insertion mutants (no amplification with gene specific primers) can be distinguished from heterozygous mutants that still contain one intact copy of the gene.

1.3.3. Generation of *kea1kea2* double mutants

First, we checked the homozygosis of the tested single mutant plants as explained in the previous paragraph. As SAIL and SALK lines have distinct selection markers, progeny selection was facilitated using Kanamycin and BASTA selection one after the other. Homozygous single mutants were grown up in vermiculite: peat-moss (1:1) in a growth chamber at 22/20 ^{o}C, 16h light (120 μmol/m^2/s) / 8 h darkness and irrigated with tap water. When the first floral stem appeared plants were separated to avoid cross fertilization. The flowers of the SALK single mutant lines were used as female parents and those from the SAIL single mutant lines were used as male parents. For the female parent, flowers in which the tips of the petals were just visible were selected. In these flowers sepals, petals and anthers were removed with a fine forceps, and only carpels remained intact. For the male parent, open flowers were removed and the convex surface of the anthers rubbed on the stigmatic surface of the exposed carpels of the female parent to make sure pollen grains were deposited on the stigma. In order to identify the seeds resulting from the cross, the flowers of the female parent that underwent cross pollination were labelled. We repeated this procedure for about 100 flowers. After 2-3 weeks, siliques derived from cross pollinated flowers were collected and allowed to dry at room temperature before collecting seeds. The seeds were germinated to generate plants of the F1 population, which were all heterozygous double mutants. F1 plants were grown to flowering, seeds resulting from self-cross collected and selected for Kanamycin and BASTA resistance. This procedure was repeated with plants of F2 population to allow the selection of a homozygous F3 population. The obtained F3 plants were again genotyped using gene specific and T-DNA primers as described above to check for the homozygosity of the F3 double mutant plants. The efficacy of the procedure was almost three double homozygous plants out of 100 crossed plants (3%). Plants of the SALK lines, SALK_009732 and SALK_045324 (KEA2), were crossed with plants of the SAIL lines SAIL_1156_H07 and SAIL_586_D02 (KEA1), to obtain two double mutant lines: SALK_045324 x SAIL_1156_H07, (hereafter called *kea1_2kea2_1* or dm1) and SALK_009732 x SAIL586_D2 (hereafter called *kea1_1kea2_2* or dm2). Preliminary studies were performed with a *kea1kea2* double mutant that we obtained as a kind gift from Drs. LR Roston and C Benning (Roston *et al.,* 2012), which is essentially the same as the *kea1_1kea2_2* mutant produced in this work by cross- pollination.

1.3.4. Seed germination and plant growth

Arabidopsis thaliana seeds were sown in seedbeds or pots containing vermiculite: peat-moss (1:1) and vernalized for 3 days in the dark at 4 ^{o}C. Then, they were transferred to a growth chamber where plants were cultivated at 22/20 ^{o}C, under an illumination of 120 µmol/ m^2/s and a photoperiod of 16 hours light and 8 hours darkness for 3-4 weeks. Alternatively, *Arabidopsis thaliana* seeds were germinated *in vitro* in petri dishes containing the basal salts of MS medium (Murashige and Skoog, 1962) diluted to ½ and solidified with 0.7 % agar. Seeds plated on petri dishes were vernalized and cultivated under the conditions described above. Before *in vitro* germination, seeds were disinfected in ethanol 70 % for 1 min followed by 50 % commercial bleach containing 2.5 % (v/v) of Tween 20 for 5 minutes and 3 washes with sterile distilled water.

To study the effects of NaCl and sucrose on plant growth, seeds were germinated *in vitro* in a medium containing a ½ dilution of MS basal salts supplemented with 0, 2 or 5 % of sucrose and 0 or 50 mM NaCl. For these experiments, petri dishes with a diameter of 15 cm were used.

The effect of 3 different light intensities, 70, 110 and 300 µmol/m^2/s, on plant growth was determined in *Arabidopsis thaliana* plants cultivated *in vitro* or in seedbeds under the conditions described above.

1.3.5. Generation of transgenic *Arabidopsis thaliana* plants

Arabidopsis thaliana was transformed by floral dipping (Clough and Bent, 1998). *Agrobacterium tumefaciens* strain GV3101 harbouring the construct for overexpression of AtKEA2 was grown under vigorous agitation at 28 ^{o}C in 200 ml YEP (Table 2.2) containing 25µg/ml kanamycin until an OD of 0.3-0.5 at 600 nm was reached. Cells were harvested by centrifugation at 5500 g at room temperature for 15 minutes and resuspended in infiltration medium (Table 2.2) to an OD at 600 nm of approximately 0.5. *Arabidopsis thaliana* plants at the initial stage of flowering were used for transformation. Before transformation, siliques and open flowers were removed from plants. Then, the inflorescences shoots were dipped into the bacterial suspension for 5 min. After dipping plants were returned to the growth chamber. The dipping procedure was repeated twice at intervals of 24 h. Thereafter plants were grown under the conditions previously described in chapter 2.3.4 for 3 to 4 weeks until flowering and

silique formation was completed. At this time, watering was stopped to allow the siliques to dry in order to facilitate harvesting of seeds, which were stored at 4 ^{o}C.

Seeds collected from primary transformants were surface sterilized as described previously (chapter 2.3.4) and germinated in petri dishes containing the selection medium composed of a ½ dilution of MS basal salts (Murashigue and Skoog, 1962) supplemented with the appropriate concentration of the selection marker. After incubation in darkness at 4 ^{o}C for 3 days, petri dishes were transferred to a growth chamber in which seedling were grown under the conditions described in chapter 2.3.4 until selection marker resistant seedlings had developed four true leaves. Seedling were then transferred to peat-moss: vermiculite (1:1) and allowed to grow until flowering and silique formation. Seeds were collected from mature dried siliques.

For overexpression and GFP localization studies we used vector pB7FWG2.0 (Plant Systems Biology, VIB, University of Gent: https://gateway.psb.ugent.be/search) (Figure 2.3). This vector facilitates the creation of an eGFP fusion protein under control of the 35S promoter, using the Gateway recombination technology. The vector confers Bar (BASTA) resistance to the transformed plants. In bacteria selection was performed with the antibiotic Spectinomycin.

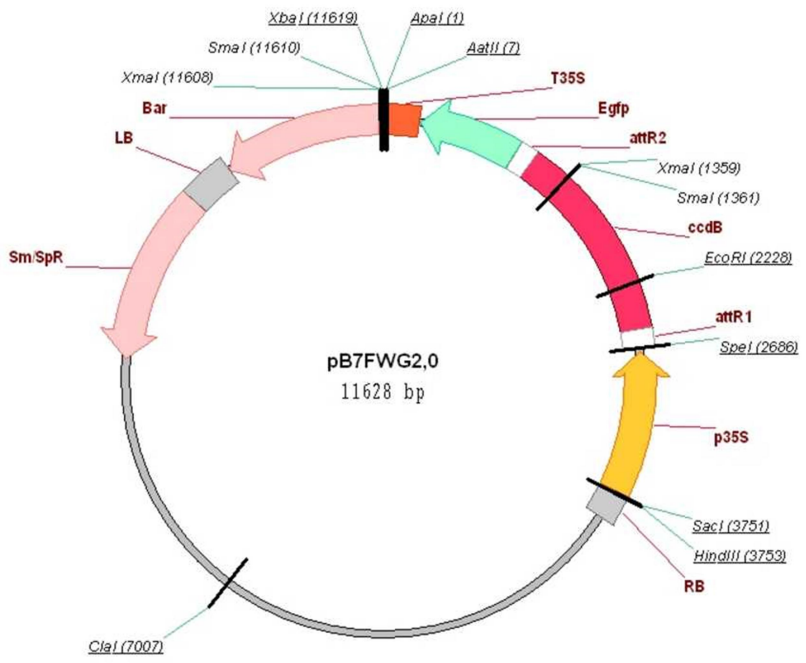

Fig.2.3. Plant Binary Vector pB7FWG2.0

2. Methods

2.1. General Molecular Biology Methods

2.1.1. PCR

The reagents used for PCR (Polymerase Chain Reaction), the concentrations of each reagent and the duration of the various stages of the reaction, depend on the purpose of amplification, the nature of the primers and the DNA polymerase used (Table 2.8).

Table 2.8. PCR mix

COMPONENT	CONCENTRATION
dNTPs	0,2 mM of each dNTP (dATP, dCTP, dGTP y dTTP)
Forward Primer	0,3 μM
Reverse Primer	0,3 μM
Buffer solution	1x
$MgCl_2$	3 mM
DNA polymerase	0,02 U/μl
DNA template	20 ng-200 ng

In general, the protocol followed in this work is summarized in Table 2.9.

Table 2.9. Conditions for PCR amplification

FASE	CYCLES	TEMPERATURE (^oC)	TIME (min)
INITIAL DENATURATION	1	94-98	3.00
AMPLIFICATION	20-25		
Denaturation	1	94-98	0.30
Hybridization	1	50-60	0.45
Elongation	1	72	1.30
FINAL ELONGATION	1	72	7.00
CONSERVATION	1	4	hold

The thermocycler used was a personal Mastercycler (Eppendorf). In this work we have used different polymerases: Phusion ™ High-Fidelity DNA Polymerase (New England Biolabs), Pfu DNA polymerase (Promega) and JumpStart ™ Accutaq ™ DNA polymerase mix (Sigma-Aldrich).

2.1.2. Separation of DNA fragments by agarose gel electrophoresis

Separation of DNA fragments was performed as described in Sambrook and Russell (2001). Horizontal agarose gels were prepared in 0.5x TBE solution (45 mM Tris, 1.25 mM Na-EDTA, 45 mM H_3BO_3, pH 8.2) containing gel red (0.4 μg/ml) to visualize the bands under UV light. 1x TAE buffer (40 mM Tris, 20 mM acetic acid, 1 mM Na-EDTA, pH 8.2) was used in cases where the extracted DNA fragments needed further processing (cloning, sequencing, etc), as borate may inhibit subsequent enzymatic reactions. The concentration of agarose used was 0.7 to 2 %, depending on the size of DNA to be separated. Samples were prepared in loading buffer (8.3 % sucrose, 0.04 % bromophenol blue and 0.017 M EDTA). The electrophoretic separation was performed in the same buffer used for preparation of gel, at a voltage between 80 and 100 V. The size of the fragments of interest was estimated by comparison with a commercial DNA molecular weight marker (1Kb DNA Ladder Molecular Weight Marker, Genecraft).

2.1.3. Extraction and purification of DNA from agarose gels

The recovery of DNA fragments from agarose gels was performed with a DNA Gel Extraction Kit (Millipore), which allows extracting the DNA from the gel by a process involving gel compression by centrifugation. For this, the band of agarose containing the DNA is deposited in a nebulizer device with a 0.45 μm filter (Durapore ®). Centrifugal force collapses the gel structure and drives the agarose through a small orifice in a gel nebulizer and the resultant gel slurry is sprayed into the sample filter cup. After centrifugation at 5000 g for 10 minutes; the DNA is collected in the filtrate. Alternatively, GenEluteTM Gel Extraction Kit (Sigma ®) was used. In this case, the bands of agarose containing DNA are solubilized and deposited on a filtration device fitted with a silica membrane that retains the DNA which is then eluted with TE buffer (10 mM Tris-HCl pH 8, 1 mM EDTA) according manufacturer's instructions.

2.1.4. DNA concentration by precipitation

For concentrating DNA by precipitation we used Pellet Paint co-precipitant (Novagen®). 2 µl of the product and 0.1 volume of 3 M sodium acetate were added to the mixture of nucleic acids. After mixing by gentle agitation, 2 volumes of ethanol (or 1 volume of isopropanol) were added and the whole was incubated for 2 minutes at room temperature and then was centrifuged at 15000 g for 5 minutes at room temperature. The obtained pellet was washed 2 times with 500 µl of 70 % ethanol, resuspended in the same volume by pipetting and centrifuged at 15000 g for 5 minutes. The resulting pellet was resuspended in 500 µl 100 % ethanol and centrifuged as above. The pellet of this centrifugation was dried at 37 ^{o}C for 5 min and resuspended in 10 µl of distilled H_2O or TE buffer.

2.1.5. Quantification of DNA or RNA

The DNA or RNA concentration was estimated spectrophotometrically using a NanoDrop ® ND-1000 Spectrophotometer or by visual comparison with a known amount of phage λ digested with EcoRI-HindIII (Molecular Weight Marker III, Roche Diagnostic) in a ultraviolet image analyzer (BioRad).

2.1.6. Plasmid Isolation

The Mini-Prep method adapted from Del Sal et al. (1988) was used. A fresh *E.coli* colony was inoculated in 2 ml of LB supplemented with the required antibiotics and incubated overnight at 37 °C. The bacterial culture was centrifuged and the pellet was resuspended in 200 µl of STET (10 % sucrose, 50 mM Tris-HCl pH 8, 50 mM EDTA pH 8, 1 % Triton X-100), and 5 µl of a solution of 5 % lysozyme. The mixture was vortexed vigorously and incubated 2 minutes 96 °C, cooled on ice for 2 minutes and centrifuged in a microcentrifuge at maximum speed for 10 minutes. The mucous sediment was discarded. To eliminate RNA contamination the supernatant was incubated 10 minutes at 68 °C after addition of 2 µl of 1% RNAse. To precipitate the plasmid DNA, 10 µl of a solution composed of 5% CTAB (hexadecyltrimethylammonium bromide) and 0.5 M NaCl was added. The solution was stirred and centrifuged at maximum speed for 15 minutes. The resulting pellet was

resuspended in 300 µl of 1.25 M NaCl and the DNA was precipitated again by adding 750 µl of 96 % ethanol. After centrifugation in a microcentrifuge at 14000 rpm for 15 minutes, the obtained precipitate was washed with 700 µl of 70 % ethanol and dried at 37 ^{o}C for 10 minutes. The DNA was resuspended in 20 µl of TE or distilled H_2O.

2.1.7. DNA digestion with restriction enzymes

DNA digestion with restriction enzymes was performed in the buffers and under the conditions recommended by the manufacturers. When it was necessary to digest with more than one enzyme and when the buffers were not compatible, the enzyme was inactivated by heating at 65 to 80 ^{o}C after digesting with the first enzyme. Thereafter the DNA was precipitated as specified in section 2.1.4., and subsequently treated with the second enzyme.

2.1.8. Cloning of DNA fragments

In most cases, DNA fragments were cloned using the Gateway technology, which allows introducing the gene of interest in a simple way in different functional analysis systems, maintaining orientation and reading frame with a high efficiency and eliminating the need for secondary sequencing or subcloning after inserting the gene into an input vector. This technology is based on the properties of integration and excision of bacteriophage lambda in the *E. coli* genome by recombination. In the gateway system, the integration and cleavage reactions are carried out *in vitro* as shown in Figure 2.4.

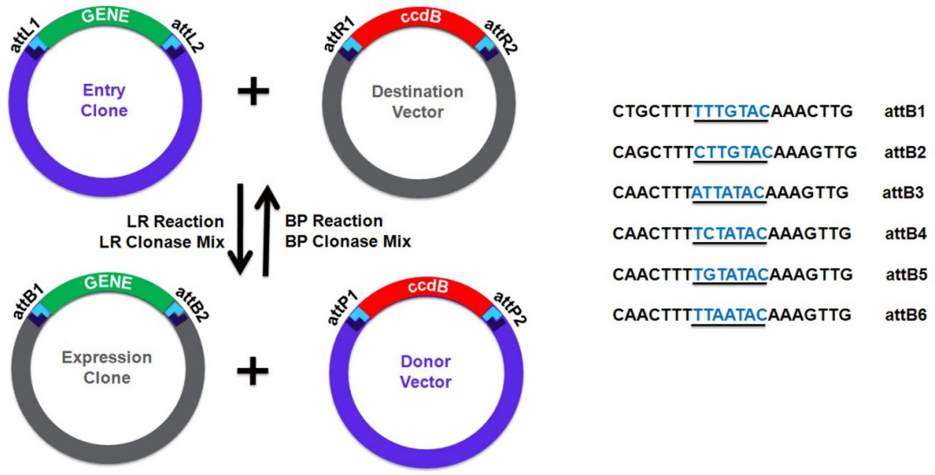

Fig. 2.4. Gateway technology used for cloning DNA fragments. The cloned gene is transferred into an input vector, flanked by two recombination sites, attL1 and attL2. The target vector contains all the necessary elements for expression of the gene of interest and two recombination sites attR1 and attR2 flanking the ccdB gene for negative selection, taken from **www.invitrogen.com.**

The attL x attR reaction is catalysed by the LR Gateway® ClonaseTM II enzyme mixture. The mixture contains, on one hand, the enzymes involved in recombination of bacteriophage lambda, Integrase (Int) and the Escisionase (Xis), and on the other hand, the factor of integration into the host (IHF) of *E. coli*. To generate the input vectors we used pENTR/D-TOPO and pENTR/SD/D-TOPO (Invitrogen), that are designed to permit the directional cloning of a PCR product between the recombination sites attL1 and attL2 (Figure 2.5). Both linearized vectors are covalently associated to vaccinia virus topoisomerase I, and the sequence GTGG has been added to the 5' end (Figure 2.5). This edge allows oriented cloning form of a PCR product generated using a forward primer to which the sequence CACC has been added. The GTGG sequence of the linearized vector anneals to the complementary CACC sequence of the PCR product, allowing oriented ligation by topoisomerase I.

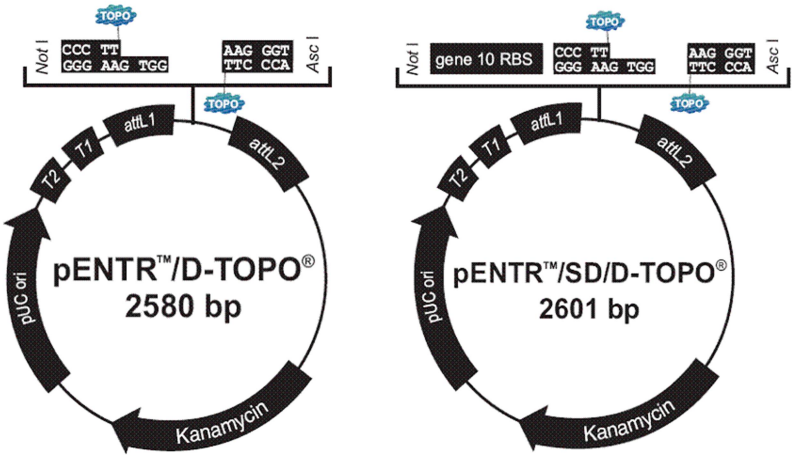

Fig. 2.5. Map of pENTR/D-TOPO and pENTR/SD/D-TOPO
Cloning was performed following the instructions of the pENTR/SD/D-TOPO Cloning Kit. Competent E coli Mach1TM cells were transformed as described and transformants selected on LB medium supplemented with 50 µg/ml kanamycin.

2.1.9. Genomic DNA extraction

Genomic DNA was isolated following a procedure adapted from Doyle et al. (1990). Approximately 500 mg of plant tissue was grinded with liquid nitrogen using a mortar and pestle until obtaining a fine powder, which was transferred into a sterile Eppendorf tube. Then 2 ml 2xCTAB buffer (Table 2.10) per gram of tissue was added to the grinded tissue. The extract was incubated for one hour at 65 °C, spun down in a microcentrifuge at 13000 rpm for 1 minute and the supernatant transferred to a new tube. The supernatant was then mixed with one volume of chloroform and the mix spun down at 3500 rpm for 5 minutes at 4 °C. The upper aqueous layer was transferred to a new tube to which 2/3 volumes of isopropanol was added to precipitate the DNA. Samples were incubated at -20 °C for at least 1 hour and up to overnight. After spinning down at maximum speed, the supernatant was removed and the pellet washed with 500 µl of 80 % ethanol and centrifuged as above. The obtained pellet was dried by leaving the tubes open at 37 ^{o}C for 10 minutes. The dried pellet was resuspended in 50-100 µl of 1xTE buffer (10 mM Tris-HCl pH 8, 1 mM EDTA) and stored as aliquots at either -80 or -20 °C.

Table 2.10. Composition of 2x CTAB extraction buffer

100 mM Tris-HCl, pH 8
1.4 M NaCl
20 mM EDTA
2 % CTAB (Cetyl Trimethyl Ammonium Bromide)
1 % polyvinylpyrolidone (40,000 MW)
0.2 % 2-mercaptoethanol

2.1.10. RNA extraction

To extract RNA from different tissues of the plant Trizol® were used, following the manufacturer's instructions. During RNA isolation, samples were treated with DNAse (RNase-Free DNase Set, Qiagen) following the manufacturer's instructions to eliminate any remaining DNA that could interfere in the RT-PCR reaction. Alternatively, RNA samples of the plants were extracted with Tri-ReagentTM (Sigma-Aldrich) following the manufacturer's instructions. In both cases, the RNA was resuspended in RNA secure ™ resuspension solution (Ambion), following the manufacturer's instructions, aliquoted and stored at -80oC.

2.1.11. Gene expression analysis by qRT-PCR

Absence of expression of AtKEA1 and AtKEA2 was also checked in the double mutant lines by real time quantitative PCR, using iQ™ SYBR® Green Supermix as fluorescent probe. In real time qPCR the accumulation of the PCR product is directly determined in the PCR tube during the cycling by measuring the increase in fluorescence due to binding of the dye to double stranded DNA. To correct for differences in cDNA input, results were normalized using Actin as a control gene. To prevent potential amplification of any contaminating genomic DNA, the samples were treated with DNAse as described above. The amplification of genomic DNA was further precluded by design of primers that span across splice junctions. RNA was first transcribed into cDNA in a reaction using reverse transcriptase as following: RNA of root, stem, leaf and flower were extracted, as described in paragraph 2.1.10. An aliquot of the resulting

cDNA was then used as a template source for multiple qPCR reactions. For experiments of reverse transcription we started from 1 μg of RNA and we used iScript™ Reverse Transcription Reagent (Bio-Rad) that synthesizes one strand of cDNA from total RNA extracted using random nonamers (primers binding randomly to RNA) and the enzyme reverse transcriptase (MMLV-RT). Prior to the reverse transcription reaction 1 μg of total RNA was incubated with 0.5 mM of each dNTPs (dATP, dCTP, dTTP and dGTP) and 3.5 μM of primers random nonamers for 10 min at 77 ^{o}C. After a brief cooling in ice, the buffer of (MMLV-RT) enzyme, (50 mM Tris-HCl pH 8.3, 40 mM KCl, 8 mM MgCl2, 1 mM DTT), 0.25 U/μl RNAse inhibitor and 0.5 U/μl (MMLV-RT), was added in a total volume of 20 μl. The reaction was carried out for 50 min at 42 ^{o}C. The expression of the two target genes, *AtKEA1* and *AtKEA2* and the reference gene, actin was assayed in three samples (two different double mutants and one wild type).Then the presence of *AtKEA1* and *AtKEA2* and the reference gene in different cDNA preparations was determined by PCR analysis using the primers listed in Table 2.11.

Table 2.11. Primers used in RT-PCR experiments

CTATTCTAGTCGACCTGCAG	35S Forward	AtKEA2-GFP expression
CTCAAGTAGTTTCTTTATTCTC	AtKEA2 1665* Reverse	
ATGTTCCCTCAGCAAGAGGT	AtKEA2 1666 Forward	AtKEA2 Expression
GTAACACGACCACAGCCA	AtKEA2 2212 Reverse	
ATGATCCCTCACCAGGAGGTC	AtKEA1 2818 Forward	AtKEA1 Expression
AATCAGTAAAACAACTACAGC	AtKEA1 3330 Reverse	
ATCTCCTGCTCGTAGTCAAC	Actin2 Reverse	Actin2 Expression
CGGTATTGTGCTGGATTCTG	Actin2 Forward	

* Annealing position in the full length cDNA calculated from the start ATG

The expression levels of *AtKEA1and AtKEA 2*, genes were quantified by real time PCR, using a Biorad iCycler thermal cycler. In real time PCR the processes of amplification and detection occur simultaneously in the same vial without post processing of the amplified products, which increases performance and reduces the chances of contamination (Bustin and Nolan 2004). Analysis by real-time PCR is based on the detection and quantification of DNA using a fluorescent probe. By measuring fluorescence during amplification, the amount of DNA synthesized at all times can be determined as the fluorescence emission produced in the reaction is proportional to the amount of DNA formed (Costa 2004). In this study the fluorescent probe used was the

intercalating agent SYBR Green I (FAM fluorophore-490), whose fluorescence emission increases significantly when bound to double-stranded DNA. Amplification was performed using Quantimix Syg Easy Kit (Biotools). The reactions were performed in a final volume of 20 µl containing 10 µl of the mixture of Quantimix Syg Easy Kit, 0.375 µM of each primer (Table 2.12), 2 µl of a dilution of 1/5000 fluorescein in dimethyl sulfoxide (DMSO), 1 µl of cDNA and 5.5 µl of Milli-Q water. The amplification protocol used was: Cycle 1 (1X), 95 °C, 3 min; Cycle 2 (35X), denaturation at 95 ° C, 30 seconds, annealing at 55 °C, 45 seconds extension at 72 ° C, 1 minute; Cycle 3 (1X), 95 ° C, 1 minute; Cycle 4 (1X), 70 °C, 1 minute; Cycle 5 (60X), 70 °C, 10 seconds. After completion of cycle 2, the necessary data to perform the quantification were obtained. Cycles 3, 4 and 5 allowed obtaining the Melting curve. Relative gene expression was calculated using the following formula: $2^{[\Delta Ct\ (Control)-\Delta Ct(sample)]}$, where $\Delta Ct = Ct_{ribosomal\ 18S} - Ct_{gene}$ and Ct (Cycle threshold) is the cycle where the sample fluorescence exceeds the chosen threshold, i.e., the cycle in which the system begins to detect the signal increase associated with exponential growth of the PCR product during the log linear phase. All reactions were performed in triplicate for each test and PCR melting curves of the amplification products were obtained in order to identify possible unspecific amplifications.

Table 2.12. Primers used in real time qPCR experiments.

CAATCATATCTGCCGTGAGG	KEA2 2676* Forward
AAATCATCCGTCTCGCTTTC	KEA2 2903 Reverse
GGTGGCCAGTTAATTGCATC	KEA1 2901 Forward
CTCTTTACTACCAGCGTCTC	KEA1 3148 Reverse
ATCTCCTGCTCGTAGTCAAC	Actin2 Reverse
CGGTATTGTGCTGGATTCTG	Actin2 Forward

*annealing position in the full length cDNA calculated from the start ATG

2.1.12. Yeast in vivo cloning

As several of the constructs used in this study were toxic when expressed in bacteria, we cloned these fragments or genes in yeast by *in vivo* recombination according to Fusco *et al.,* (1999). To this end the fragment to be cloned was amplified by PCR using a high fidelity DNA polymerase. To facilitate homologous recombination of the

fragment into the yeast vector, the primers used to amplify the fragment contained 20-30 bp overhangs with sequence homology to the sites in the vector where the fragment was to be inserted (Figure 2.6). Next, the vector was cut by one or two restriction enzymes between the recombination sites. For linearization of the vector we used minimally 500 ng vector in 10 µl volume and 0.5 µl (5 Units) of restriction enzyme. The enzymes were inactivated by heating for 15 minutes at 65 °C. 200 to 250 ng of linearized vector was mixed with 5 µl of the PCR reaction mixture (Table 2.13) and used to transform yeast according to the yeast transformation protocol described (Table 2.5). The transformation mix was spread on selective medium SC-URA (Table 2.4) and incubated for 2 to 3 days at 28 °C. Presence of the recombined vector harboring the insert was tested by colony PCR. The plasmid was extracted from some positive colonies to test the correctness of the constructs by sequencing.

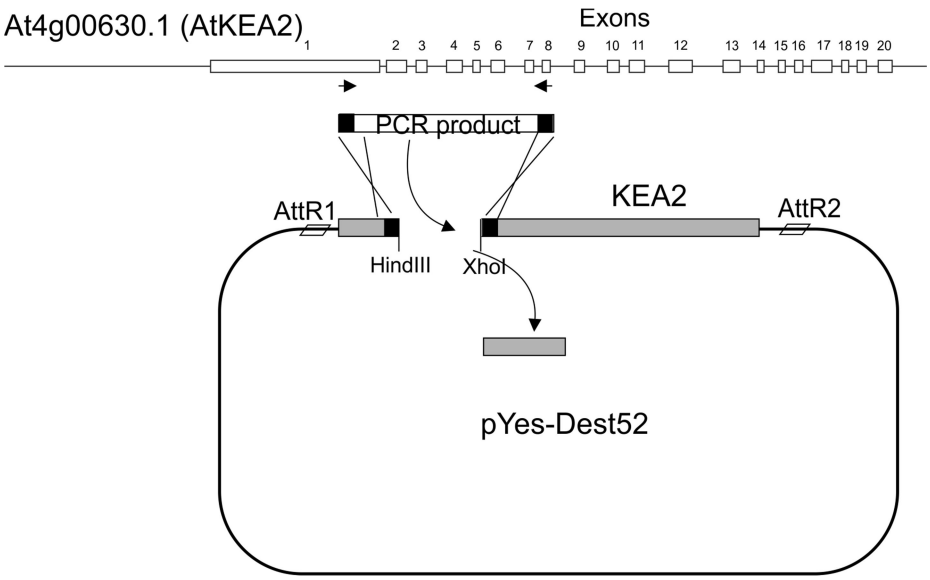

Fig. 2.6. Insertion of part of the AtKEA2 genomic sequence into the AtKEA2 cDNA. The start of the *AtKEA2* gene including 7 introns was amplified by PCR from the genomic sequence, and inserted by *in vivo* recombination into vector pYES-DEST52 harbouring the *AtKEA2* cDNA. Arrows indicate the used primers. Black boxes represent homologous regions in PCR product and KEA2 that facilitate the recombination resulting insertion of the PCR product into the vector.

Table 2.13. PCR reaction components used for yeast *in vivo* cloning

COMPONENT	Concentration
dNTPs	0.2 mM of each dNTP (dATP, dCTP, dGTP y dTTP)
Forward Primer	0.5 µM
Reverse Primer	0.5 µM
Buffer solution	1x
DNA polymerase[1]	0.02 U/µl
DNA template	20 ng

[1] *Phusion™ High-Fidelity DNA Polymerase* (New England Biolabs); Total Volume: 25µl/reaction (complete with MilliQ® water)

2.2. Gene Constructs made in this study

2.2.1. Cloning of full length AtKEA2intron1-4

In order to study the localization and function of AtKEA2 in plants, we made an AtKEA2-GFP fusion protein. The full length cDNA of AtKEA2 was previously cloned in yeast expression vector pYes-Dest52 by *in vivo* recombination in yeast (Aranda-Sicilia *et al.,* 2012). Due to toxicity of the DNA sequence, we could however not transfer this construct to bacterial cloning vectors. To circumvent the problem of toxicity of the full length *AtKEA2* gene in bacteria, the first 4 introns of the genomic sequence of AtKEA2 were inserted into the full length cDNA by homologous recombination in yeast. To this end the first part of the gene encoding the N-terminus, was amplified by PCR from genomic DNA, using primers that annealed to position 1492 and 2212 bp of the full length cDNA (Table 2.14). These primers amplify a 1545 bp fragment from the genomic AtKEA2 sequence, including the first 7 exons and the first 22 bp of the exon 8 (i.e. spanning 7 introns). The pYes-*AtKEA2* vector was linearized by cutting with HindIII and XhoI, that both cut the AtKEA2 cDNA between positions 1492 and 2212 (Figure 2.6). The PCR product and the linearized pYES-*AtKEA2* vector were used to transform the yeast strain BYa by standard LiAc transformation (Gietz *et al.,* 1995). The correct insertion of the PCR product in pYES-*AtKEA2* was checked by PCR. Plasmids from independent positive colonies were

extracted and sequenced as described by Singh and Weil (2002). Final sequencing of the resulting plasmid showed that we had successfully inserted only the first 4 introns, most likely because the vector was not completely digested with XhoI. Next, the *AtKEA2*$_{intron1\text{-}4}$ sequence was introduced by BP recombination of the pYES-*AtKEA2*$_{intron1\text{-}4}$ with Gateway vector pDONR221, facilitating subsequent generation of plant overexpression vectors. The *AtKEA2*$_{intron1\text{-}4}$ was transferred by LR recombination from pDONR221 to plant binary vector pB7FWG2 fused to the eGFP coding sequence for subcellular localization (Karimi *et al.,* 2002).

Table 2.14. PCR primers used for cloning

AtKEA2$_{intron1\text{-}4}$	
For: TTTACACTTCTTGGGGCAGG	Annealing at position 1492 in cDNA
Rev: GTAACACGACCACAGCCA	Annealing at position 2212 in cDNA
cTP-sAtKEA2	
For: TCAAACAAGTTTGTACAAAAAAGCAGGCTCCGCGGCCGCCCCCTTCACCATGGATTTT GCGTCTAGCGTTC	
Rev: GGGAAGCTTCCTCCTCATTAACCTCTTGCTGAGGGAACATTCGTTTCGATCTAATAGCTG	
N-Terminus AtKEA2	
For: AGCTATCAAACAAGTTTGTACAAAAAAGCAGGCTCCGCGGCCGCCCCCTTCATGAG ATCGAAACGAAATGTATCG	
Rev: CTTTGTACAAGAAAGCTGGGTCGGCGCGCCCACCCTTCTCAAGTAGTTTCTTTATTCTC	
N-Terminus Deletion Δ1	
For: As for N-terminus	
Rev: CTTTGTACAAGAAAGCTGGGTCGGCGCGCCCACCCTTTAAACTCTCAAAAACTGTTGCG	
N-Terminus Deletion Δ2	
For: As for N-terminus	
Rev: CTTTGTACAAGAAAGCTGGGTCGGCGCGCCCACCCTTACTCTCTTCAGAAGTATTGTACCC	
N-Terminus Deletion Δ3	
For: As for N-terminus	
Rev: CTTTGTACAAGAAAGCTGGGTCGGCGCGCCCACCCTTATTTGCAACATCCTCCTCGGC	
Short AtKEA1 (TOPO)	
For: CACCATGATCCCTCACCAGGAGGTC	
Rev: GATTACGACTGTGCCTCCTTCG	(-Stop)
Rev: TCAGATTACGACTGTGCCTCCT	(+Stop)
N-Terminus AtKEA1	
For: TTGTACAAAAAAGCAGGCTCCGCGGCCGCCATGGAGTATGCGTCTACTTT	
Rev: GATGTTGAAAAGCAACAAAAC	

Wild-type Arabidopsis thaliana plants (ecotype Col-0) were transformed with the AtKEA2intron1-4-eGFP construct by the floral dip procedure (Clough and Bent, 1998). Seeds were obtained from the primary transformants and screened by in vitro

germination on a ½ dilution of MS basal salts supplemented with 15 mg/l BASTA. Fluorescence was observed in T1 and T2 progeny. Both double mutant kea1kea2 lines were also transformed with the AtKEA2intron1-4-eGFP construct. Transformed plants were selected based on recovery of the wild-type phenotype. Transgene presence in the selected lines was verified by PCR analysis using a 35S forward primer and a gene specific reverse primer.

2.2.2. Cloning of short AtKEA2 without N-terminal domain fused to the chloroplast transit peptide

DNA encoding the chloroplast transit peptide (cTP) sequence (Residues M1-R60) was amplified from the plasmid with the complete *AtKEA2* sequence using primers listed in Table 2.14. The PCR product and the plasmid containing the short pYes-*AtKEA2* sequence (Residues M556-I1174) (Aranda-Sicilia *et al.,* 2012) linearized by NotI were used to create the cTP-*sAtKEA2* in pYes-Dest52 by *in vivo* recombination as described above. The cTP-*sKEA2* sequence was transferred to plant binary vector pB7FWG2 and used for stable transformation of wild-type *Arabidopsis thaliana* plants as described above for the full-length sequence.

2.2.3. Cloning of full length AtKEA1

To clone the full-length *AtKEA1* sequence we used a similar strategy to that used before to clone full length *AtKEA2* (Aranda-Sicilia *et al.,* 2012). The *AtKEA1* gene was originally annotated to correspond to locus At4g00630 (old gene accession: AAC13638.1). We obtained cDNA for this short version (*AtsKEA1*, without the N-terminal domain) from the laboratory of Dr. J.M. Ward (Univ. Minnesota, USA). The cDNA was sequenced and transferred by PCR and TOPO cloning to the pENTRSD/D-TOPO vector (Invitrogen), using primers indicated in the Table 2.14. The cDNA was transferred by LR recombination to vector pYES-DEST52 (Invitrogen). The full-length *AtKEA1* gene was obtained using homologous recombination in yeast as described by Fusco et al. (1999). The missing part of the gene was amplified by PCR from *Arabidopsis thaliana* cDNA using primers indicated Table 2.14. The PCR product and the pYES-*AtsKEA1* linearized by NotI and HindIII were used to transform the yeast strain BYa by standard LiAc transformation (Gietz *et al.,* 1995). Yeast was grown for 2-3 days on SC medium (Table 2.4) without uracil. The correct insertion of the PCR product was first checked by PCR on colonies using the above primers. Plasmids from

independent positive colonies were extracted and sequenced as described by Singh and Weil (2002).

2.2.4. Construction of deletion mutants of the AtKEA2 N-terminal domain

The N-terminal domain of AtKEA2, without the chloroplast transit peptide sequence, and 3 deletion constructs were amplified from a vector containing the complete *AtKEA2* cDNA sequence (Aranda-Sicilia *et al.,* 2012), using primers listed in Table 2.14, and inserted by *in vivo* recombination into pYes-Dest52 (Invitrogen) linearized with EcoRI and XbaI. The cloned constructs correspond to amino acids R57-E555 (complete N-terminus), R57-L483 (Δ1), R57- N316 (Δ2) and R57- S245 (Δ3).

2.3. Biochemical and Cell Biological Methods

2.3.1. Isolation and fractionation of yeast microsomal membranes

Yeast cells of strain BYa harboring plasmids for expression of the N-terminal domain fragments were grown overnight to saturation in 2 % glucose, 0.7 % yeast nitrogen base (without amino acids; Difco) with yeast synthetic drop out medium supplement without Uracil (Sigma). Cells were pelleted by centrifugation for 5 minutes at 3000 g and resuspended in the same medium, but replacing glucose by galactose to induce expression of the proteins, to an OD_{660} of 0.4, and grown for 4 hours. Cells were harvested by centrifugation for 5 minutes at 3000 g and washed with cold distilled H_2O. The cells were resuspended in 0.2 M Tris-HCl pH 8; 150 mM KCl; 15 mM EDTA-Na pH 8; 10 mM DTT and 1:100 dilution of protease inhibitor cocktail (SIGMA). Cells were broken in a bead-beater (Biospec) by vigorously vortexing with glass beads of 425-600 mm diameter (SIGMA) by 3 pulses of 15 seconds, with 30 seconds of cooling on ice in between. After removal of cell debris and glass beads by centrifugation at 3000 g for 15 minutes, the supernatant was centrifuged at 100.000 g for 1 hour. The obtained microsomal membrane pellet was resuspended in 10 mM Tris-HCl pH 7.5; 1 mM DTT; 1 mM EDTA; 20 % glycerol and 1:1000 dilution of protease inhibitor cocktail, and stored at -80 °C together with the supernatant as soluble protein fraction. Routinely, starting from a 1 liter yeast culture, cells were broken in a total volume of 50 ml with 25 ml of glass beads, and the final pellet resuspended in 500 µl of GTED20 (20 % glycerol, 100 mM Tris-HCl pH 7.5, 1 mM EDTA and 1 mM DTT).

Yeast microsomal membranes were further fractionated by centrifugation in a linear sucrose gradient. All steps were performed at 4°C. First a step-gradient was prepared by layering on top of each other 7 ml each of 60, 46, 33 and 20 % (w/w) sucrose in 10 mM Tris-HCl, pH 7.5, 1 mM EDTA, 1 mM DTT and 30 µl protease inhibitor cocktail (SIGMA) in 30 ml centrifuge tubes. Next the tubes were sealed with parafilm and slowly tilted 90 degrees (total tilt in about 1 minute), and left in a horizontal position. After 3 hours the tubes were slowly tilted back to an upright position. Next the microsomal membrane pellet (1 ml) was layered on top of the sucrose gradient and centrifuged 18 hours at 100000 *g* in a Beckman SW28 swinging bucket rotor. Two ml fractions were collected by carefully pipetting, holding the pipette to the gradient surface. Sucrose density of the fractions was measured in a refractometer and protein content determined. For western blotting 500 µl of the fractions were used after precipitation.

2.3.2. Isolation of Arabidopsis thaliana total protein

Arabidopsis thaliana total protein was isolated as described in Roux *et al*. (2011). Leaves of Arabidopsis thaliana were frozen at -20 °C and grinded in mortar and pestle until a fine powder was obtained. Extraction buffer composed of 50 mM Tris-HCl pH 7.5, 150 mM NaCl, 5 % glycerol, 1 mM EDTA, 5 mM DTT (dithiotrheitol), 0.5 % (w/v) PVPP, 1 % (v/v) Protease inhibitor cocktail (Sigma), 1 mM PMSF (pehenylmethylsulfonyl fluoride), 0.5 % (v/v) NP-40 (Nonidet P-40) was added at a ratio of 2 ml buffer per g tissue and the suspension was transferred to a centrifuge tube. The tube was shaken at 4 °C for 30 minutes. The extract was passed through 6 layers of gauze and centrifuged at 12000 g and 4 °C for 20 min. The supernatant was aliquoted in 2 ml Eppendorf tubes (1.5 ml/tube).

2.3.3. Purification of GFP tagged proteins from Arabidopsis thaliana for co-immune precipitation

Magnetic GFP-Trap®_MA beads (Chromotek) were vortexed and 25 µl bead slurry was added to 500 µl ice-cold lysis buffer (10 mM Tris-HCl pH 7.5, 150 mM NaCl, 0.5 mM EDTA and 0.5 % NP-40). Beads were separated magnetically and the supernatant discarded. This step was repeated twice. 500 µl of *Arabidopsis thaliana* total protein extract was added and the mixture was incubated for 1 hour at 4 °C on a roller mixer. The beads were separated magnetically and resuspended in 500 µl dilution buffer (lysis

buffer without NP-40). This wash step was repeated twice. Next, the beads were resuspended in 20 µl of 2x Laemmli buffer (120 mM TrisHCl pH 6.8, 20 % glycerol, 4 % SDS, 0.04 % bromophenol blue, 10 % β-mercaptoethanol) and incubated 10 min at 95 ^{o}C. The beads were separated magnetically, and the supernatant used for SDS gel electrophoresis.

2.3.4. Chloroplast isolation

Chloroplasts were isolated from leaf protoplasts. Protoplasts were first isolated using the tape *Arabidopsis thaliana* sandwich method (Wu, 2009). The upper side of 7 to 10 leaves (1 to 2 grams) of 3 to 5 week old plants were attached to time tape (coloured tape). The lower side of the leaves was attached to magic tape (transparent tape). Next, the magic tape was slowly removed, peeling of the lower epidermis of the leaves. The leaves were floated (time tape up) in 10 ml of enzyme solution (0.25 % (w/v) Macerozyme R-10, 1 % (w/v) Cellulase Onozuka R-10, 400 mM KCl, 20 mM Mes-KOH, pH 5.7, 10 mM $CaCl_2$, 10 mM β-mercapthoethanol and 0.5 M manitol) in a petri dish with agitation (40 rpm) for 30 to 90 minutes. The solution was chilled on ice and transferred carefully to a round bottomed centrifuge tube and centrifuged for 4 minutes at 100 g. Subsequent steps were carried out at 4 ^{o}C. The protoplasts were washed once with 5 ml solution W5 (125 mM $CaCl_2$, 5 mM glucose, 5 mM KCl, 154 mM NaCl, 2 mM Mes-KOH and 0.5M manitol) and centrifuged for 4 minutes at 100 g. Finally protoplasts were resuspended in protoplast resuspension solution (PRS, 0.3M sorbitol, 20 mM Tricine pH 8.4, 5 mM EGTA, 5 mM Na_2EDTA, pH 8, 10 mM $NaHCO_3$, 0.1 % BSA) at 80 to 100 µg chlorophyll/ml. The suspension was transferred to a 5 ml syringe from which the end had been removed and replaced with a 20 µm nylon mesh filter. The suspension was gently pushed through the filter breaking the protoplasts and releasing chloroplasts. The chloroplasts were collected by centrifugation for 1 minute at 270 g, and resuspended at 250 to 400 mg chlorophyll/ml in cold chloroplast resuspension solution (CRS, 0.3 M sorbitol, 20 mM HEPES pH 7.6, 5 mM $MgCl_2$, 2.5 mM Na_2EDTA pH 8, 10 mM $NaHCO_3$, 0.1 % BSA), and stored on ice until use.

2.3.5. Determination of chlorophyll concentration

10 µl of chloroplast or protoplast suspension was diluted in 990 µl of 80 % acetone, and centrifuged at 3000 g for 2 minutes. The absorbance at 652 nm of the supernatant was

determined, and the chlorophyll concentration calculated from: [Chl] = (A_{652} X 100)/36 mg/ml

2.3.6. Preparation of thylakoid, envelope and stromal protein fractions

We used a simple method to separate thylakoid, envelope and stromal proteins by differential centrifugation. Protoplasts were diluted to 100 mg/ml chlorophyll in PRS and broken as described above. Chloroplasts were spun down and resuspended in 100 µl CRS. The chloroplasts were diluted with 1 ml of 10 mM MOPS-NaOH pH 7.8, 4 mM $MgCl_2$ and 10 µl Protease Inhibitor Cocktail (SIGMA). To break the chloroplasts, the suspension was frozen at -80 ^{o}C for 15 minutes, and allowed to thaw on ice. This procedure was repeated twice. The chloroplasts were centrifuged at 4 ^{o}C and 12000 g for 5 min. The pellet, containing thylakoids was resuspended in 1 ml GTED20, supplemented with 5 µl Protease Inhibitor Cocktail (SIGMA). The supernatant was centrifuged for 15 minutes at 100.000 g to separate the envelope and stromal fraction. The pellet containing envelope membranes was resuspended in 500 µl GTED20 supplemented with 2.5 µl protease inhibitor cocktail. The 12000 g pellet (thylakoids); 100.000 g pellet (envelopes) and 100.000 g supernatant (stromal proteins) were frozen at -80 ^{o}C until further use.

2.3.7. Extraction of membrane proteins from yeast microsomal membranes

Yeast microsomal membrane fractions (200 µg protein) were incubated at 4 $^{\circ}$C under gentle stirring for 60 minutes in the presence of one of the following membrane protein extracting reagents: 0.6 M KI, 0 1 M Na_2CO_3 pH 11.5, 2.5 M urea or 1 % Triton X-100. Extraction was made in a final volume of 450 µl of a buffer containing 20 % glycerol, 10 mM Tris-HCl, pH 7.5, 1 mM EDTA, 1 mM DTT and a 1/50 dilution of protease inhibitor cocktail (Sigma). Subsequently, the membrane fractions were centrifuged for 30 minutes at 100.000 g. The pellets were resuspended in the same buffer as above (without addition of chaotropic agents or detergent), and the supernatant saved. Both resuspended pellet and supernatant were centrifuged again to avoid cross contaminations and final pellets and supernatants were saved at -80 ^{o}C until further use.

2.3.8. Gel electrophoresis and immunoblotting

SDS gel electrophoresis and electrotransfer were performed using a Bio-Rad Mini-Protean-3 and Mini trans-blot. 5 to 25 µg of protein resuspended in GTED20 with a

1:1000 dilution of Protease Inhibitor Cocktail (SIGMA) was precipitated by addition of an equal volume of ice cold 22 % TCA and incubation at 0 ^{o}C for 20 minutes. Precipitated protein was pelleted by centrifugation for 15 minutes at top speed in an Eppendorf centrifuge. The supernatant was removed, and the pellets centrifuged again for 5 minutes to remove residual supernatants. The pellet was washed with 500 µl of ice-cold water, and resuspended in 10 µl GTED20 and 10 µl 2x Laemmli buffer. The mix was shaken for 30 minutes at room temperature. Proteins were separated by SDS-PAGE on 7.5 % or 10 % acrylamide gels using the Laemmli buffer system (Laemmli, 1970). Proteins were electrotransferred to a PVDF (polyvinylidene difluoride) membrane (Pall Gelman) at 100 V during 90 minutes at 0 ^{o}C, using 25 mM Tris, 192 mM Glycine and 20% (v/v) methanol as transfer buffer. After transfer the membranes were incubated for 1 hour in blocking buffer (20 mM Tris-HCl pH 8.0, 0.01 % Tween 20, 150 mM NaCl and 2.5 % milk powder). Next, the membranes were incubated overnight at 4 ^{o}C in 5 ml blocking buffer with a 1:2500 dilution of monoclonal antibodies raised against the V5 epitope (AbCam SV5-Pk1), Pma1p (Invitrogen/Molecular probes), GFP (Roche) or polyclonal antibodies to FtsZ1,2 (Rabbit anti FtsZ1 and 2, Agrisera). Next day the blot was washed 3 times (5 minutes each time) at room temperature with 5 ml blocking buffer, and incubated for 1.5 hour in 5 ml blocking buffer lacking milk powder with a 1:10000 dilution of anti-mouse or anti-rabbit IgG-alkaline phosphatase conjugate. Afterwards, the membranes were washed again 5 times during 5 minutes with 5 ml blocking buffer without milk powder. Finally the membranes were incubated at room temperature in 10 ml of 0.1 M Tris-HCl pH 9.5, 0.1M NaCl, 5 mM $MgCl_2$, 0,033 % NBT (Nitroblue Tetrazolium) and 0,0165 % BCIP (5-Bromo-4-chloro-3-indolyl phosphate) to reveal the protein-antibody interactions.

2.3.9. Protein determination

Protein content was determined by the method of Bradford (Bradford, 1976) with the Bio-Rad protein assay reagent and bovine serum albumin as standard.

2.3.10. Chlorophyll determination

Chlorophyll was extracted using the published online protocol by Poorter *et al* (http://www.publish.csiro.au/prometheuswiki/tiki-pagehistory.php?page=Chlorophyll extraction and determination&preview=11). Mortars and pestles were cooled at -20 ^{o}C for at least 30 minutes before extraction. The extraction was carried out in the dark at 4

^{o}C. A few young leaves (about 150 mg) were cut and ground with liquid nitrogen with the precooled mortar and pestle. 1 to 2 ml 80 % ice-cold acetone was added and the mixture was ground until homogeneity. The solution was transferred to precooled centrifuge tubes and centrifuged 5 min at 3000 g. The supernatant was transferred to a 50 ml falcon tube, and the pellet was re-extracted with 2 ml 80 % ice cold acetone. After centrifugation the supernatants were pooled. The re-extraction was repeated until the green colour of pellet was gone (normally two times). The volume of the combined supernatants was adjusted to 25 ml and kept in the dark and cold.

Prior to the determination of the chlorophyll content, the supernatant was acclimated to room temperature (but kept in the dark). The absorbance at 646, 652, 663 and 710 nm was determined using 80 % acetone as blank. The chlorophyll a and b concentrations in mg/l were determined from the formulae:

$Chl_a=12.21*(A_{663}-A_{710})-2.81*(A_{646}-A_{710})$
$Chl_b=20.13*(A_{646}-A_{710})-5.03*(A_{663}-A_{710})$
$Chl_{a+b}=7.18*(A_{663}-A_{710}) +17.32*(A_{646}-A_{710})$

The data presented are the means of 5 independent chlorophyll extractions from different plants. Each determination was performed in triplicate.

2.3.11. Preparation of cells for chloroplast counting

Whole leaves of 2 to 3 week-old *Arabidopsis thaliana* seedlings (2 to 4 leaves) were fixed in 3.5 % (v/v) glutaraldehyde for 1 hour in the dark. The fixative was removed and replaced by 0.1 M Na_2EDTA pH 9 and the fixed leaf was incubated for 2.5 hours at 60 °C in a shaking water bath (Pyke and Leech, 1991). Samples were stored at 4 ^{o}C prior to chloroplast counting. For chloroplast counting, a small piece of macerated leaf sample was put on a slide in distilled H_2O and covered by a cover glass. Mesophyll cells were separated by tapping gently on the cover glass. Chloroplasts were counted using an optical microscope from individual pictures taken at different focal planes. Cell and chloroplast area were measured using ImageJ or Corel Photo-Paint.

2.3.12. Confocal Microscopy

Confocal microscopy was performed at the Estación Experimental del Zaidín (EEZ) microscopy service, equipped with a Nikon C-1 confocal laser scanning microscope. GFP-tagged protein was detected using standard argon 488 nm laser for excitation, and a 590/50 nm bandpass filter for emission. Auto-fluorescence of chlorophyll was observed with a 650 nm Long Pass filter detecting red emission. All experiments were

performed with 2 to 3 week-old seedlings at the stage of 2 to 4 true leaves. Alternatively observations were made at the microscopy services of the University of Granada, equipped with a high speed multiphoton Leica TCS-SP5 spectral confocal microscope system.

2.3.13. Transmission electron microscopy

Ultrastructure of chloroplasts from double mutant and wild type cells was studied by transmission electron microscopy (Hyman and Jarvis, 2011). Samples were prepared for electron microscopy from 2 week-old seedlings grown as indicated in section 2.3.4., selecting the yellow sections in the double mutant plants. Transmission electron microscopy was performed at Scientific Services of the University of Granada (http://cic.ugr.es/servicios-y-unidades/ficha.php?codServicio=6&unidad=27).

IV. RESULTS

1. Selection of mutant lines

1.1. Characteristics of the used T-DNA insertion lines

Four different T-DNA lines with insertions in the *AtKEA1* and *AtKEA2* genes were identified from the TAIR website and obtained from the NASC stock center:

- SALK lines (KEA2) Kanamycin resistance

SALK_009732
SALK_045324

- SAIL lines (KEA1) BASTA resistance

SAIL_1156_H07
SAIL_586_D02

According to the TAIR website, both SALK lines are homozygous for the T-DNA insertion. We determined the exact site of the T-DNA insertion from the published genomic sequence of the flanking regions (Figure 3.1). In both SALK lines the T-DNA is inserted in an exon of the AtKEA2 genomic sequence. The AtKEA1 SAIL_1156_H07 line was also reported to be homozygous, while the AtKEA1 SAIL_586-D02 line was heterozygous. The SAIL_586_D02 line T-DNA insertion is located in an exon, while the T-DNA insertion in SAIL_1156_H07 is located in an intron.

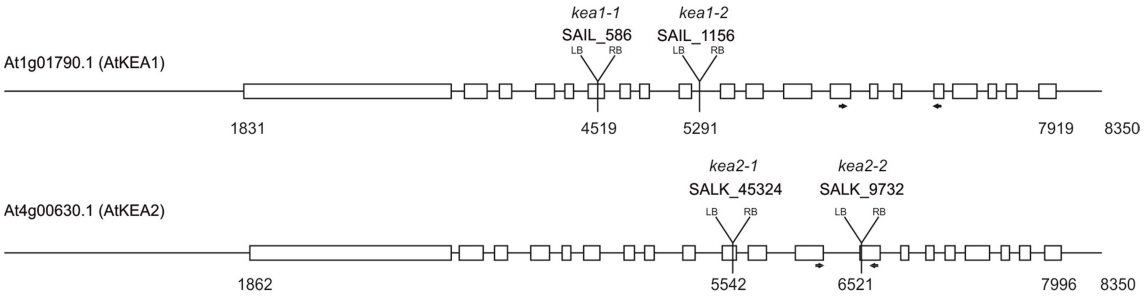

Fig. 3.1. AtKEA1 and AtKEA2 T-DNA insertion positions and orientation. White boxes indicate exons. LB: left border, RB: right border. Numbers below the sequence indicate nucleotide positions. The arrows below the sequence indicate the location of the primers used for RT-PCR expression analysis.

In order to select real homozygous lines, we performed a PCR analysis using gene specific and T-DNA primers, as described in material and methods. For line SALK_045324, in 4 out of 6 plants gene specific primers failed to amplify the AtKEA2 gene (Figure 3.2A), while an amplification product of the expected size was obtained using a T-DNA left border primer and a gene specific forward primer (Figure 3.2B),

meaning these plants were homozygous for the T-DNA insertion. Seeds were collected from the homozygous plants in order to perform subsequent experiments.

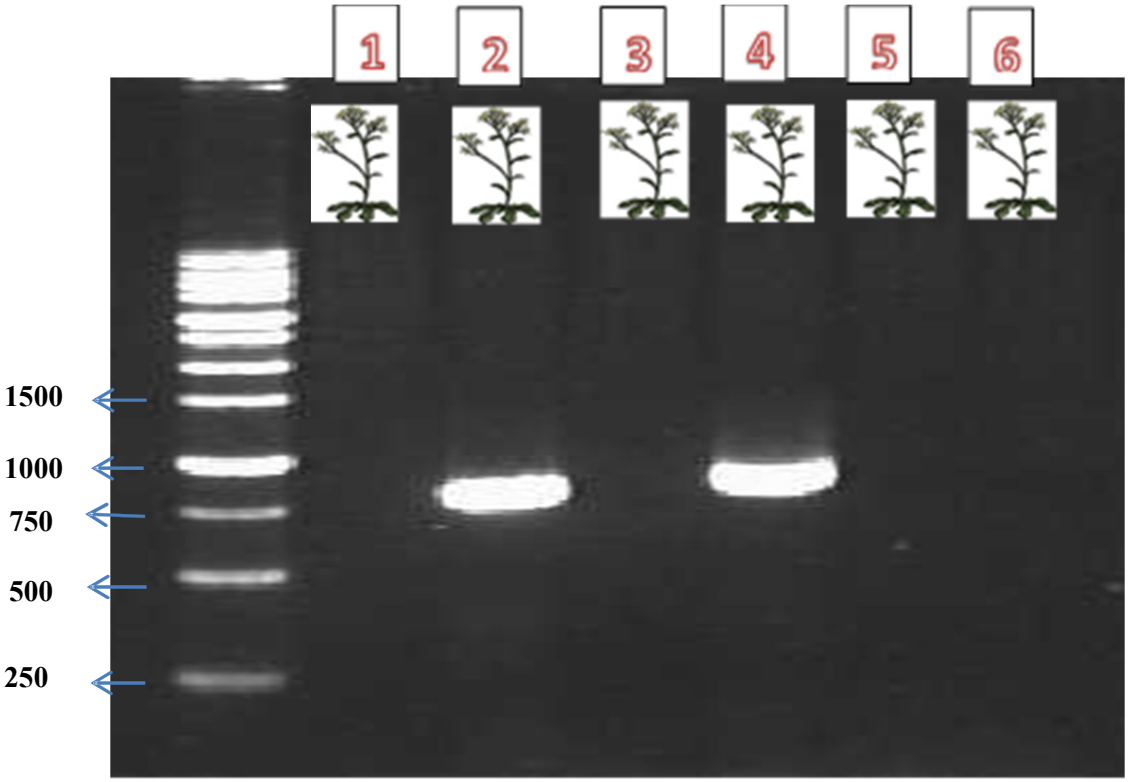

Fig. 3.2A. Genotyping of SALK_045324. No signal is observed in plants 1, 3, 5 and 6, indicating that the *AtKEA2* gene is interrupted by the T-DNA. In plants 2 and 4 a fragment of expected size is amplified, indicating that the lines do not harbor the T-DNA insertion or are heterozygous. Base pairs of molecular standards are indicated on the left side of the figure.

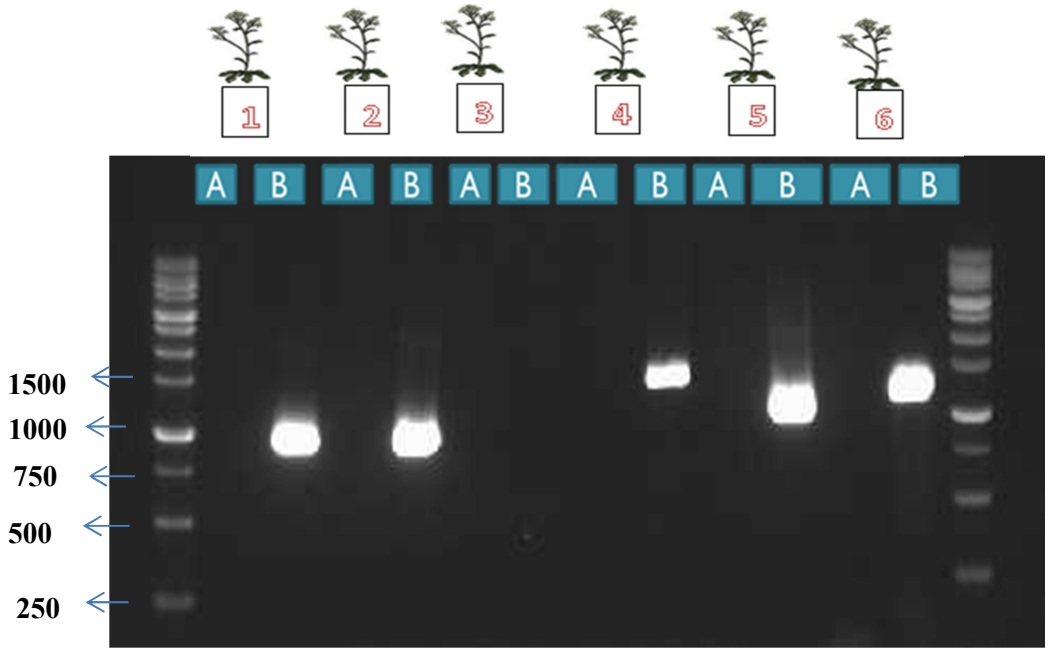

Fig. 3.2B. Genotyping of SALK_045324. A) Left border T-DNA primer lbp1.3 and a reverse *AtKEA2* gene specific primer or B) left border T-DNA primer lbp1.3 and a forward *AtKEA2* gene specific primer.

Except for plant No. 3, all samples show amplification using the T-DNA left border primer and the gene specific forward primer. These results, combined with those in Figure 3.2A indicate that plants 1, 5 and 6 are homozygous for the T-DNA insertion, while 2 and 4 appear to be heterozygous. Plant No. 3 was excluded for further studies as PCR analysis failed. Similar analyses were performed for the other T-DNA insertion lines to select homozygous lines for further studies.

1.2. Generation of *kea1kea2* double mutant T-DNA insertion lines

kea1kea2 double mutants were obtained by crossing homozygous *kea1* and *kea2* single mutants as described in material and methods. Crosses were as follows: SALK_045324 x SAIL_1156_H07, (hereafter called *kea1_2kea2_1* or dm1) and SALK_009732 x SAIL586_D2 (hereafter called *kea1_1kea2_2* or dm2). Plants of the F2 population were genotyped by PCR using specific primers (Table 2.7, Materials and Methods). In this study, we have also used a third *kea1kea2* double mutant (hereafter named dm3) obtained as a kind gift from Drs. L.R. Roston and C. Benning. Absence of expression of

AtKEA1 and *AtKEA2* was checked in the single mutants and in the double mutants by RT-PCR (Figure 3.3).

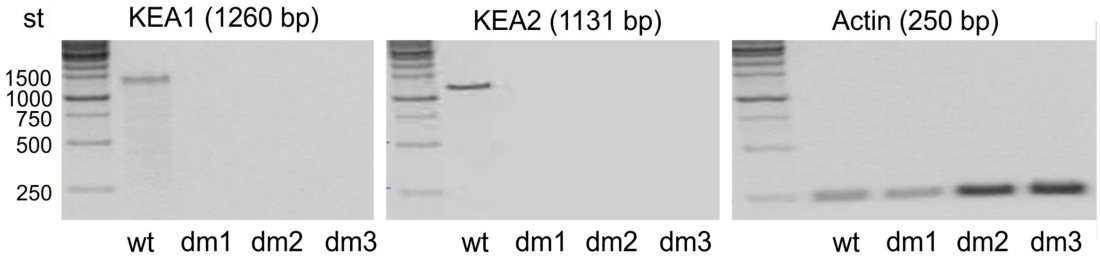

Fig. 3.3. Determination of expression of KEA1 and KEA2 in double mutant plants determined by RT-PCR using gene specific primers amplifying a 1260 bp fragment from KEA1 and a 1131 bp fragment from KEA2. As a control the expression of actin was also assayed.

The expression levels of *AtKEA1* and *AtKEA2* were also determined by real time qPCR as described in Materials and Methods (Figure 3.4).

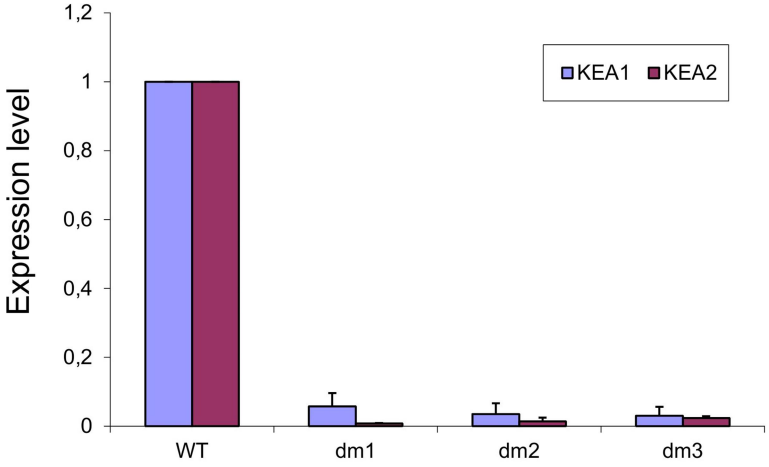

Fig. 3.4. Determination of the expression level of KEA1 and KEA2 in double mutant plants. The expression level was determined using primers amplifying fragments of 263 bp (*AtKEA2*) and 283 bp (*AtKEA1*). Values are expressed as relative expression compared to the levels in wild type plants. Data are means ± SD of at least 3 independent experiments.

2. Phenotypic analysis of mutant plants

We analyzed the expression pattern of *AtKEA1* and *AtKEA2* in different tissues of the wild type plants (Figure 3.5B). RT-PCR showed that *AtKEA1* and *AtKEA2* are highly expressed in leaves compared to roots, stems or flowers. The finding that *AtKEA1* and *AtKEA2* have a similar expression pattern points to redundant functions for both genes. In *Arabidopsis thaliana* AtKEA1 and AtKEA2 are close homologs, and the only

members of the KEA family of K^+/H^+ exchangers with a long N-terminal domain. However, in several relatively closely related plant species, only one copy of this gene subfamily can be found, also indicating that these genes result from a recent gene duplication and have redundant functions (Chanroj *et al.,* 2012).

2.1. Growth and appearance in normal conditions

In accordance with a redundant function for AtKEA1 and AtKEA2, we did not observe any obvious phenotype when the single T-DNA mutants were grown in standard growth conditions (Figure 3.5A). However, the two independent double mutant lines obtained were clearly much smaller, and had a yellowish appearance as compared to wild type plants (Figure 3.5A, C, D). The yellowish appearance of the mutant plants was observed above all in newly formed proliferating zones in leaves of young plants, and disappeared in later growth stages (Figures 3.6, 3.7, 3.8). The observed recovery of pigmentation is typical of virescent mutants that show defects in photosynthetic pigments in young and emerging tissues, but gradually turn green along the leaf proximal-distal axis. This is often related to altered expression of genes involved in early chloroplast biogenesis causing delayed chloroplast development (Chi *et al.,* 2010; Jarvis and López-Juez, 2013; Qi *et al.,* 2015).

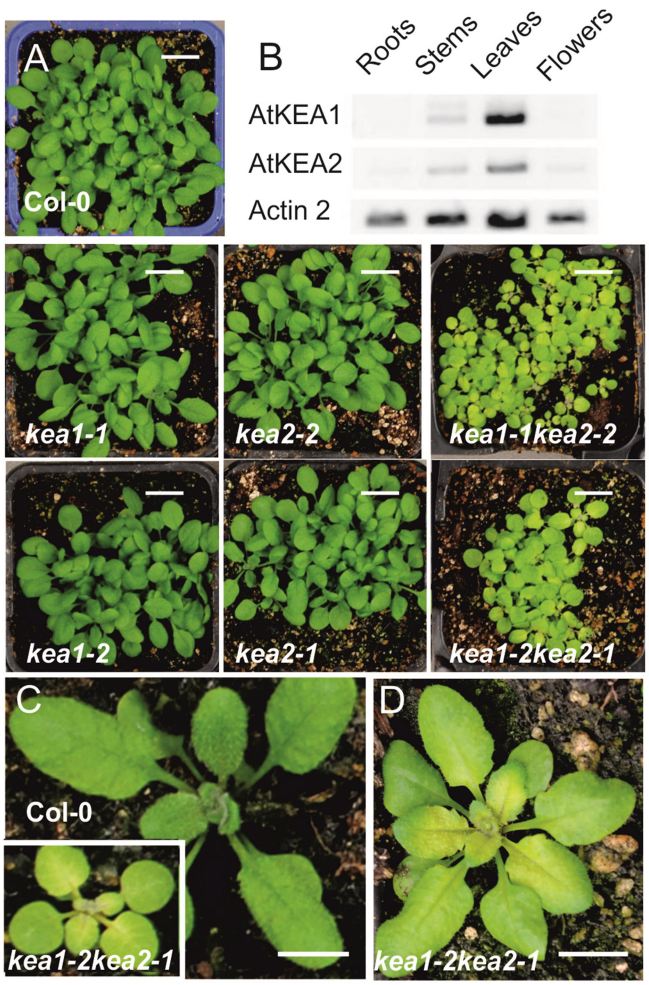

Fig. 3.5. ***Arabidopsis thaliana kea1kea2*** **double mutant leaves appear chlorotic in a developmental gradient (A)** The indicated KEA1 and KEA2 T-DNA insertion lines were grown for 3 weeks in peat-moss:vermiculite 1:1 at 22/20 ^{o}C,16 h light (120 µmol/m^{2}/s) /8 h darkness and irrigated with tap water. Single mutants appear similar to wild type Col-0 plants. The two independent *kea1kea2* double mutant lines were stunted in size and had pale yellowish leaves in a developmental gradient with younger leaves being particularly affected. **(B)** RT-PCR showing a similar expression pattern of *AtKEA1* and *AtKEA2* genes in WT plants. Three- **(C)** and four- **(D)** week old WT and *Arabidopsis thaliana kea1kea2* mutant plants grown under the conditions described in A. Newly emerging leaves of the double mutant plants are pale yellowish, while pigmentation partially recovers in old leaves. Bars = 1 cm.

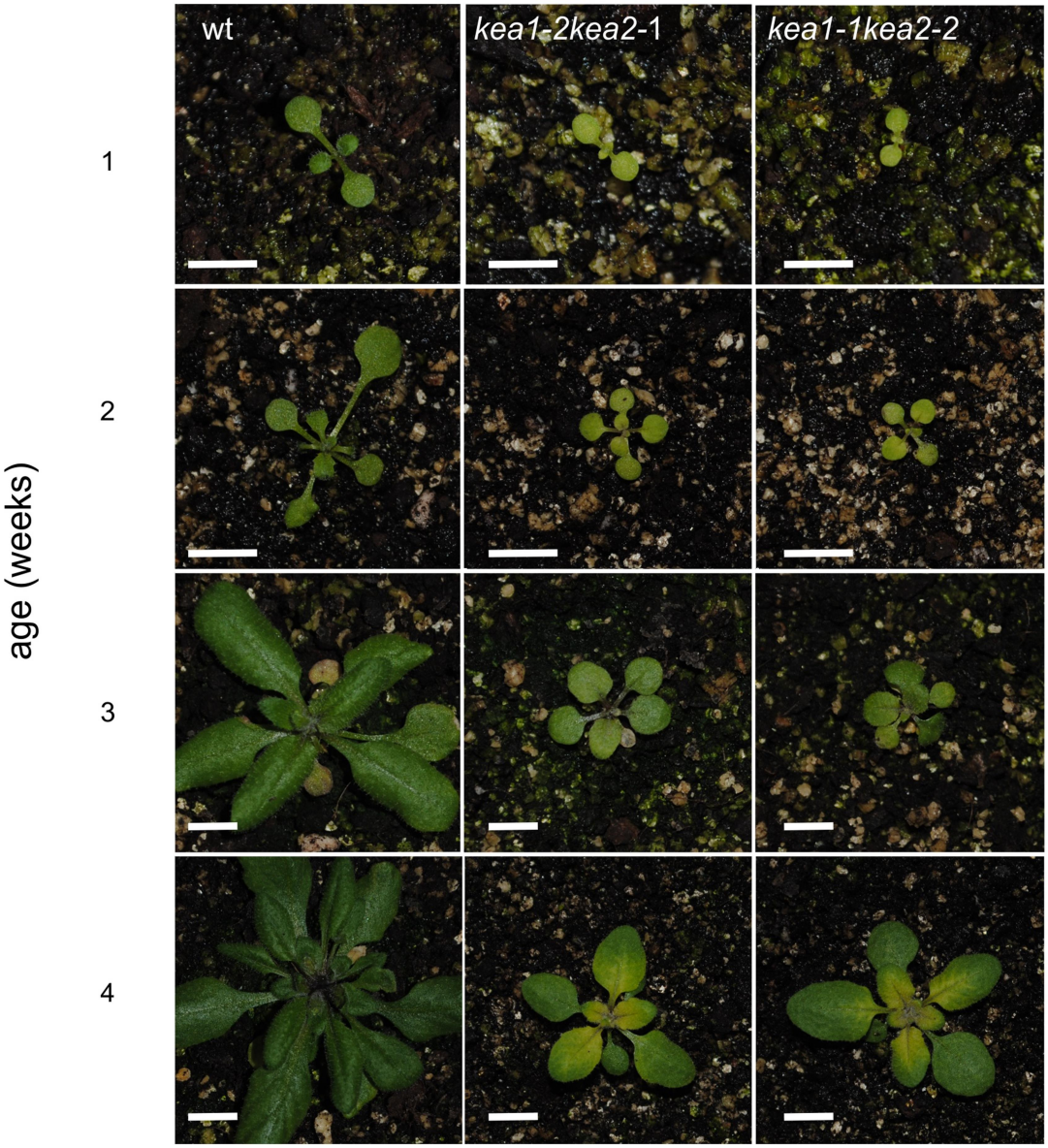

Fig. 3.6. Newly emerging leaves of *atkea1atkea2* double mutant plants appear chlorotic. Double *kea1kea2* mutants show reduced growth and newly emerging leaves are pale yellowish, while pigmentation partly recovers in later growth stages and older leaves. Four week old WT plant is shown without stem. Bar = 0.5 cm.

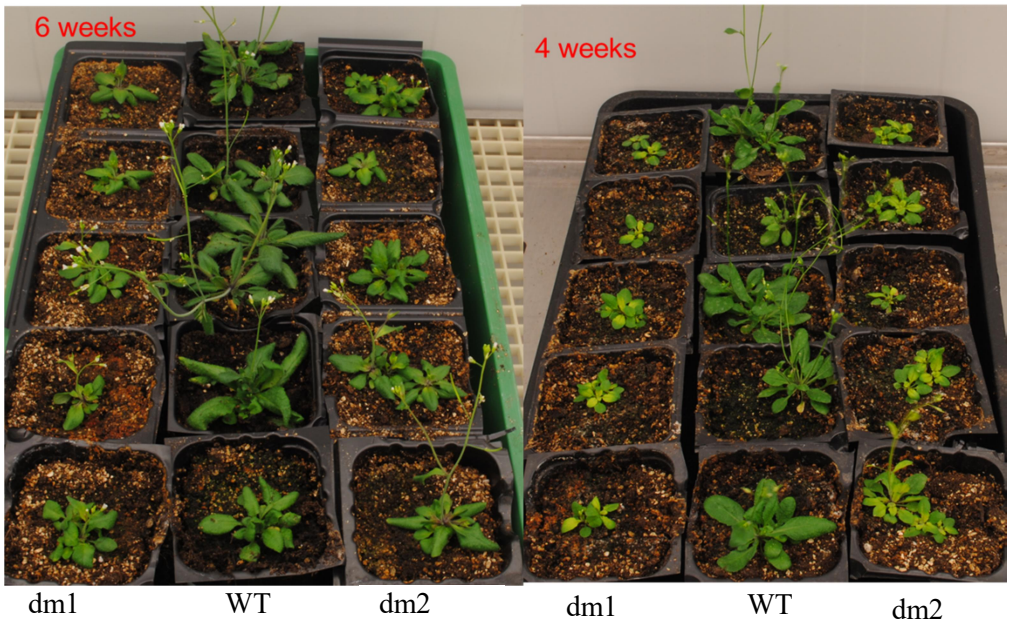

Fig. 3.7. Recovery of pigmentation in old plants and old leaves. Picture shows that after 4 weeks of culture the double mutant plants still appear chlorotic, while after 6 weeks they show the same pigmentation as WT plants. Double mutants remain smaller than WT plants both at 4 and 6 weeks of cultivation.

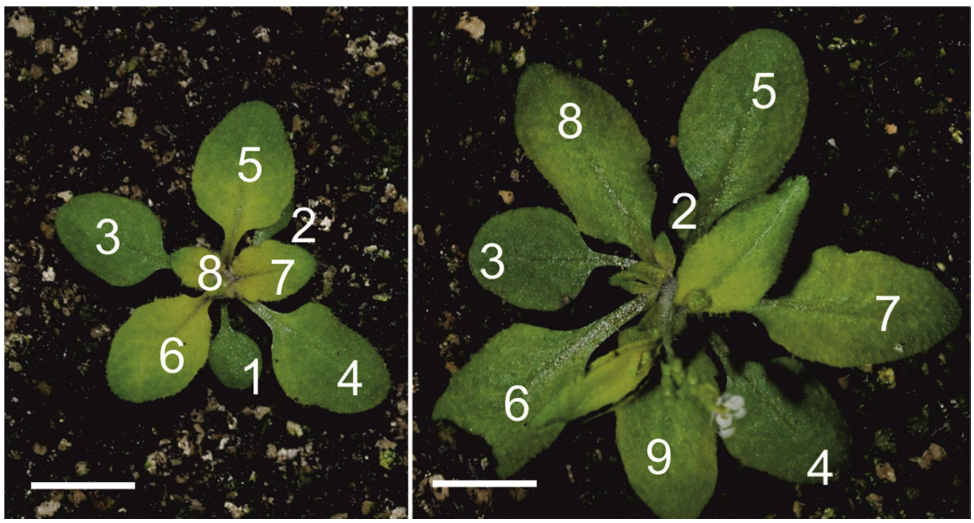

Fig. 3.8. ***kea1-1kea2-2*** **mutant at 4 (left) and 5 (right) weeks.** The plants are oriented to show numbering of visible leaves from old to new. Leaves #5-8 at 4 weeks show yellowish areas which turn green progressively from top to base by 5 weeks, corresponding to the transition from proliferation to expansion and mature zone. Bars = 0.5 cm

2.2. Analysis of chlorophyll and protein abundance in chloroplasts

The chlorotic appearance of the young double mutant leaves indicates reduced chlorophyll content. To quantify these differences chlorophyll content was determined in 3 week old WT and double mutant plants. As expected, the double mutants have lower total chlorophyll (chlorophyll a+b) content (Figure 3.9). Chlorophyll a and b are both reduced to the same extend, as can be seen from the constant chlorophyll a/b ratio (Figure 3.9).

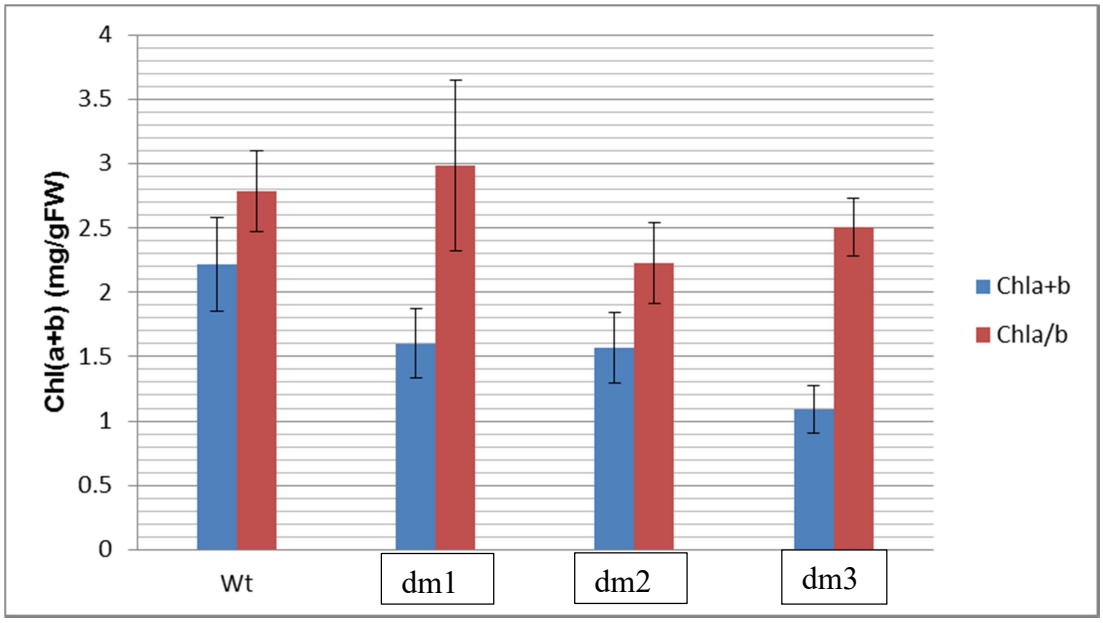

Fig. 3.9. Chlorophyll a+b content and chlorophyll a/b ratio in wild type and double mutant leaves. Chlorophyll was extracted from leaves of 3 week old plants grown under the conditions described in Fig. 3.5 and its content was determined as indicated in material and methods.

The particularly reduced pigmentation evident in the young leaf tissues of *kea1kea2* plants and the recovery in later leaf stages suggests that loss of chloroplast inner envelope K^+/H^+ antiporter activity may delay chloroplast development. To verify such a role for AtKEA1 and AtKEA2, the abundance of essential thylakoid membrane photosynthetic protein complexes as well as other thylakoid and stromal proteins was determined in the green and yellow sections of double mutant leaves as indicated in Figure 3.10. These determinations were performed in the laboratory of Dr. Ute

Armbruster (Howard Hughes Medical Institute, Department of Plant and Microbial Biology, University of California, Berkeley, CA 94720 USA).

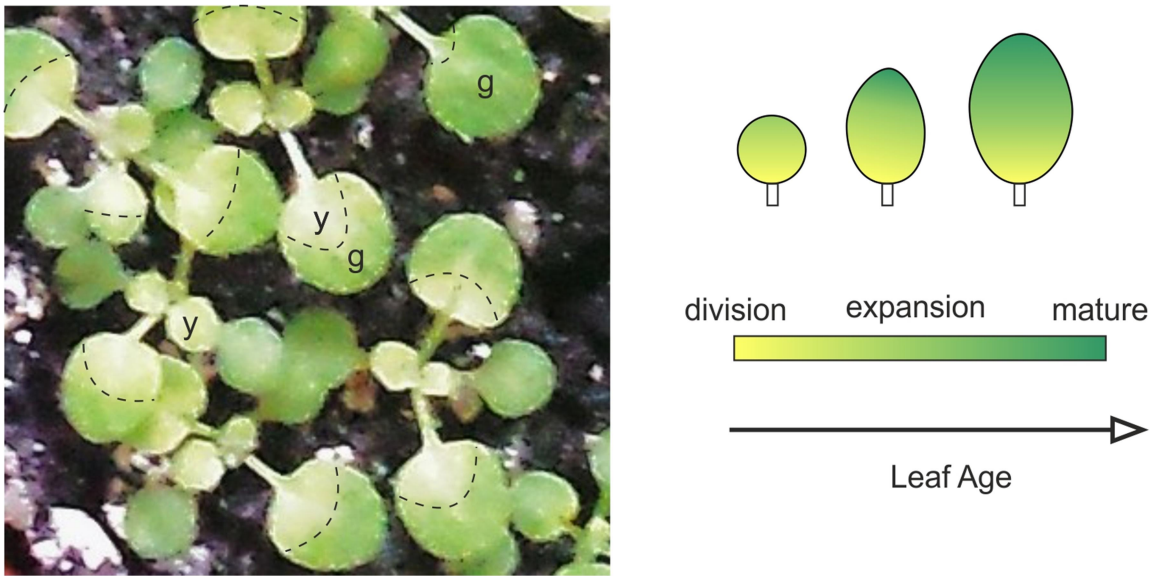

Fig. 3.10. Leaf development in double mutant plants. The picture shows green (g) and yellow/pale (y) sections identified in two week old plants that correspond to division/expansion zones and mature zones (Beemster *et al.,* 2014).

The selected subunits serve as good indicators for the abundance of the respective complexes, because subunits either do not accumulate at all or only in marginal amounts in the absence of their functional complexes. Results in Figure 3.11 show that in yellow leaf sections of double mutant plants particularly the two subunits of the PSII reaction center, PsbA and PsbD, were decreased (~20 % of WT), but also subunits of photosystem I (PSI), PsaD, cytochrome b_6f complex ($Cytb_6$) and the light-harvesting complex II (Lhcb2) were strongly reduced as compared to WT (~40 %). The ATP synthase (AtpB) and Rubisco (RbcL) accumulated to about 60 % of WT, while KEA3 and Alb3 (involved in protein insertion in the thylakoid membrane) were present at WT levels. In the differentiated mature parts of *kea1kea2* leaves, levels of all analyzed protein subunits recovered to WT levels. These results support the view that the activity of AtKEA1 and AtKEA2 is particularly important for younger leaf cells. Together, the effect of AtKEA1 and 2 loss-of-function on pigmentation and photosynthetic protein complex accumulation particularly in the young developing leaf tissues may suggest a function of envelope K^+/H^+ antiport in chloroplast biogenesis.

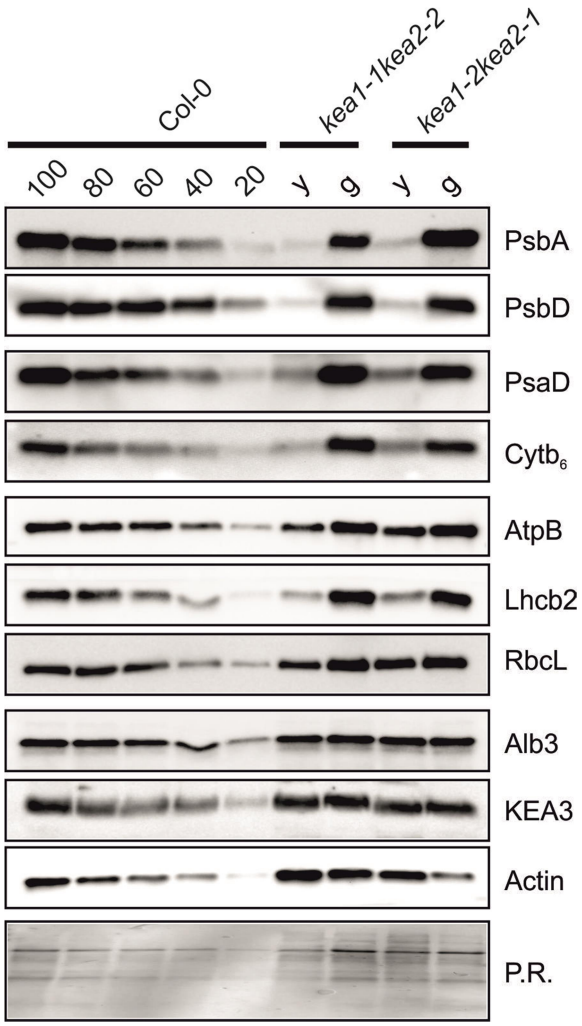

Fig. 3.11. Levels of essential photosynthetic protein complexes are severely decreased in developing leaves of *kea1kea2* mutants. Determinations were made in green and yellow zone of leaves separated as shown in Fig 3.10.Total protein from 0.5 mg fresh weight of WT, or green (g) and yellow (y) sections of *kea1kea2* leaves was separated by SDS-gel electrophoresis and transferred to PVDF membranes for immunostaining. Different amounts (20-100 %) of WT protein were analysed to estimate the relative abundance of proteins in *kea1kea2* leaves P.R.: Ponceau Red stained proteins serve as the loading control. PsbA: photosystem II protein D1, PsbD: photosystem II subunit D2, PsaD: Photosystem I subunit D, Cytb6: Cytb6f complex subunit, AtpB: ß subunit of ATP synthase, Lhcb2: subunit 2 of Light harvesting complex 2, RbcL: Rubisco large subunit, Alb3: Albino 3 thylakoid insertase, KEA3: *Arabidopsis thaliana* thylakoid membrane K^+/H^+ antiporter KE

2.3. Analysis of photosynthetic parameters

This study was made in collaboration with Dr. Ute Armbruster at the University of Berkeley. Spectroscopic measurements shown in Figure 3.12 indicate that the maximum quantum yield of PSII (Fv/Fm) was strongly affected in the young yellow sections of the leaves. A light response curve further showed that photosynthetic capacity is

saturated at lower light intensities in *kea1kea2 Arabidospsis* mutants again particularly in the young developing leaf sections. This confirms that the observed abnormalities in thylakoid protein and pigment composition cause defects in chloroplast function.

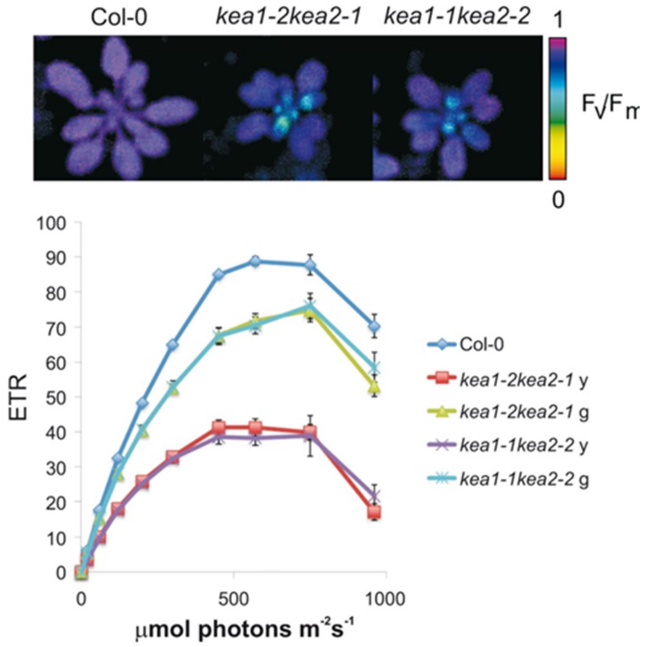

Fig. 3.12. Photosynthetic parameters are affected in young developing leaves of mutants. (A) Young developing leaves of *kea1kea2* mutants show decreased PSII quantum efficiency. **(B)** Electron transport rates (ETR) are decreased particularly in young tissues of *kea1kea2* leaves and saturate at lower light intensities (g: green sections, y; yellow sections). *kea1-2kea2-1y*: yellow sections of dm1, *kea1-2kea2-1g*: green sections of dm1, *kea1-1kea2-2y*: yellow sections of dm2 and *kea1-1kea2-2g*: green sections of dm2.

2.4. Chloroplast ultrastructure

Transmission electron microscopy (TEM) images of chloroplasts from the yellow sections of the leaves showed that lack of AtKEA1 and AtKEA2 causes a general disorganization of internal structures (Figure 3.13). Thylakoid membranes showed less stacking and were slightly wrinkled. Above all, thylakoid membranes were not properly aligned along the longitudinal axis in the double mutant chloroplasts. Starch grains in chloroplasts from double mutant plants have an irregular swollen shape compared to the elongated WT starch grains, and are surrounded by a much bigger cavity. Additionally, we noticed an increase in the number of plastoglobuli in the double mutant chloroplasts, indicating increased photo-oxidative stress in the mutant plants.

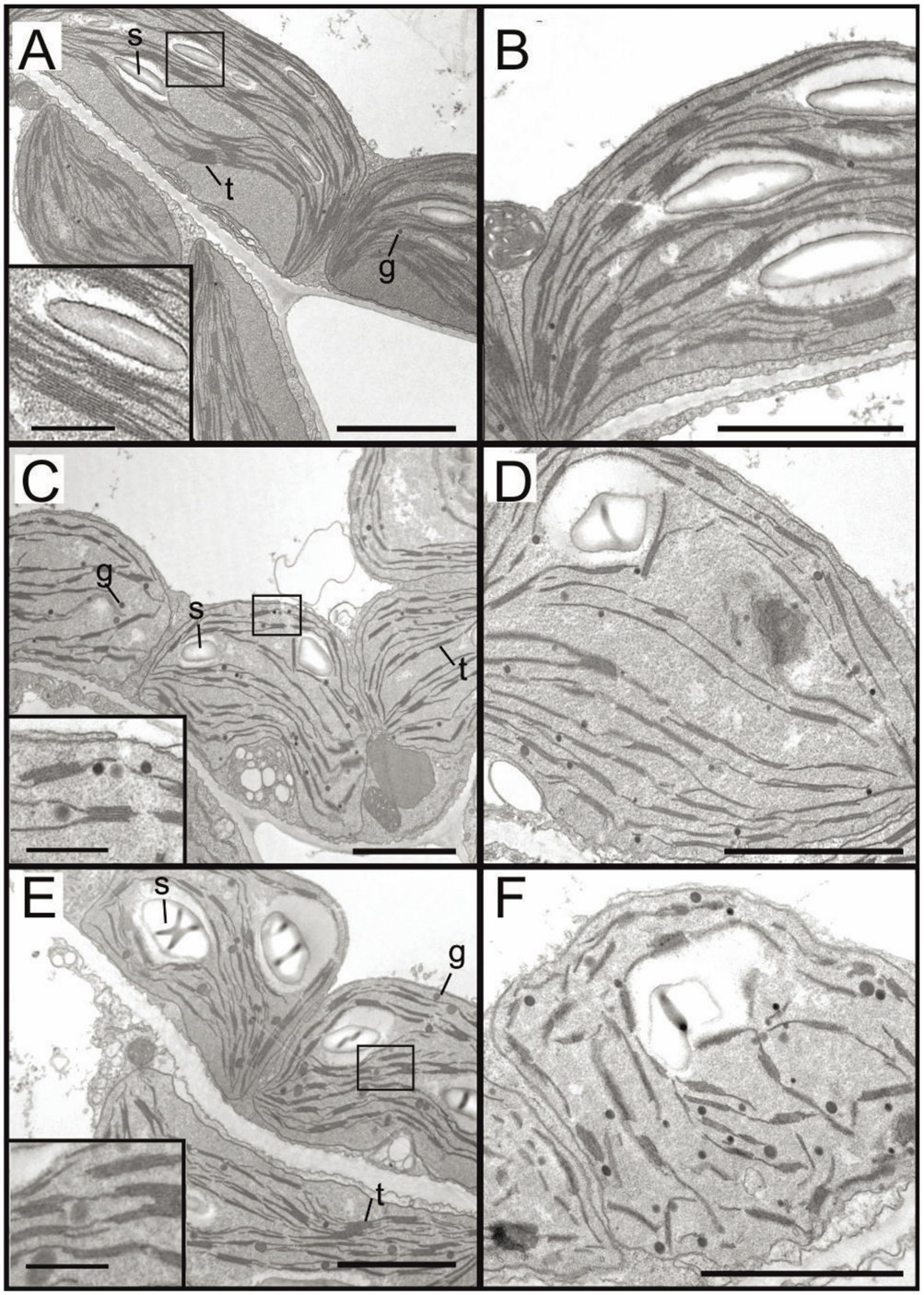

Fig. 3.13. Double mutant *kea1kea2* chloroplasts show altered thylakoid organization and starch grain alignment. TEM images of chloroplasts from WT plant (A, B) and *kea1_1kea2_2* (C, D) and *kea1_2kea2_1* (E, F) are shown. Plants were grown for 3 weeks under the conditions described in Fig 3.5. Chloroplasts of WT plants have a typical stretched bean like shape and show internal structures, i.e. thylakoid membranes (t) and starch grains (s) aligned according to this elongated shape. Chloroplasts from double mutants are rounder, and the internal structures show a less organized alignment along the longitudinal axis. Chloroplasts from double mutants show less stacked thylakoids, shorter grana and higher amount of plastoglobuli (g) than chloroplasts from WT plants. Bars = 2 μm. Insets show close ups of thylakoid stacks. Inset bars = 0.5 μm.

2.5. Chloroplast number and size

Young leaves of 2 week old plants were observed with a light microscope. In most cases chloroplasts from double mutant leaves were bigger and round shaped, which could be an indication of osmotic swelling (Figure 3.14). Cells from double mutant plants also appeared to contain less chloroplast. A general overview of a leaf using a confocal microscope, detecting only chlorophyll fluorescence, also indicated a lower density of chloroplasts in leaves from double mutant plants (Figure 3.15). To quantify in more detail the chloroplast number and size in the double mutant plants, cells were fixed in glutaraldehyde and treated with EDTA as described in material and methods. The number of chloroplasts per cell was counted for about 200 chloroplasts from each mutant by focusing through different planes of the cell. Results in Figure 3.16 show that the number of chloroplasts in cells from double mutants was about 60 % of the number in wild type cells. The size of double mutant chloroplasts was also slightly bigger and more heterogeneous (Figure 3.16). These characteristics are typical of chloroplast division mutants (Osteryoung and Pyke, 2014).

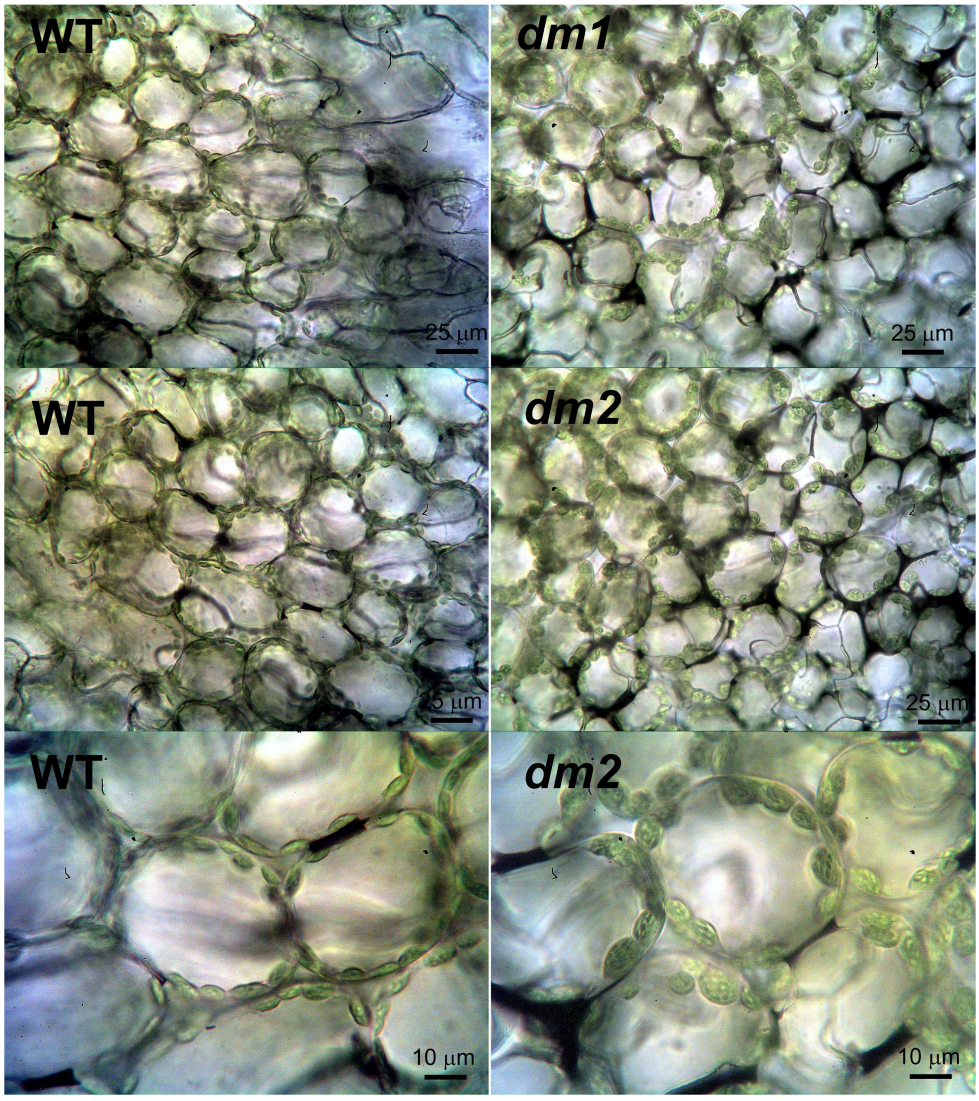

Fig. 3.14. Chloroplasts in double mutant cells are round and swollen. Leafs from 11 day old plants were observed with a light microscope with a 40x objective (top two rows) or a 100x objective (bottom row).

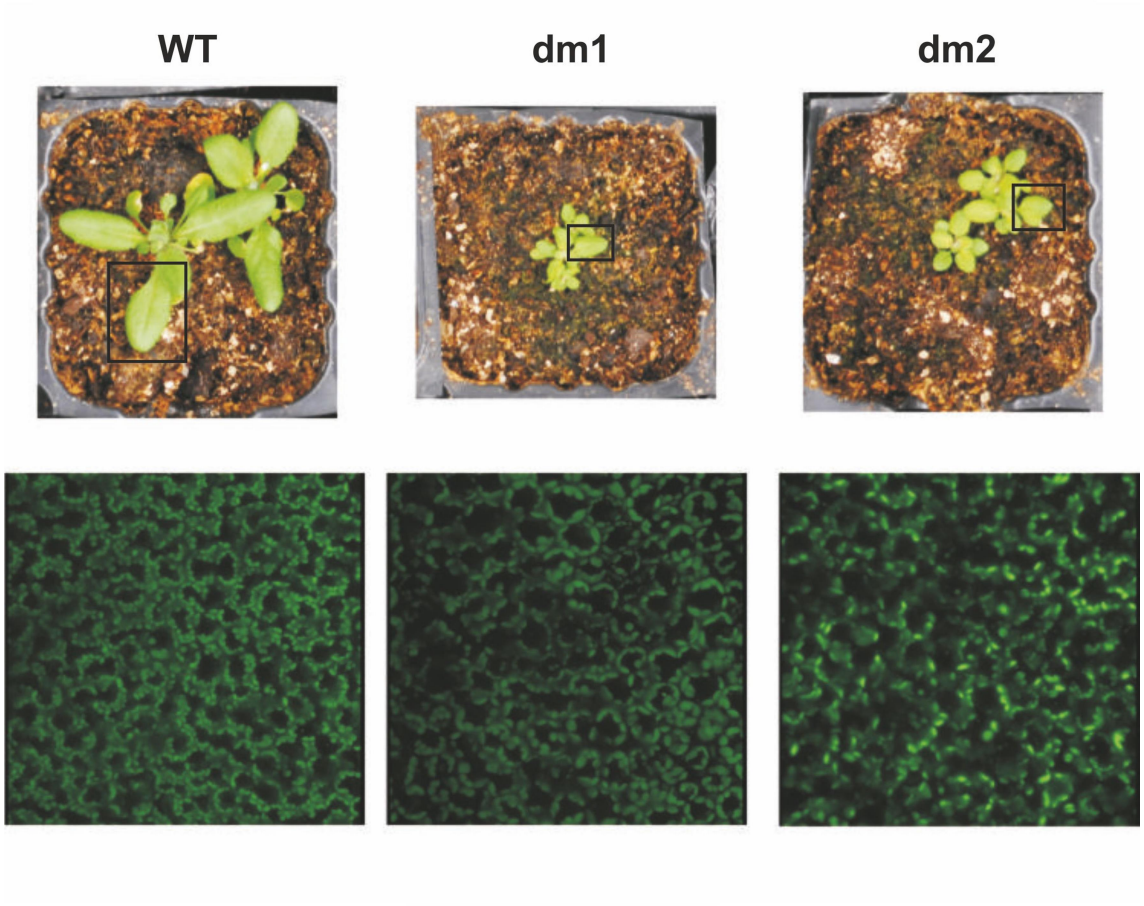

Fig. 3.15. Double mutant leaves have a lower chloroplast density. Plants were grown for 3 weeks as indicated in Fig 3.5. A leaf section, indicated by black rectangles, was chosen for confocal microscopy imaging. Chlorophyll autofluorescence was assessed in different planes and a final Z-stack image was reconstructed from 12 slices.

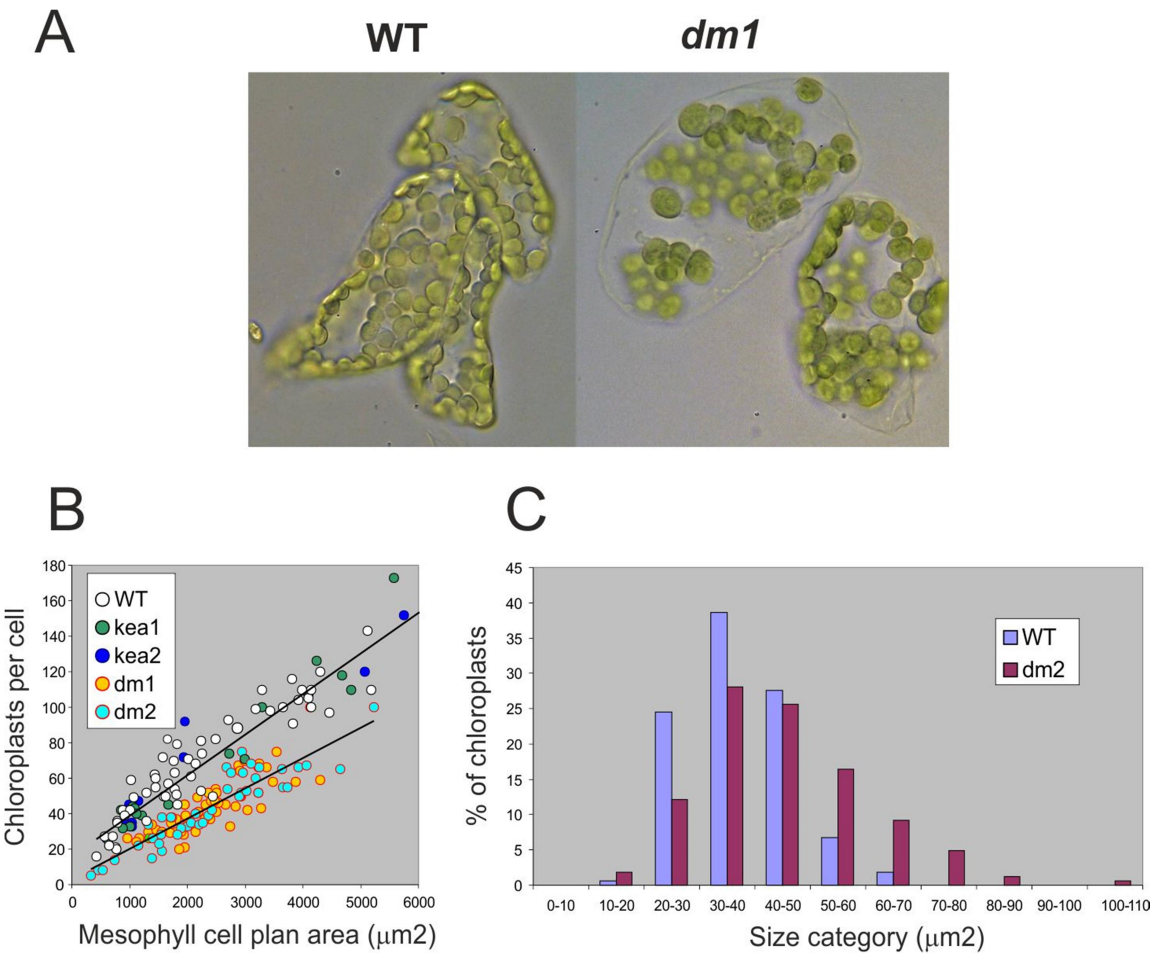

Fig. 3.16. Double mutants have bigger chloroplasts and less chloroplast per cell. A) Optical microscope image of WT and double mutant leaf cells fixed in glutaraldehyde and treated with EDTA (Pyke and Leech, 1991). **B)** Graph showing chloroplasts per leaf mesophyll cell area. Chloroplasts were counted by focusing on different planes through the cells with every point in the graph representing one cell. Cells from double mutant plants contain about 60 % of the number of chloroplasts compared to wild type cells. **C)** Chloroplasts size. Chloroplasts in double mutants are larger than in WT plants. Size of individual chloroplasts was determined by measuring the area in Corel Photo Paint. 100 % = 200 chloroplasts for mutants and WT. Mean size of wild type chloroplasts is 36 ± 9 μm^2. Mean size of double mutant chloroplasts is 45±15 μm^2.

2.6. Effect of Sucrose and NaCl on growth

Initial characterization of *kea1kea2* double mutant phenotypes was performed with seedlings growing on agar plates supplemented with 2 % sucrose. We observed that in these conditions the phenotype of double mutant plants was much less severe and disappeared completely with time.

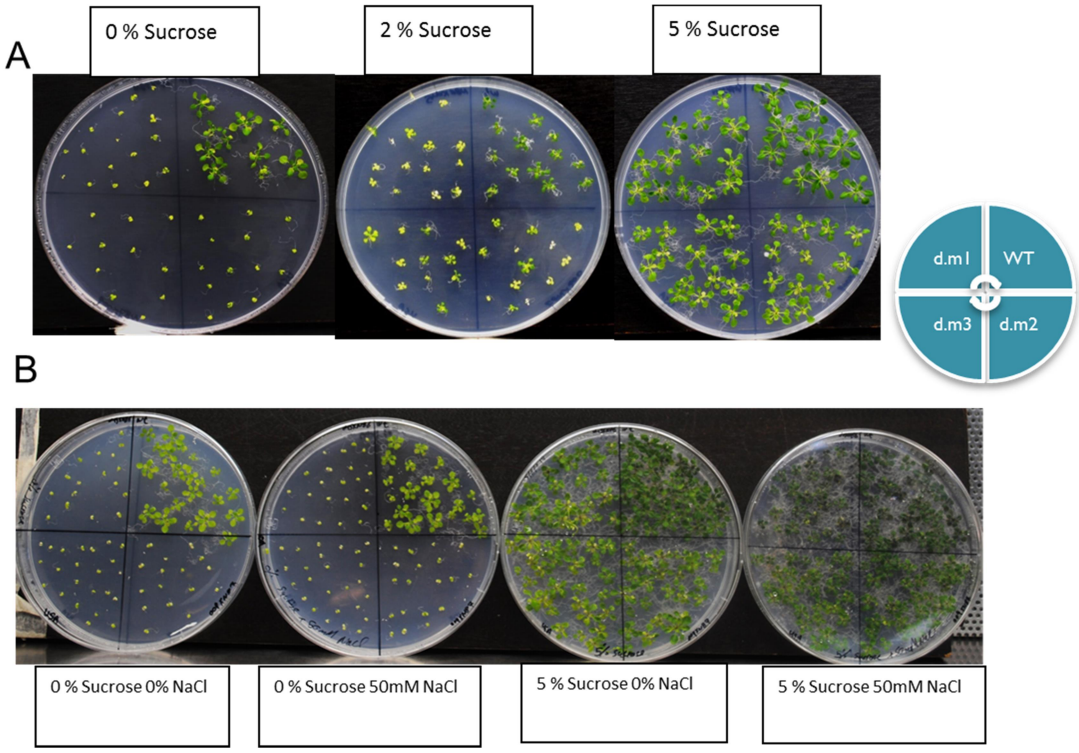

Fig. 3.17. Effect of sucrose and NaCl on growth of *kea1kea2* and WT plants. Seeds were germinated on a medium composed by a ½ dilution of MS basal salts supplemented and non-supplemented with sucrose (A) or sucrose and NaCl (B) at the indicated concentrations. Pictures shown that mutant phenotypes are rescued by external NaCl and sucrose.

As AtKEA1 and AtKEA2 are predicted to be located in the chloroplast inner envelope membrane, it is likely that their absence affects photosynthesis or carbon fixation reactions. When plant growth is less dependent on carbon fixation, for instance by external sucrose supply, it is expected that growth will be restored to some extent. To test this hypothesis, we studied the effect of sucrose supplementation on the growth of double mutant plants (Figure 3.17). It is observed that in the presence of 5 % sucrose the double mutant plants did not show differences in size as compared to the wild type plants. The mutant plants conserved however the notable pale yellow leaf colour (Figure 3.17A). These results suggest that absence of AtKEA1 and AtKEA2 causes defects in chloroplast biogenesis or development resulting in yellow colour and reduced photosynthesis and carbohydrate production. The lack of carbohydrate production can be remediated by addition of sucrose. Curiously, when in addition to sucrose also NaCl was added to the culture medium, seedlings recovered both pigmentation and size (Figure 3.17B). NaCl stress is known to cause synthesis of cellular osmolytes. Possibly the defects in chloroplast biogenesis in double mutant plants are caused by high osmotic

pressure inside the chloroplasts, as K^+ is not exported by AtKEA1 or AtKEA2. NaCl could improve the osmotic balance of the cytoplasm, preventing the developmental defects in chloroplasts from double mutant plants.

2.7. Effect of light intensity on growth

As AtKEA1 and AtKEA2 might be involved in regulating efficiency of photosynthesis reactions, we tested the effect of light intensity on the growth of double mutant and wild type plants.

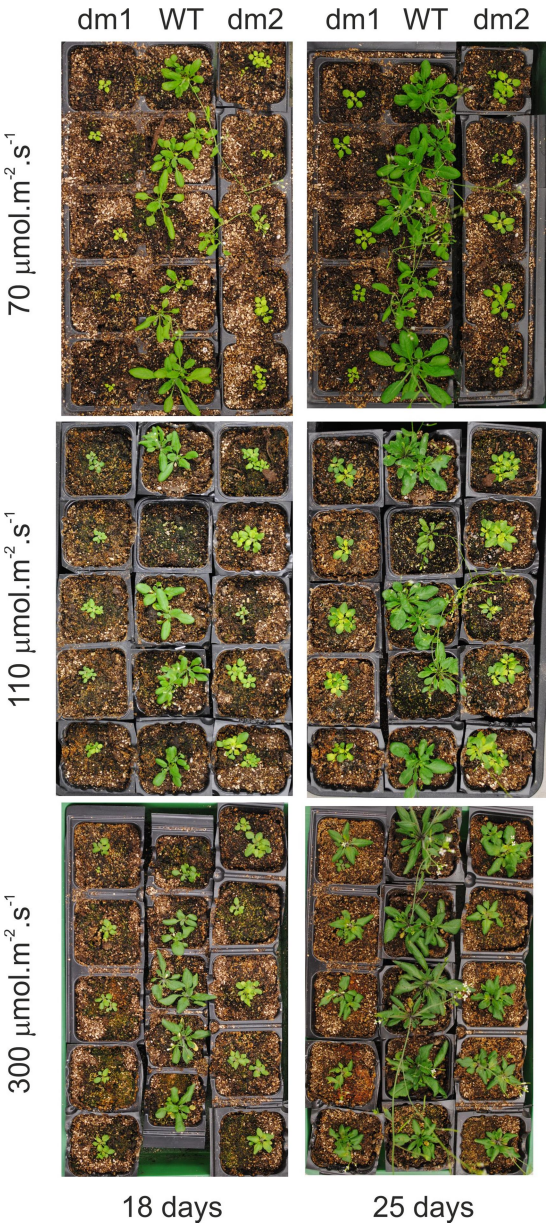

Fig. 3.18. Effect of light intensity on growth of WT and *kea1kea2* mutant plants. *Arabidopsis thaliana* plants were cultivated under the conditions described in Fig. 3.5 at the indicated light intensities.

At all light intensities tested, the double mutant plants were much smaller, and showed a yellowish appearance (Figure 3.18) indicating a lower chlorophyll content as compared to WT plants. Higher light intensities seemed to inhibit slightly the leaf expansion in wild type plants, while it stimulated growth of the double mutant plants to some extend (Figure 3.18). This indicates that photosynthesis reactions are less efficient in *atkea1atkea2* double mutant plants, requiring higher light intensities for full activity.

3. Transformation of wild type and double mutant plants with GFP tagged AtKEA2

To study in more detail the function of AtKEA2, we transformed wild type and double mutant plants with the full length *AtKEA2* gene, including the first 5 introns, tagged with a C-terminal GFP protein. The full length *AtKEA2*-GFP construct was cloned in a plant expression vector pB7WG2, which harbours a BASTA resistance marker. Although this was adequate for transforming wild type plants, double mutant plants are resistant to both BASTA and Kanamycin. For this reason, we have tried to introduce the gene construct in a vector harbouring hygromycin resistance, but we did not succeed in transforming double mutant plants with this construct. We therefore used the gene construct conferring BASTA resistance to transform the double mutants. We have observed that seeds obtained from double mutant plants which underwent transformation generated two types of plants; some recovered the WT phenotype while others showed the double mutant phenotype (Figure 3.19A). When these two types of plants were analysed by PCR, the presence of the *AtKEA2* gene was detected in plants showing the WT phenotype, but not in plants with mutant phenotype (Figure 3.19B). The bigger size of the gene fragment amplified by PCR in wild type plants was due to the presence of introns that were absent in the C-terminal region of the *AtKEA2*-GFP construct used for transformation of double mutants. As observed for heterozygous T1 plants (Figure 3.19A) homozygous T3 plants restored the normal growth phenotype (Figure 3.19C). It can thus be concluded that the stunted growth and yellowish phenotype of the *kea1kea2* double mutants was a result of the absence of AtKEA1 and AtKEA2. To further confirm the presence of a functional AtKEA2-GFP protein in the transgenic plants, we performed western blotting on total protein extracts from leaves of wild type or transgenic plants, using a monoclonal antibody raised against the GFP protein. In such total protein extracts, no signal was obtained (data not shown). Next,

we specifically enriched the preparation for the tagged protein, using the GFP-trap system, consisting of GFP-specific antibodies linked to magnetic beads. Using the latter procedure we could clearly demonstrate the presence of recombinant protein of the expected size in the transformed plants, while no signal was detected in wild type plants (Figure 3.19D). These data indicate that only low levels of AtKEA2 are required for proper AtKEA2 function, which is surprising given the high number of chloroplasts in *Arabidopsis thaliana* leaves.

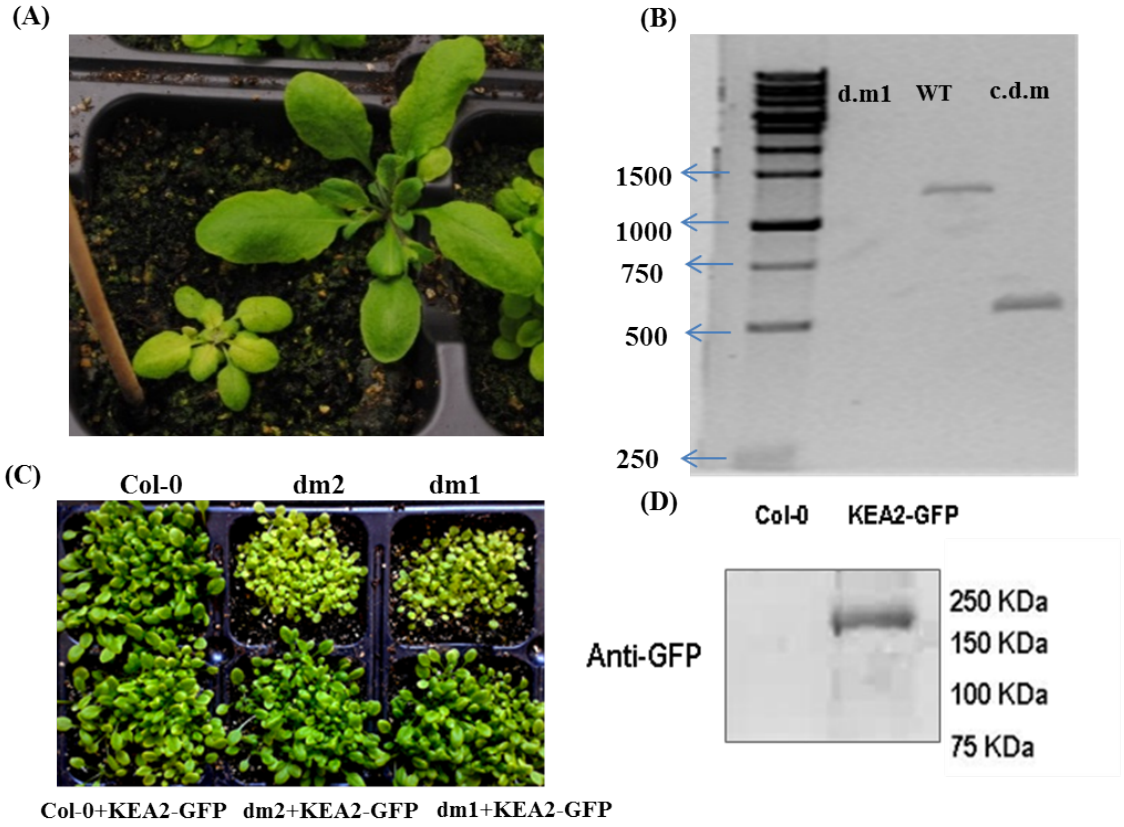

Fig 3.19. Complementation of growth defects by expression of AtKEA2-GFP. WT (Col-0) and *kea1kea2* double mutant (dm1 and dm2) plants were transformed with a construct encoding an AtKEA2-GFP fusion protein. (**A**) Two plants obtained from seeds of a double mutant plant transformed with AtKEA2-GFP were grown for 4 weeks under the conditions described in Fig. 3.5. Two different phenotypes are observed (**B**) The presence of *AtKEA2* was checked by PCR on genomic DNA of the plants shown in (A) as well as in WT plants. dm1: plant with double mutant phenotype. WT: wild type plant. cdm: plant with WT phenotype. **(C)** Growth of WT, double mutants and homozygous (KEA2-GFP) T3 double mutant plants. Plants were grown for 2 weeks in the same conditions described in (A). (**D**) Immunodetection of AtKEA2-GFP. Total protein was extracted from wild type plants transformed (KEA2-GFP) or not (Col-0) with the AtKEA2-GFP construct and separated by SDS gel electrophoresis. Presence of the protein was assayed after electrotransfer to a PVDF membrane using an anti-GFP antibody.

4. Subcellular localization of AtKEA2

To determine the subcellular localization of AtKEA2, we stably transformed *Arabidopsis thaliana* plants with the construct for expression of the AtKEA2-GFP fusion protein. In isolated mesophyll chloroplasts from transformed plants, GFP fluorescence can be clearly seen as a ring surrounding the chloroplasts, indicating the KEA2-GFP protein is located in the inner or outer envelope membrane. These data were confirmed by Kunz et al. (2014), who showed AtKEA1 and AtKEA2 are localized to the inner envelope in guard cell chloroplasts. GFP fluorescence was however not observed in all chloroplasts, and some local patches of GFP fluorescence were observed at both sides of the chloroplasts (Figure 3.20).

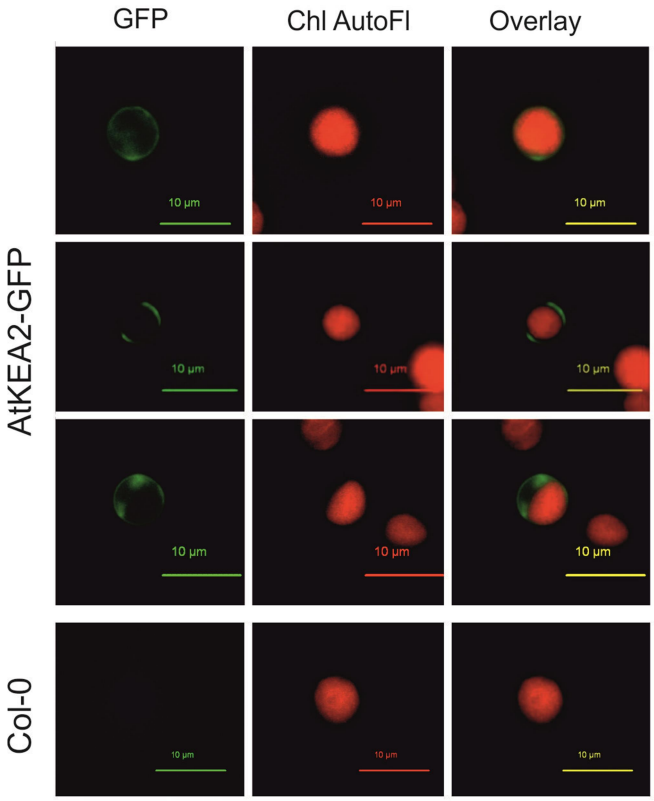

Fig. 3.20. AtKEA2 is localized to the chloroplast envelope. In isolated chloroplasts from Col-0 plants expressing the AtKEA2-GFP gene, GFP fluorescence is observed as a ring around the chloroplasts, clearly indicating inner envelope location. The fluorescence pattern is much more homogeneous as compared to the GFP fluorescence observed from chloroplasts in living mesophyll cells.

In leaf mesophyll cells AtKEA2-GFP fluorescence appears punctuate (Figure 3.21A, B, C). Closer observation shows that GFP fluorescence is above all present in small developing chloroplasts, and concentrated at the poles, but excluded from the division site (Figure 3.21, insets 1, 2, 3 and 6). In mature chloroplasts, AtKEA2-GFP

fluorescence is much less abundant, and only remains in discrete spots (Figure 3.21 insets 4 and 5), somewhat reminiscent of the localization of the mechano sensitive channels MSL2 and MSL3 (Haswell and Meyerowitz, 2006).

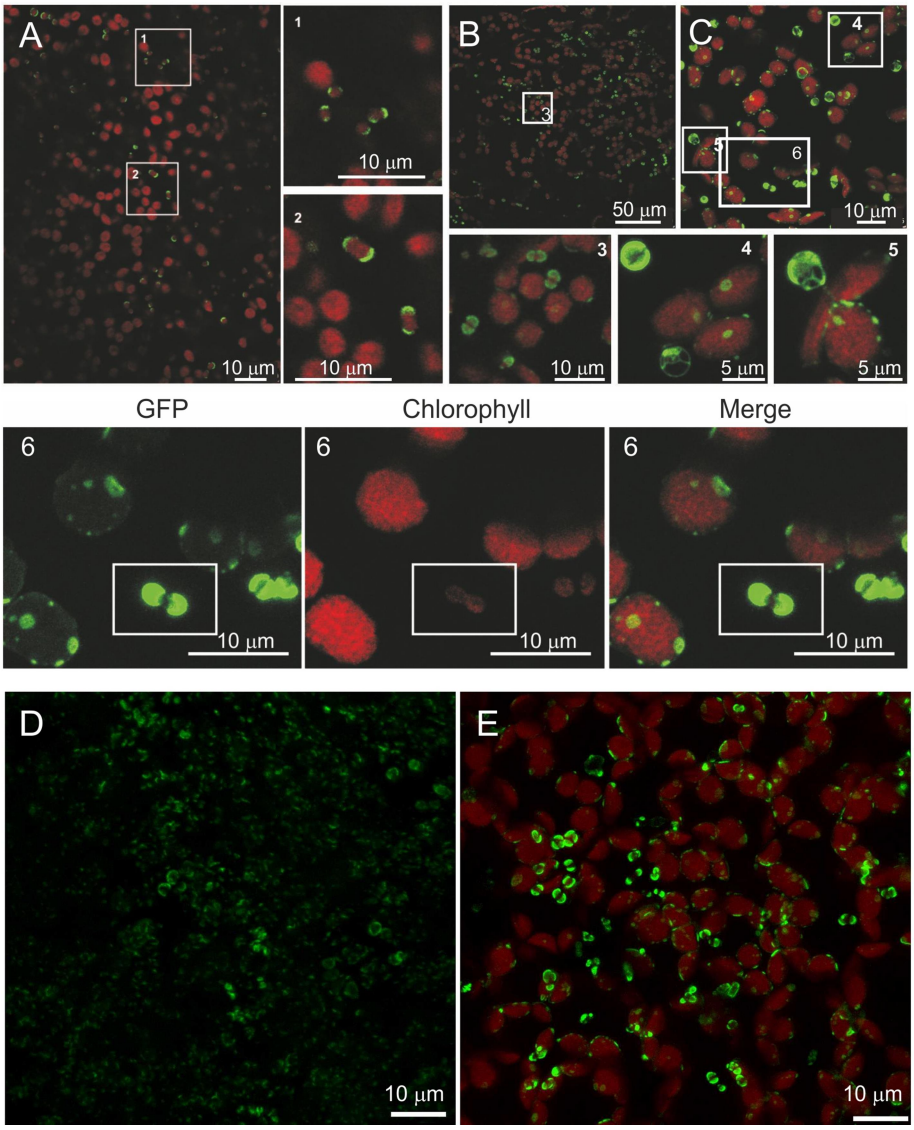

Fig. 3.21. AtKEA2-GFP localizes to small dividing chloroplasts. AtKEA2-GFP fluorescence coincides with chloroplasts, it is most brightly observed in small chloroplasts that show little chlorophyll fluorescence, and is mostly localized to the poles (inset 1, 2, 3 and 6). In bigger-older chloroplasts AtKEA2-GFP fluorescence remains in spots at the envelope membrane (inset 4 and 5). In some chloroplasts, AtKEA2-GFP fluorescence is interconnected by a wireframe network along the inner envelope (inset 4 and 5). A, B and C show a complete picture at the original resolution. Insets 1 to 5 show digitally enlarged regions from these pictures. In inset 6 the separate GFP and Chlorophyll autofluorescence is shown. GFP: GFP fluorescence. Chlorophyll: Chlorophyll fluorescence. Merge: Overlay of chlorophyll and GFP fluorescence. D and E show AtKEA2-GFP fluorescence in cotyledons of dark (D) versus light (E) grown seedlings. Cotyledons of 10 day-old seedlings were examined.

To quantify the above observations (Figure 3.21), we scored for 200 chloroplasts whether or not fluorescence was seen at the two poles, as a function of the size of the chloroplasts (Figure 3.22).

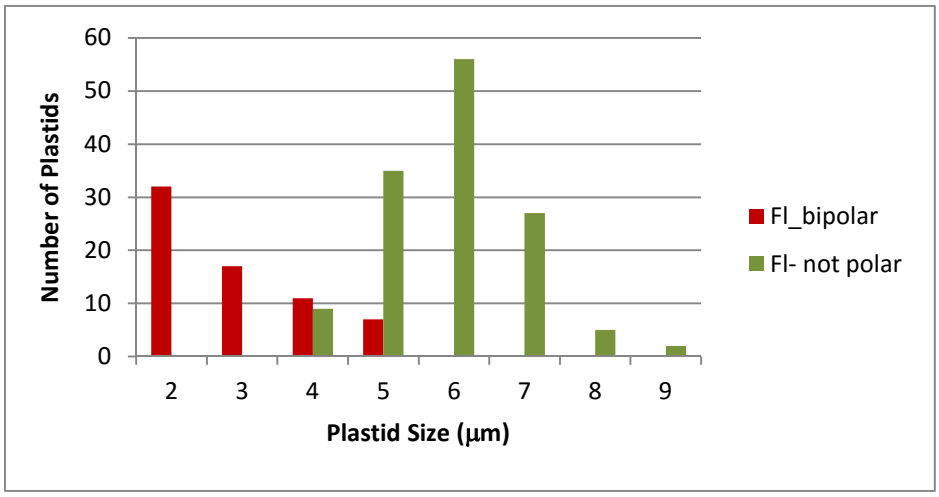

Fig. 3.22. AtKEA2 is located to the two poles of small chloroplasts. In Fig 3.21A and B the presence of bipolar GFP fluorescence and size of the chloroplasts (maximal longitude) were determined.

5. Analysis of the N-terminal domain of AtKEA2

AtKEA1 and AtKEA2 are members of the KEA1a family of KEA antiporters. KEA1a proteins are composed of 3 parts (Figure 3.23): An N-terminal extension of approximately 600 amino acids, a central Na_H antiporter domain, and a C-terminal KTN nucleotide binding domain, also known as TrkA-N or RCK domain.

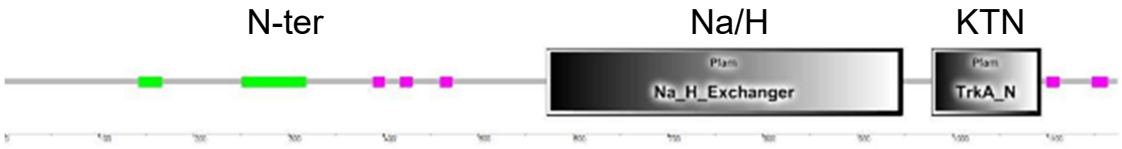

Fig. 3.23. Domain organization of KEA1a proteins. Domains in AtKEA2 were analyzed using the Simple Modular Architecture Research Tool (SMART, http://smart.embl-heidelberg.de/). N-ter; N-terminal domain of AtKEA2, Na/H; Pfam Na_H exchanger domain PF00999, KTN; Pfam TrkA_N domain PF02254, Green; predicted coiled-coil regions, magenta; regions of low complexity.

The N-terminal extension is unique to the KEA1a members of green plants. While the Na_H exchanger domain and the KTN domain are relatively well conserved between green algae and plants, the N-terminal domain is much more variable, and most amino acid stretches that are conserved in higher plants are absent in the algal isoforms (Figures 3.24 and 3.25). This indicates that the N-terminal domain could have become increasingly important from bryophytes onwards. Most transmembrane prediction algorithms predict the presence of a transmembrane span at the C-terminal end of the N-terminus (http://aramemnon.uni-koeln.de/, http://topcons.cbr.su.se/ Figure 3.25).

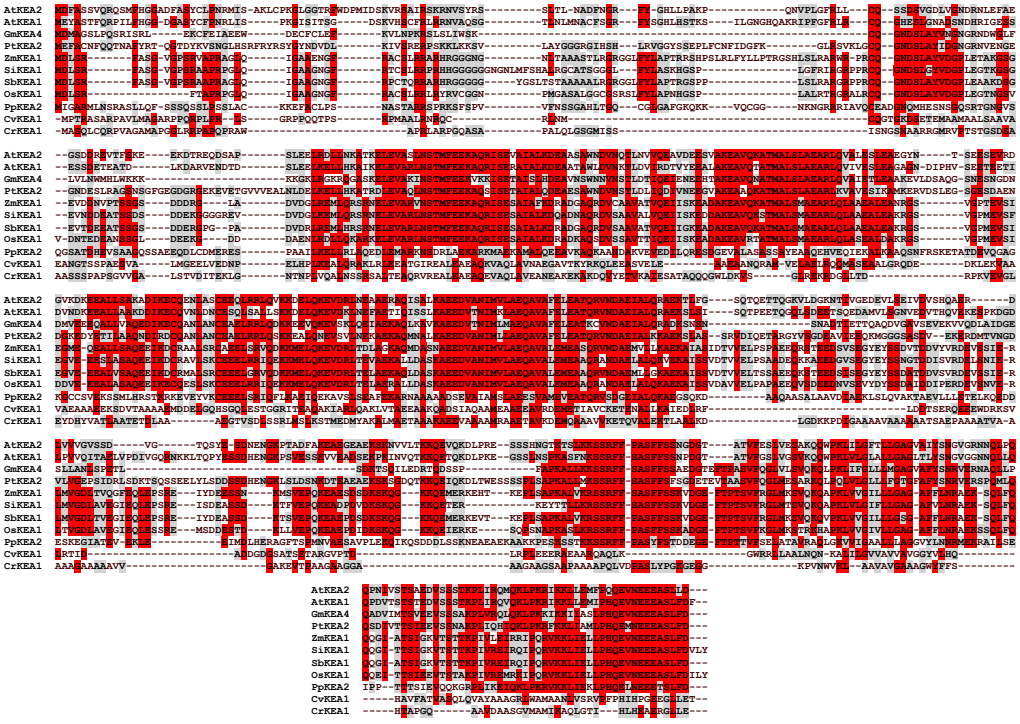

Fig. 3.24. Amino acid sequence of the N-terminal domain. Proteins were identified at the Phytozome website (http://phytozome.jgi.doe.gov/pz/portal.html#) and aligned with Clustalw. Accession numbers: AtKEA1; *Arabidopsis thaliana* AT1G01790.1, AtKEA2; *Arabidopsis thaliana* AT4G00630.1, GmKEA4; *Glycine max* Glyma18g46420.1, PtKEA2; *Populus trichocarpa* POPTR_0014s07660.1, ZmKEA1; *Zea mays* GRMZM2G093643_P01, SiKEA1; *Setaria italica* Si021020m, SbKEA1; *Sorghum bicolor* Sb06g033310.1, OsKEA1; *Oryza sativa* LOC_Os04g58620.1, PpKEA2; *Physcomitrella patens* Pp1s262_91V6.1, CvKEA1; *Chlorella variabilis* E1ZPZ2, CrKEA1; *Chlamydomonas rheinhardtii* Cre04.g220200.t1.1. Numbering of the sequences is according to Chanroj *et al*. (2012). Identical amino acids are shown with red background; similar amino acids are shown with grey background. As an example, the N-terminus of *Chlamydomonas reinhardtii* only shares 13 % identity to the AtKEA2 N-terminus, which contrasts to the 60 % and 69 % identity for the Na/H domain and KTN domain respectively (Fig 3.25).

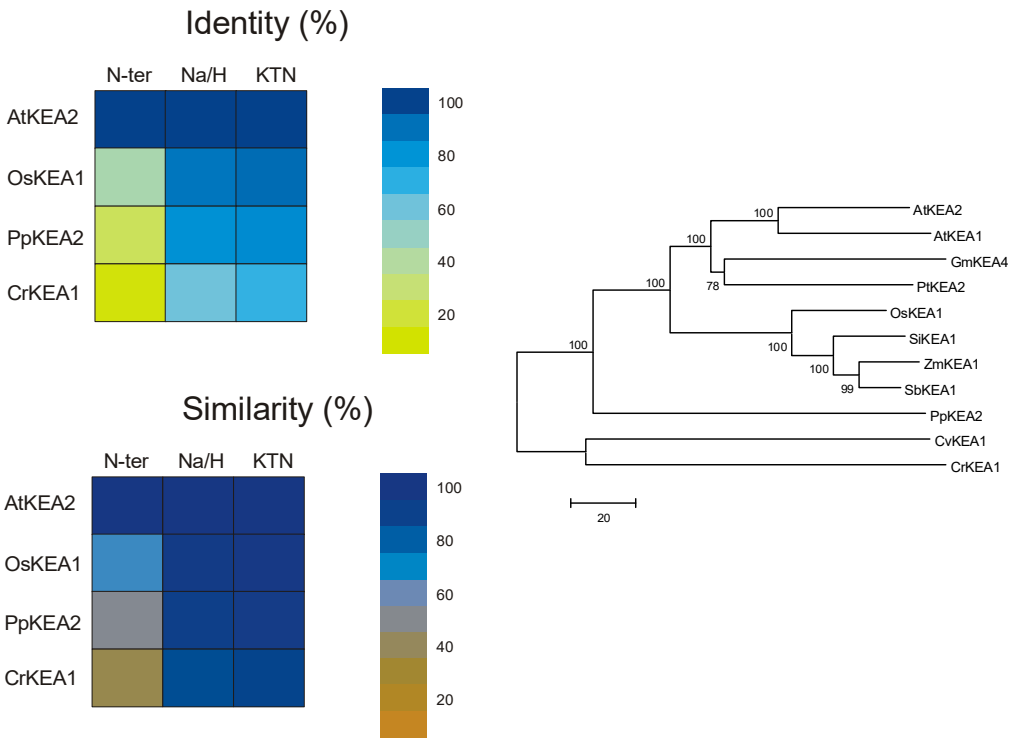

Fig. 3.25. Comparison of sequence homology and phylogenetic analysis of KEA1a proteins. Sequence identity and similarity were calculated based on the ClustalW sequence alignment. A phylogenetic tree of the N-terminal domain was constructed using the maximum likelihood method in MEGA5 (Tamura *et al.,* 2013).

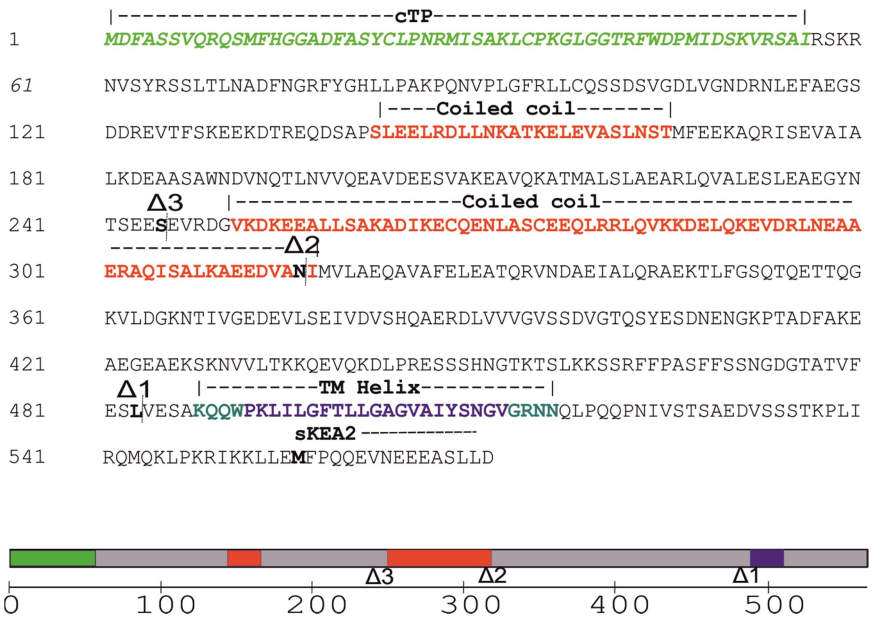

Fig. 3.26. Sequence alignment of the N-terminal domain of KEAIa proteins. Indicated are the deletion mutants made in this study (marked Δ1, Δ2, Δ3), coiled coil regions (according to SMART-EMBL), a putative trans membrane helix and the chloroplast transit peptide (cTP).

The N-terminal domain is rich in charged amino acid residues (Figure 3.26), with a total of 16 % negative charges and 12 % positive charges. The N-terminus is predicted to adopt a long alpha helicoidal conformation, with a high probability for the presence of coiled coil structures (Figures 3.26 and 3.27). Coiled coils consist of two or more alpha-helices winding around each other in a supercoil. On a primary structure level, amino acid sequences with the capacity to form left-handed alpha-helical coiled-coils are characterized by a heptad repeat pattern in which residues in the first and fourth position are hydrophobic, and residues in the fifth and seventh position are predominantly charged or polar. The N-terminal domain has no significant homology to any protein of known function. PSI-Blast search algorithms will indicate some homology to other coiled coil containing proteins like tropomyosin, or spectrin, but the low complexity and repeat nature of the underlying sequence motif of hydrophobic and polar residues interferes with sequence comparison algorithms, which often leads to false predictions of homology between long coiled-coil proteins (Pevsner 2005). Coiled coil containing proteins can have a large variety of functions, mainly related to their capacity to act as "molecular velcro" to stick proteins or membranes or even cells together (Rose *et al.,* 2005). As such coiled coil proteins are important amongst others in cytoskeleton

interactions, cell division, DNA interactions, endocytosis, and vesicle budding and transport or chloroplast movements.

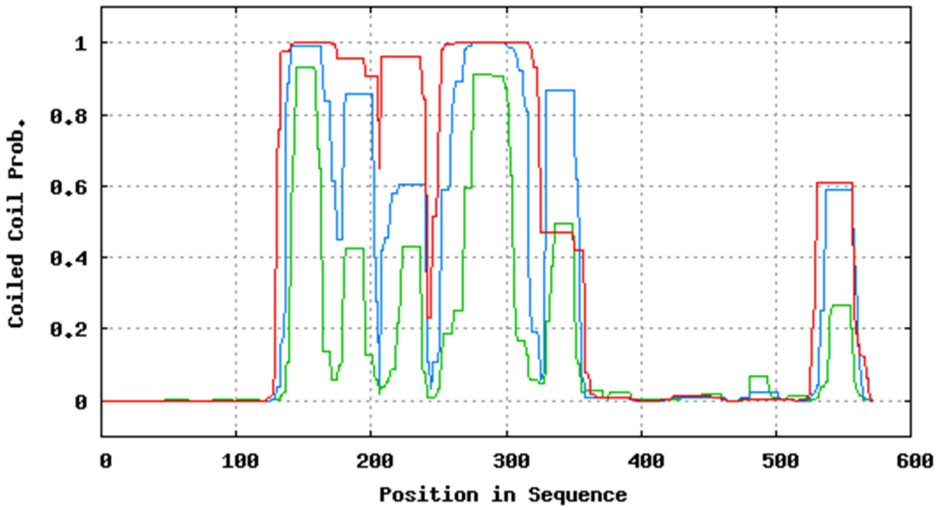

Fig. 3.27. Prediction of coiled coil regions in the AtKEA2 N-terminal domain. Coiled coils were predicted with the coils/pcoils program (http://toolkit.tuebingen.mpg.de/pcoils) based on the sequence shown in Fig. 3.25. A search window of 14 (green), 21 (blue) or 28 (red) amino acids was used to detect coiled coils.

To gain more insight into the possible function of the N-terminal domain of KEA1a type proteins, we tried to predict its 3 dimensional structure using a homology modelling approach. The modelling was performed using two web-based protein homology/analogy recognition engines, I-TASSER (Yang *et al.,* 2015) (Iterative Threading ASSEmbly Refinement; http://zhanglab.ccmb.med.umich.edu/I-TASSER/) and Phyre2 (Kelley *et al.,* 2015) (http://www.sbg.bio.ic.ac.uk/phyre2/html/page.cgi?id=index). Basically both methods rely on comparing a protein sequence of interest with a large database of sequences, to construct an evolutionary or statistical profile of that sequence and to subsequently scan this profile against a database of profiles for known structures. The result is an alignment between two sequences, one of unknown structure and one of known structure. One can then use this alignment, or set of equivalences, to construct a model of one sequence on the basis of the structure of another. Both Phyre2 and I-TASSER gave similar results. We used the N-terminal domain of AtKEA2, without the chloroplast targeting sequence as query sequence. Both approaches yielded a reasonable

top match to the Bacillus subtilis cell division inhibitor protein Ezra (Cleverley et al., 2014) (Figure 3.28). It has to be taken into account that the model is based on only 10 % identity between the two protein sequences, that coiled-coil conformations are notoriously difficult to detect based on sequence alone and that coiled-coil patterns interfere with sequence homology algorithms (see above). It is however certainly possible that the helicoidal N-terminus of AtKEA2 adopts the type of spectrin repeats as in the Ezra protein. Using rice OsKEA1 N-terminus or Clamydomonas rheinhardtii CrKEA1 N-terminus as query protein yielded a very similar result. The Ezra protein is important for inhibition of aberrant FtsZ division ring formation at the cell poles and has also a function as scaffolding protein coordinating lateral growth with cell wall biosynthesis (Land et al., 2014). The bacterial division machinery is partially conserved between chloroplasts and gram-negative bacteria, but no homologs of Ezra have been identified in gram-negative bacteria so far (Nakanishi et al., 2009; Osteryoung et al., 2014)

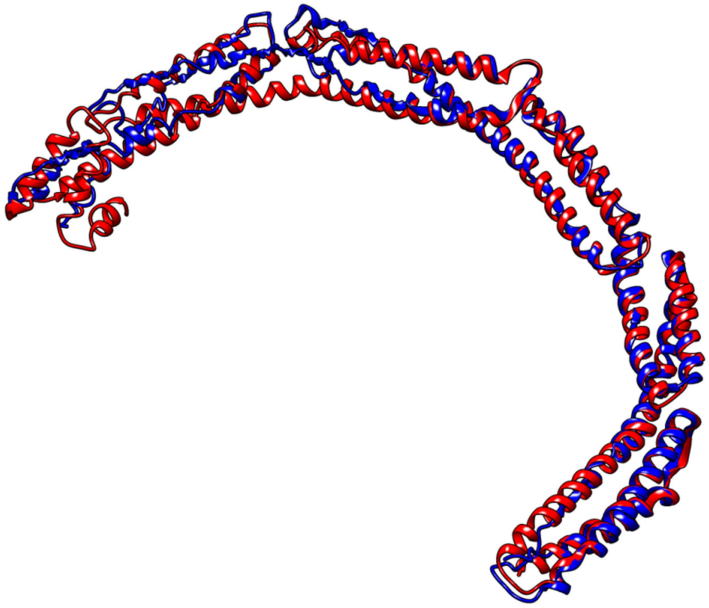

Fig. 3.28. Predicted AtKEA2 N-terminus structure. The predicted KEA2 N-terminal structure as modelled by I-TASSER is shown superimposed on the structure of the cytoplasmic domain of the septation ring formation regulator Ezra of *Bacillus subtilis* pdb template structure 4uxv (DOI: 10.2210/pdb4uxv/pdb). The predicted AtKEA2 N-terminus structure is shown in blue, the Erza template structure is shown in red. The predicted structure has a C-score of -0.90. C-score is a confidence score for estimating the quality of predicted models by I-TASSER. It is calculated based on the significance of threading template alignments and the convergence parameters of the structure assembly simulations. C-score is typically in the range of [-5, 2], where a high C-score signifies a model with a high confidence. Other structures predicted by I-TASSER have C-scores lower than -2.5.

5.1 Study of AtKEA2 N-terminal domain membrane interactions by deletion analysis in yeast

The AtKEA2 N-terminal domain was initially considered to be a soluble extension, although some prediction programs predict the presence of a transmembrane (TM) helix at the C-terminal end (Figure 3.29). To test whether the N-terminal domain constitutes a soluble or a membrane associated protein, we cloned the N-terminal domain and 3 deletion mutants (Figure 3.26) in yeast under control of the galactose inducible promoter. The complete protein expressed in yeast growing on galactose was recovered in the microsomal fraction only, and is thus strongly bound to the membrane (Figure 3.30).

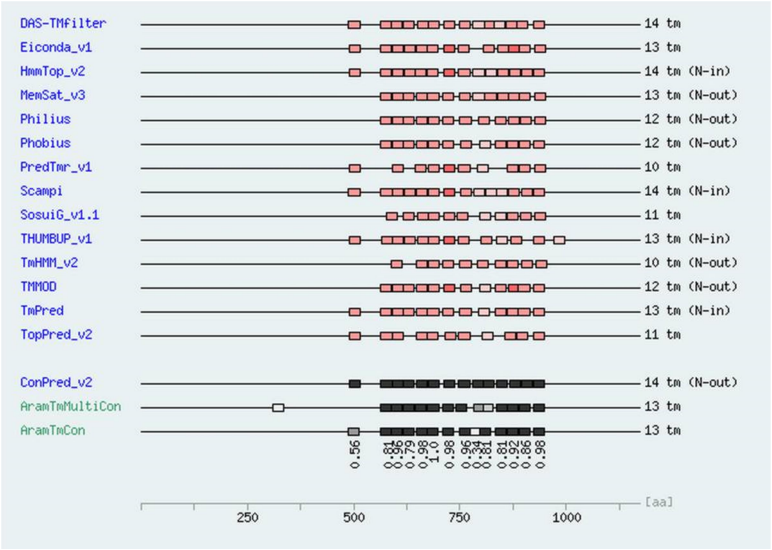

Fig. 3.29. Prediction of transmembrane helices in AtKEA2. Most programs predict one extra Tm span just before the central Na/H exchanger core that contains 10 to 13 TM helices. (http://aramemnon.uni-koeln.de/).

After deletion of the most C-terminal amino acid stretch (Δ1), a substantial amount of the protein is recovered in the 100.000 g supernatant fraction, indicating that this region indeed contains a true transmembrane helix (Figure 3.30). However, although the protein is recovered from the soluble fraction after deletion of the trans membrane helix (Δ1) or after deletion of the amino acids up to the second predicted coiled coil domain (Δ2), a large fraction of the protein is still recovered in the membrane pellet, showing that the region comprising the two coiled coils is also associated to the membrane

(Figure 3.30). Finally, after deletion of the second coiled-coil domain (Δ3), the protein could no longer be detected (Figure 3.30).

In a linear sucrose gradient, the protein shows a broad distribution, typical of endoplasmic reticulum membrane localization (Figure 3.31), indicating that protein sedimentation is not the result of the formation of insoluble misfolded aggregates.

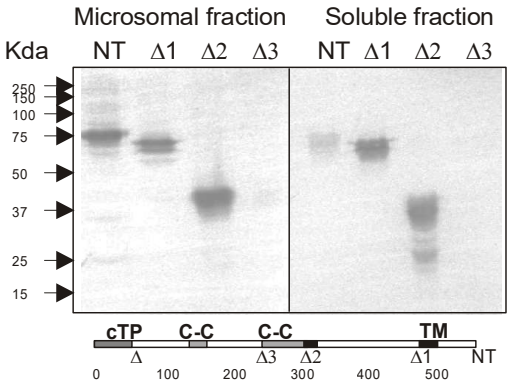

Fig. 3.30. Western blot showing membrane localization of the AtKEA2 N-terminal domain expressed in yeast. The N-terminus of AtKEA2 as well as several deletion mutants were cloned in yeast, fused to a C-terminal V5-H6 epitope tag. Microsomal membranes and soluble proteins were isolated from yeast cells. Western blotting of microsomal and soluble fractions was performed using a mouse V5 monoclonal antibody. The schematic figure on the bottom shows the location of the deletions. cTP; chloroplast targeting peptide, C-C; predicted coiled coils (according to SMART-EMBL), TM; putative transmembrane helix. NT; complete N-terminus, without the cTP sequence (R57-E555). Δ1; as NT but deleted at position Δ1 (R57-L483), eliminating the putative trans membrane helix. Δ2; as NT, deleted at position Δ2 (R57-N316). Δ3; as NT deleted at position Δ3 (R57-S245).

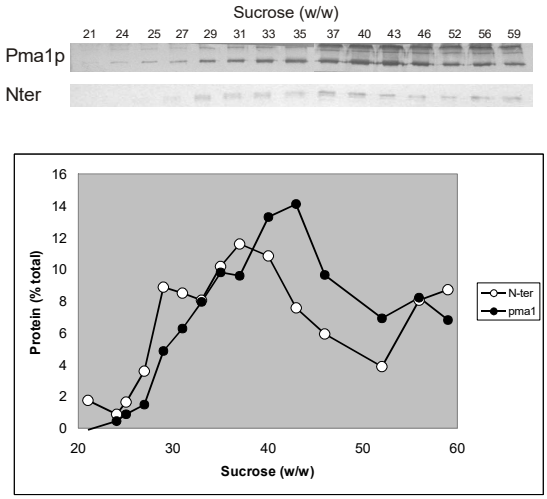

Fig. 3.31. Distribution of AtKEA2 N-terminus in a linear sucrose gradient. Microsomal membranes of yeast, expressing the AtKEA2 N-terminus fused to a V5-H6 epitope were loaded on a 30 ml linear sucrose gradient and centrifuged overnight as indicated in material and methods. Fractions were analyzed for the presence of the N-terminus by western blotting. As a control the plasma membrane H^+-ATPase Pma1p was used. Density of the bands was estimated in ImageJ, using the formula ($Band_m$-$Back_m$)* Area, where $Band_m$ is the intensity of the band, $Back_m$ the intensity of a similar region of background color, and Area the surface area of the band analyzed. Intensity is in linear color space from 0 to 255 for a greyscale image. AtKEA2 N-terminus, white circles; Pma1p, black squares.

To test the type of membrane interactions, we tried to extract the AtKEA2 N-terminus and the N-terminus without its putative TM span from the membrane fraction by using detergent or chaotropic agents (Figure 3.32).

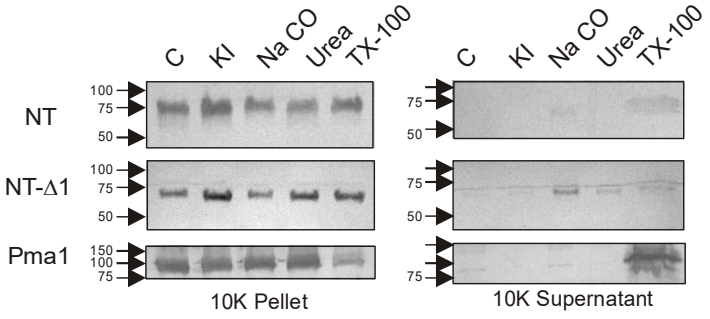

Fig. 3.32. Solubilization of the AtKEA2 N-terminus. Microsomal membranes of yeast cells expressing the AtKEA2 N-terminus were treated with the chaotropic agents KI (0.6M), Na_2CO_3 (0.1M, pH 11,5) or Urea (2.5M), or with the detergent Triton X-100 (1%), as indicated in material and methods. After treatment the fractions were centrifuged at 100.000 g for 30 min. The pellet and supernatant were analyzed for the presence of N-terminal domain by western blotting using a monoclonal antibody against the V5-H6 epitope. As a control, a monoclonal antibody against the plasma membrane H^+-ATPase Pma1p was used.

While a detergent like Triton X-100 is expected to be able to solubilize true hydrophobic integral membrane proteins from the membrane, chaotropic agents extract preferentially peripheral membrane bound proteins, by disrupting interactions between hydrophobic patches of the otherwise hydrophilic protein with lipids or membrane embedded proteins. None of the treatments, not even Triton X-100 treatment, could extract the complete AtKEA2 N-terminus from the membrane fraction (Figure 3.32). After deletion of the putative transmembrane domain, a substantial amount of the protein could be extracted by alkaline washes with Na_2CO_3, pH 11.5, showing this part of the protein is indeed more peripheral bound to the membrane. However, none of the treatments succeeded in fully solubilizing the AtKEA2 N-terminal domain. As a control we show that the yeast plasma membrane proton ATPase Pma1p, a true integral membrane protein, is only solubilized from the membrane by treatment with detergent Triton X-100 (Figure 3.32).

5.2. Interaction of AtKEA2-GFP with the division ring formation protein FtsZ

The localization of AtKEA2 to the poles of developing chloroplasts, as well as the developmental phenotypes observed and the reduced number of chloroplasts in double mutant plants suggests a role for AtKEA2 in chloroplast development and division. The homology modelling approach of the N-terminal domain indicates that this role for AtKEA2 might be related to specific interactions with chloroplast cytoskeleton-like proteins involved in chloroplast development and division. An important protein interacting with the Ezra protein is the tubulin-GTPase FtsZ that forms the inner chloroplast division ring (Z-ring) (Osteryoung and Pyke, 2014). We therefore studied interactions between FtsZ and AtKEA2 by Co-immunoprecipitation. The AtKEA2-GFP protein could be pulled down from total protein extracts using the GFP-Trap system. We tested in the same fractions for the presence of FtsZ1 and FtsZ2 (see material and methods). Although the AtKEA2 protein could be detected in these fractions, western blotting using polyclonal antibodies against FtsZ1 and FtsZ2 did not give any signal (Figure 3.33).

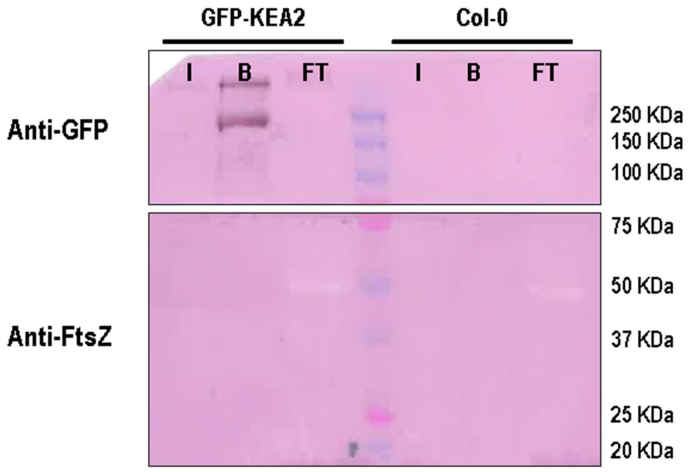

Fig. 3.33. Study of interaction of AtKEA2-GFP with FtsZ1 and FtsZ2. AtKEA2-GFP was purified using the GFP-Trap system (see material and methods). Proteins were eluted from the beads, and essayed for the presence of AtKEA2-GFP using an anti-GFP antibody. I: Input total protein fraction. B: Protein eluted from the magnetic beads after binding. FT: Flow through fraction of unbound proteins. The anti-GFP antibody conjugated to magnetic beads effectively binds AtKEA2-GFP as can be seen from the western blot signal in the bound fraction. No positive signal is however observed when this fraction is probed with the FtsZ polyclonal antibody. In total protein extracts the concentration of both proteins appears to low to be detected by the used antibodies.

As an alternative approach, we incubated yeast microsomal membranes expressing the AtKEA2 N-terminal domain with chloroplast stromal proteins. As control we incubated stromal proteins with yeast microsomal membranes not expressing the AtKEA2 N-terminus. The mixture was centrifuged again, and the pellet assayed for the presence of FtsZ1 and FtsZ2 proteins. We did not observe a clear difference between the pattern observed in microsomes expressing the AtKEA2 N-terminus or not (data not shown). These results indicate there is no direct interaction between AtKEA2 and FtsZ1 or FtsZ2. It has however to be taken into account that the polyclonal antibody to FtsZ1 and FtsZ2 in our hands shows little specificity and a rather weak signal with high background in western blot analysis of chloroplast proteins (Figure 3.34).

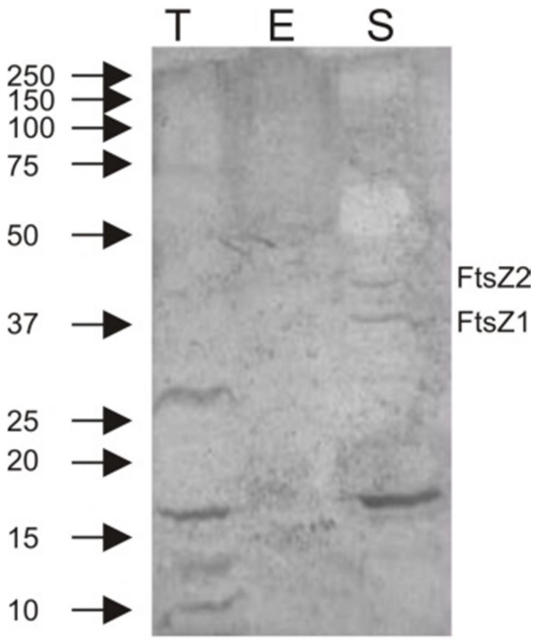

Fig. 3.34. Western Blot of chloroplast Thylakoid (T), Envelope (E) and Stromal (S) proteins using a polyclonal antibody to FtsZ1 and FtsZ2 (Agrisera).

5.3. Role of the N-terminal domain in localization of AtKEA2

The localization of AtKEA2 to the poles in developing chloroplasts envelope membrane suggests specific interactions of some domains of AtKEA2 with proteins or lipids at these locations. We hypothesized that the unusual N-terminal domain of >550 residues might have a role in such an interaction. To test this hypothesis, we deleted the N-terminal domain from the AtKEA2 protein, and stably transformed *Arabidopsis thaliana* WT plants with this construct. Indeed, the protein without the N-terminal domain was distributed throughout the envelope membrane (Figure 3.35), strongly supporting that the N-terminus contains the signal required for faithful localization of the AtKEA2 protein. While we could readily select double mutant plants transformed with the full length AtKEA2-GFP protein based on recovery of the WT growth phenotype (Figure 3.19A and 3.19C), we could not do the same with double mutant plants transformed with the AtKEA2-GFP protein without the N-terminus, as none of the plants recovered normal growth and greening. This indicates that the N-terminal domain is required for the physiological function of the antiporter. It was previously shown that the AtKEA2 protein without the N-terminal domain is an active K^+/H^+ antiporter when expressed in yeast (Aranda-Sicilia *et al.,* 2012). Thus our results

strongly suggest that targeting of AtKEA2 to the poles of young developing chloroplasts by the N-terminal domain is essential for the role of this antiporter in chloroplast and plant development.

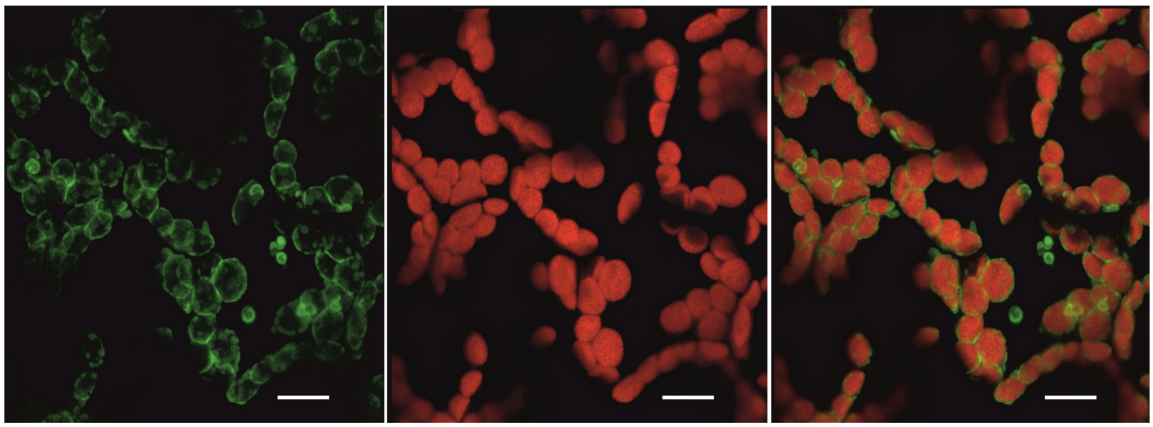

Fig. 3.35. The N-terminal domain is required for polar localization of AtKEA2. The transport domain of AtKEA2-GFP protein (residue M556-I1174) distributes evenly around plastids. Bars = 10 μm. The transport domain of AtKEA2 protein was stably expressed in WT *Arabidopsis thaliana*. From left to right: GFP fluorescence, chlorophyll fluorescence and overlay of GFP and chlorophyll fluorescence.

V. DISCUSSION

In this Thesis the Potassium/Proton antiporters AtKEA1 and AtKEA2 were studied. The plant KEA transporters are members of the CPA2 family of Cation / Proton antiporters, and share homology to bacterial K^+ efflux systems KefB and KefC. In the laboratory where the present work was carried out, it was previously determined that AtKEA1 and AtKEA2 are Cation/Proton antiporters with K^+/H^+ exchange activity that are localized to the chloroplast (Aranda-Sicilia *et al.,* 2012), but no information on the physiological function of the proteins in plants was available.

pH and K^+ homeostasis are fundamental to photosynthetic reactions in plastids, though the molecular basis of pH and cation homeostasis is largely unknown. The maintenance of an alkaline stromal pH and thus a pH gradient across the envelope membrane was suggested to depend on an active H^+-extruding ATPase in combination with K^+ and Cl^- fluxes (Demmig and Gimmler, 1983; Heibert *et al.,* 1995; Neuhaus and Wagner, 2000; Pottosin *et al.,* 2005). Light induced electrogenic K^+ uptake is predicted to cause osmotic swelling of the organelle. Photosynthesis reactions are sensitive to such chloroplast volume changes, and a plausible role for KEA antiporters in the envelope membrane is thus volume control by catalyzing pH gradient coupled K^+ efflux. During the course of these thesis Kunz et al. (2014) indeed published that *Arabidopsis thaliana kea1kea2* double mutants have enlarged swollen chloroplasts that are very fragile. This was taken as evidence that the osmotic homeostasis was perturbed in these chloroplasts. It was also shown that chloroplasts from double mutant plants had a reduced thylakoid pH gradient and reduced photosynthetic quantum yield in the young sections of the leaves, indicating that perturbed ionic and osmotic homeostasis led directly to reduced photosynthetic efficiency. It was suggested that K^+ export by AtKEA1/AtKEA2 could operate in parallel to K^+ efflux from the thylakoid lumen mediated by the channel TPK3, while H^+ uptake by AtKEA1/AtKEA2 could counterbalance light induced proton uptake into the thylakoid lumen, thus creating a pathway for proton/potassium exchange between cytosol and thylakoid lumen.

In this thesis we show that, although AtKEA1 and AtKEA2 might be involved in maintaining osmotic and ionic balance as suggested above, the effects of disruption of AtKEA1 and AtKEA2 are much more profound, and impact on early chloroplast and thylakoid membrane development. Our data are in agreement with the report by Sheng et al. (2014), who showed that disruption of the rice AtKEA1/2 homologue, OsKEA1, caused symptoms related to defects in chloroplast development.

To obtain information on the function of AtKEA1 and AtKEA2, we studied the phenotypes of *Arabidopsis thaliana* mutants with T-DNA insertions in the AtKEA1 and AtKEA2 sequence. We also studied the localization of the AtKEA2 protein in chloroplasts in more detail by transforming *Arabidopsis thaliana* with a construct for expression of an AtKEA2-GFP fusion protein.

AtKEA2 is an inner envelope protein

Experiments with isolated chloroplasts from plants stably expressing the AtKEA2-GFP construct clearly show that the protein localizes to the inner envelope. GFP fluorescence is observed as a ring surrounding the chloroplasts, although some local patches can be observed (Figure 3.20). These data were confirmed during the course of this work by the report Kunz et al. (2014).

AtKEA1 and AtKEA2 are important for chloroplast development

Arabidopsis thaliana kea1 and *kea2* T-DNA single mutants do not show any obvious alteration of growth. *kea1kea2* double mutants are however much smaller and show pale/yellowish leaves (Figures 3.5, 3.6). This indicates that AtKEA1 and AtKEA2 have redundant functions, in accordance with their high (98%) sequence identity.

Intriguingly, *kea1kea2* double mutants showed reduced growth and a reduced Chl content primarily in newly developing leaves, but less obvious in later growth stages (Figures 3.5 to 3.9). Newly emerging leaves are first yellow, but turn green progressively, closely following leaf development from proliferation to expansion zones (Figure 4.1).

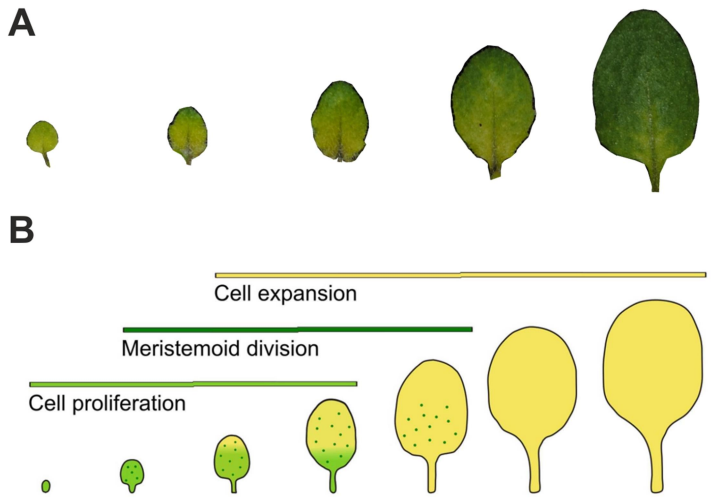

Fig. 4.1. (A). A leaf from a *kea1kea2* double mutant *Arabidopsis thaliana* plant at different developmental stages. Greening progresses from tip to base. (**B). A scheme of Arabidopsis thaliana leaf development**. Leaf development consists of a proliferation and expansion phase. Young leaves increase in size by cell division (proliferation). During a transition phase, cell division first ceases at the tip, and gradually most cells exit the cell cycle and start to expand in a basipetal (from tip to base) manner. While most cells enter the expansion phase, some cells, the meristemoid cells, undergo further divisions and form special cell types like stomatal cells and epidermal cells or vascular cells. Adapted from (Vanhaeren et al. 2015).

Early leaf growth is sustained by cell proliferation and subsequent cell expansion that initiates at the leaf tip and proceeds in a basipetal direction. Genes differentially expressed during the transition from cell proliferation to expansion are especially those involved in cell cycle, photosynthesis, and chloroplast retrograde signaling. Furthermore, it was found that differentiation of the photosynthetic machinery is important for regulating the exit from proliferation (Andriankaja *et al.,* 2012). Recovery of pigmentation is typical of virescent mutants that show defects in photosynthetic pigments in young and emerging tissues, but gradually turn green along the leaf proximal-distal axis. This is often related to altered expression of genes involved in early chloroplast biogenesis, especially thylakoid membrane formation, causing delayed chloroplast development (Chi *et al.,* 2010; Jarvis and López-Juez, 2013; Qi *et al.,* 2016). The observed growth phenotype is thus a clear indication that AtKEA1 and AtKEA2 have a role in chloroplast development. Why pigmentation recovers in virsecent mutants is not well described. We suggest that when growth slows down, chloroplasts of *kea1kea2* plants, which are delayed in development can catch up, resulting in less severe phenotypes in older leaves.

In accordance with a role for AtKEA1 and AtKEA2 in chloroplast development young yellow leaves of double mutant plants show strongly reduced amounts of protein complexes involved in photosynthetic electron transport (Figure 3.11). Thylakoid membranes in plastids of yellow sections of double mutant leaves are disorganized, not aligned, and show strongly reduced stacking compared to thylakoids in WT seedlings (Figure 3.13). These results point again to a role of inner envelope AtKEA1/2 in thylakoid biogenesis, formation and maintenance. Thus, the observed reduction in photosynthetic parameters of *kea1kea2* double mutants (Figure 3.12) is most likely a consequence of impaired or delayed chloroplast differentiation.

A striking observation is that AtKEA2 protein is concentrated to the poles in young developing chloroplasts, while it is localized in non-polar spots in mature chloroplasts (Figure 3.21). Furthermore, we observed that AtKEA2 protein accumulation is highest in small developing plastids and dividing plastids of first true leaves. AtKEA2 protein accumulation appears to be regulated developmentally and in response to light, because it is significantly reduced or absent in etiolated seedlings and mature differentiated chloroplasts (Figure 3.21). The localization of AtKEA2 to young developing and dividing chloroplasts further supports a role for K^+/H^+ antiport in early chloroplast development

The long N-terminal domain attaches AtKEA1/2 to a specific location

Our data show that the long N-terminal domain in KEAIa antiporters is important for the polar localization. This N-terminal domain of >550 residues upstream of the antiporter domain is a unique feature of plant and algal KEAIa sequences. The domain is rich in charged residues, and is predicted to form coiled-coil structures (Chanroj *et al.,* 2012). Most coiled-coil domains hold together molecules, subcellular structures, and even tissues (Rose *et al.,* 2005). In accordance, it was shown previously that AtKEA1 and AtKEA2 proteins are present in large protein complexes of unknown functions at the inner envelope (Roston *et al.,* 2012). In chloroplasts, roles for coiled-coil proteins have been reported in chloroplast division, thylakoid membrane development and chloroplast relocation in response to light, fundamentally by interaction with cytoskeleton-like elements. The homogeneous distribution in the envelope membrane of the AtKEA2 protein without the N-terminal extension (Figure 3.35) demonstrates that the N-terminus is essential to target AtKEA2 to specific domains. Furthermore, although the AtKEA2 protein without the N-terminal domain constitutes an active

antiporter (Aranda-Sicilia *et al.,* 2012), it fails to complement the growth defects of the double mutant plants, suggesting that the specific localization of the protein is crucial for its function. By expressing the N-terminal domain of AtKEA2 in yeast, we show that this domain of AtKEA2 most likely contains a trans-membrane stretch at the C-terminal end, but that the region containing the coiled-coil domains binds to the membrane as well (Figures 3.30 to 3.32). Association of oligomers of AtKEA2 could depend on membrane tension or curvature, which is highest at the poles, but more relaxed at the mid-cell (Laloux and Jacobs-Wagner, 2014; Strahl *et al.,* 2015). Tension or compression dependent interaction of coiled-coil domains with lipid membranes has been reported for instance for the Bar-domain superfamily of proteins (Frost *et al.,* 2009; Rabe *et al.,* 2014). This would also explain why AtKEA2-GFP fluorescence in isolated round chloroplasts is more homogeneously distributed in the inner envelope (Figures 3.20 and 3.21). Alternatively, the localization could be due to protein-lipid or protein-protein interactions at subdomains in the envelope with specialized functions (Laloux and Jacobs-Wagner, 2014).

Relation of AtKEA2 and AtKEA1 to chloroplast fission and osmoregulation

In relation to WT plants, *kea1kea2* double mutants contain less chloroplasts, with a slightly bigger and heterogeneous size (Figures 3.14 to 3.16), which is a feature of chloroplast division mutants (Osteryoung and Pyke, 2014). The size of mutant leaves is smaller than WT at the same age (Figures 3.5 to 3.7), in agreement with the observation that plastid division and cell division and expansion are linked (Vanhaeren *et al.,* 2015). It also appears that mesophyll cells from double mutant plants are smaller (Figure 3.16), although this was not statistically verified.

Like AtKEA1 and AtKEA2, chloroplast inner envelope mechanosensitive channels MSL2 and MSL3 were shown to be important for osmoregulation in plastids (Haswell and Meyerowitz, 2006). The MSL channels also play an important role in plastid division and FtsZ division ring placement, although the mechanism is not clear (Wilson and Haswell, 2012). MSL2 and MSL3 show a similar patchy localization in mature chloroplasts as observed for the AtKEA1 and AtKEA2 antiporters (Haswell and Meyerowitz, 2006). It is thus tempting to suggest that both MSL channel and KEA antiporters share a function in the pathway that links osmoregulation to plastid fission. In this sense the putative structural homology of the AtKEA2 N-terminal domain to the

B subtilis cell division inhibitor protein Ezra is intriguing (Figure 3.28) (Cleverley *et al.,* 2014). The Ezra protein is important for inhibition of aberrant FtsZ division ring formation at the cell poles in gram-positive bacteria (Land *et al.,* 2014). The chloroplast division machinery is partially derived from the cyanobacterial gram-negative ancestor, and no Ezra homologs are found in chloroplasts (Nakanishi *et al.,* 2009; Osteryoung and Pyke, 2014). Possible the AtKEA2 N-terminal domain has evolved in chloroplasts to perform a function similar to the Ezra protein in gram-positive bacteria. However, we could not show any direct protein-protein interactions of AtKEA2 with the division protein FtsZ (Figure 3.33), indicating that the observed effects on chloroplast division are indirect.

Role of AtKEA1 and AtKEA2 in abiotic stress tolerance

We observed in this work that the chlorotic and small-size phenotype of the double mutant *kea1kea2* plants partially recovers in media supplemented with NaCl (Figure 3.17). A similar observation was made by (Kunz *et al.,* 2014). These authors also determined that ultrastructure of chloroplasts from NaCl grown double mutant plants resembled those of wild type plants and that photosynthetic parameters recovered in the double mutant plants grown in media supplemented with NaCl. It was suggested that these effects were due to higher cytoplasmic osmotic values due to salt accumulation which could counteract the high osmotic value of double mutant chloroplasts. Sheng at al. (2014) showed that the OsKEA1 gene is induced by KCl and NaCl, and that seed germination is delayed in kea1 mutant rice plants at high KCl concentrations. Most strikingly however the kea1 mutant rice plants showed enhanced drought tolerance. The authors suggest that this was due to over accumulation of H_2O_2 in the mutant plants, causing stomatal closure through increased ABA production. In our electron microscopy pictures (Figure 3.13) we also see an increased number of plastoglobuli, indicating increased photooxidative stress which might also be related to increased ROS production. It thus appears that enhancement of abiotic stress tolerance by disruption of KEA antiporters is not related to the primary function of these transporters, but caused by indirect effects.

Model: biogenesis centers for thylakoids

Formation of thylakoid membranes requires the synthesis, import and assembly of lipids, proteins and pigments to form the complexes for electron transport and ATP synthesis. One unanswered question is how lipids that are assembled at the envelope membrane, as well as pigments and photosynthetic complexes reach their final destination. Three hypothesis are currently proposed: i) formation of invaginations from the envelope membrane ii) a vesicle transport mechanism and iii) transfer of lipids by lipid binding proteins (Rast *et al.,* 2015). Distinct biogenesis centers at the envelope membrane for the formation of thylakoid membranes have been proposed for decades (Vothknecht and Westhoff, 2001; Rast *et al.,* 2015). The specific localization of AtKEA2 to the poles of young developing chloroplasts combined with the effect of AtKEA2 and AtKEA1 disruption on thylakoid membrane formation suggests that the chloroplast poles have a special function in chloroplast development, and possibly represent such 'biogenesis centers'. Biogenesis centers have been shown to exist in cyanobacteria where they form a separate membrane fraction at the thylakoid membrane-plasma membrane contact points (Nickelsen and Zerges, 2013). Contact points of thylakoid membranes with the plasma membrane can be clearly seen in 3D micrographs of a cyanobacterium (Nierzwicki-Bauer *et al.,* 1983). Evidence to support this model in higher plants has been challenging due to the transient nature of membrane remodeling in plastids (Shimoni *et al.,* 2005). It was suggested that during the transition of proplastids to chloroplasts, thylakoid membranes originate from invaginations of the inner envelope in algal chloroplasts or proplastids of vascular plants, while in mature chloroplasts the membrane system is maintained by vesicle transport (Rast *et al.,* 2015). AtKEA2 K^+/H^+ antiport at biogenesis centers could be responsible for formation or swelling of invaginations or vesicles before budding off from the envelope. Chloroplast vesicle transport mechanisms have been proposed to exist in plants, but seem to be absent in green algae (Westphal *et al.,* 2003; Vothknecht *et al.,* 2012). Compared to land plants, the KEA N-terminal domain in green algae is much shorter and misses almost all the conserved domains, which would infer a specific function for this domain in land plants (Chanroj *et al.,* 2012). As chloroplasts mature, thylakoids are likely maintained by thylakoid envelope contact sites. Thylakoid

membranes converge at two poles in wild-type chloroplasts, but in *kea1kea2* mutants, thylakoids are disorganized, and not aligned with the axis of the organelle (Figure 3.13). These results support the idea that AtKEA1 and AtKEA2 mediated K^+ and pH homeostasis at these 'centers' or micro domains is important for the proper formation and alignment of the thylakoid membrane.

VI. CONCLUSIONS

1. AtKEA1 and AtKEA2 are chloroplast inner envelope Cation/Proton Antiporters that are abundant most of all in aerial tissues. Contrary to double disruption mutants, single *atkea1* or *atkea2* mutants do not show a clear phenotype, indicating their function is redundant.
2. Double mutant *atkea1atkea2* plants are small in size and show a chlorotic phenotype in a developmental gradient. Proliferating leaf zones are chlorotic, but pigmentation recovers in expansion and mature zones. Such phenotype is typical of virescent mutants, generally affected in chloroplast biogenesis.
3. AtKEA1 and AtKEA2 play a role in chloroplast biogenesis, thylakoid membrane formation and chloroplast division. Chloroplasts from young leaves of double mutant plants are swollen have disorganized and less stacked thylakoid membranes and dramatically reduced amounts of photosynthetic protein complexes and pigments. Photosynthetic performance is reduced in young leaf sections.
4. AtKEA2 has a long N-terminal extension that contains domains predicted to adopt coiled-coil conformations. The domain shows homology to a bacterial cell division regulator. The domain is essential for the physiological function of KEA2 in *Arabidopsis thaliana*.
5. AtKEA2 is targeted specifically to the poles or caps of young dividing chloroplasts. This localization depends on the presence of the AtKEA2 N-terminal domain. In yeast the N-terminal domain is shown to bind very strongly to the membrane fraction.
6. The localization of AtKEA2 to the poles in young chloroplasts or to micro domains in the inner envelope in mature chloroplasts suggests that these locations have a special role in thylakoid membrane formation.

VII. REFERENCIES

Abrahamsen, M.S., Templeton, T.J., Enomoto, S., Abrahante, J.E., Zhu, G., Lancto, C.A., Deng, M., Liu, C., Widmer, G., Tzipori, S., Buck, G. A., Xu,P., Bankier, A.T., Dear, P. H., Konfortov, B.A., Spriggs, H.F., Iyer, L., Anantharaman,V., Aravind, L., and Kapur,V.(2004). Complete genome sequence of the apicomplexan, Cryptosporidium parvum. *Science*, *304(*5669), 441–445.

Ache, P., Becker, D., Deeken, R., Dreyer, I., Weber, H., Fromm, J., & Hedrich, R. (2001). VFK1, a Vicia faba K+ channel involved in phloem unloading. *The Plant Journal*, *27*(6), 571-580.

AGI. The *Arabidopsis thaliana* Genome Initiative (2000). Analysis of genome sequence of the flowering plant *Arabidopsis thaliana*. *Nature*, 408 (6814), 796-815.

Ahmad, I., & Maathuis, F. J. (2014). Cellular and tissue distribution of potassium: physiological relevance, mechanisms and regulation. *Journal of Plant Physiology*, *171*(9), 708-714.

Aldridge, C., Cain, P., & Robinson, C. (2009). Protein transport in organelles: protein transport into and across the thylakoid membrane. *FEBS Journal*, *276*(5), 1177-1186

Amtmann, A., Armengaud, P., & Volkov, V. (2004). Potassium nutrition and salt stress. *Membrane Transport in Plants. Blackwell, Oxford*, 293-339.

Andrés, Z., Pérez-Hormaeche, J., Leidi, E. O., Schlücking, K., Steinhorst, L., McLachlan, D. H., Schumacher, K., M. Hetherington, A., Kudla J., Cubero B., & Pardo, J. M. (2014). Control of vacuolar dynamics and regulation of stomatal aperture by tonoplast potassium uptake. *Proceedings of the National Academy of Sciences USA*, *111*(17), E1806-E1814.

Andriankaja, M., S. Dhondt, S. De Bodt, H. Vanhaeren, F. Coppens, L. De Milde, P. Mühlenbock, A. Skirycz, N. Gonzalez, Gerrit T. S. Beemster and D. Inzé (2012). "Exit from Proliferation during Leaf Development in *Arabidopsis thaliana*: A Not-So-Gradual Process." *Developmental Cell 22*(1): 64-78.

Aranda-Sicilia, M. N., Cagnac, O., Chanroj, S., Sze, H., Rodríguez-Rosales, M. P., & Venema, K. (2012). *Arabidopsis thaliana* KEA2, a homolog of bacterial KefC, encodes a K+/H+ antiporter with a chloroplast transit peptide. *Biochimica et Biophysica Acta (BBA)-Biomembranes*, *1818*(9), 2362-2371.

Arkin, I., Xu, H., Jensen, M., Arbely, E., Bennett, E., Bowers, K., Chow, E., Dror, R., Eastwood, M., Flitman-Tene, R., Gregersen, B., Klepeis, J., Kolossvary, I., Shan, Y. and Shaw, D. (2007). Mechanism of Na+/H+ Antiporting. *Science*, 317(5839), pp.799-803.

Armbruster, U., Carrillo, L., Venema, K., Pavlovic, L., Schmidtmann, E., Kornfeld, A., Jahns, P., Berry, J., Kramer, D. and Jonikas, M. (2014). Ion antiport accelerates photosynthetic acclimation in fluctuating light environments. *Nature Communications*, p.5439.

Aronsson H, Jarvis P (2009) The chloroplast protein import apparatus, its components, and their roles. *The Chloroplast*, 89-123

Ashraf, M., & Harris, P. J. C. (2013). Photosynthesis under stressful environments: an overview. *Photosynthetica*, *51*(2), 163-190.

Askegaard M, Eriksen J, Johnston AE. (2004) Sustainable management of potassium. In: Schjorring P, Elmholt S, Christensen BT **(**editors**)**. Managing soil quality: challenges in modern agriculture. Wallingford: *CABI Publishing*, 85–102.

Austin, J. R., Frost, E., Vidi, P. A., Kessler, F., & Staehelin, L. A. (2006). Plastoglobules are lipoprotein subcompartments of the chloroplast that are permanently coupled to thylakoid membranes and contain biosynthetic enzymes. *The Plant Cell*, *18*(7), 1693-1703.

Axelsen, K. B., & Palmgren, M. G. (2001). Inventory of the superfamily of P-type ion pumps in Arabidopsis thaliana. *Plant Physiology*, *126*(2), 696-706.

Barragan, V., Leidi, E., Andres, Z., Rubio, L., De Luca, A., Fernandez, J., Cubero, B. and Pardo, J. (2012). Ion Exchangers NHX1 and NHX2 Mediate Active Potassium Uptake into Vacuoles to Regulate Cell Turgor and Stomatal Function in Arabidopsis thaliana. *The Plant Cell*, 24(3), pp.1127-1142.

Basak, I., & Møller, S. G. (2013). Emerging facets of plastid division regulation. *Planta*, *237*(2), 389-398.

Bassil, E., Tajima, H., Liang, Y., Ohto, M., Ushijima, K., Nakano, R., Esumi, T., Coku, A., Belmonte, M. and Blumwald, E. (2011). The *Arabidopsis thaliana* Na+/H+ Antiporters NHX1 and NHX2 Control Vacuolar pH and K+ Homeostasis to Regulate Growth, Flower Development, and Reproduction. *The Plant Cell, 23*(9), pp.3482-3497.

Bassil, E., Ohto, M., Esumi, T., Tajima, H., Zhu, Z., Cagnac, O., Belmonte, M., Peleg, Z., Yamaguchi, T. and Blumwald, E. (2011). The *Arabidopsis thaliana* Intracellular Na + /H + Antiporters NHX5 and NHX6 Are Endosome Associated and Necessary for Plant Growth and Development. *The Plant Cell*, 23(1), pp.224-239.

Bassil, E., & Blumwald, E. (2014). The ins and outs of intracellular ion homeostasis: NHX-type cation/H+ transporters. *Current Opinion in Plant Biology*, *22*, 1-6.

Bechtold, N., & Pelletier, G. (1998). In planta Agrobacterium mediated transformation of adult *Arabidopsis thaliana* plants by vacuum infiltration. *Arabidopsis thaliana Protocols*, 259-266.

Becker, T., Jelic, M., Vojta, A., Radunz, A., Soll, J., & Schleiff, E. (2004). Preprotein recognition by the Toc complex. The *EMBO Journal*, 23(3), 520-530.

Berardini, T. Z., Reiser, L., Li, D., Mezheritsky, Y., Muller, R., Strait, E., & Huala, E. (2015). The *Arabidopsis thaliana* information resource: Making and mining the "gold standard" annotated reference plant genome. *Genesis*, 53(8), 474-485.

Berkowitz, G. A., & Peters, J. S. (1993). Chloroplast inner-envelope ATPase acts as a primary H+ pump. *Plant Physiology, 102*(1), 261-267.

Bernardi, P. (1999). Mitochondrial transport of cations: channels, exchangers, and permeability transition. *Physiological reviews*, *79*(4), 1127-1155.

Booth, I.R., M.A. Jones, D. McLaggan, Y. Nikolaev, L.S. Ness, C.M. Wood, S. Miller, S. Tötemeyer, and G.P. Ferguson. (1996). Bacterial ion channels. InTransport Processes in Eukaryotic and Prokaryotic Organisms, Vol. 2

(W.N. Konings, H.R. Kaback and J.S. Lolkema, eds.), Elsevier Press, New York, pp. 693-729

Bouche, N. and Bouchez, D (2001). *Arabidopsis thaliana* gene knockout: phenotypes wanted. *Current Opinion in Plant Biology*, 4, (2), 111-117.

Boutigny S., Sautron E., Finazzi G., Rivasseau C., Frelet-Barrand A., Pilon M., Rolland N., Seigneurin-Berny D. (2014). HMA1 and PAA1, two chloroplast-envelope PIB-ATPases, play distinct roles in chloroplast copper homeostasis, *Journal of Experimental Bot*any, *65***,** 1529-1540.

Brink S, Bogsch EG, Mant A, Robinson C (1997). Unusual characteristics of amino terminal and hydrophobic domains in nuclear encoded thylakoid signal peptides. *European Journal of Biochemistry*, 245, 340-348.

Britto DT, Kronzucker HJ (2008). Cellular mechanisms of potassium transport in plants. *Physiologia Plantarum* 133, 637-650.

Britvec, M., Pecina, M., Reichenauer, T., Soja, G., Ljubesic, N., & Eid, M. (2001). Ultrastructure changes in grapevine chloroplasts caused by increased tropospheric ozone concentrations. *Biologia* (Slovak Republic).

Brouder SM, Volenec JJ. (2008). Impact of climate change on crop nutrient and water use efficiencies. *PhysiologiaPlantarum* 133, 705–24.

Bustin, S. A., & Nolan, T. (2004). AZ of quantitative PCR. La Jolla. *CA: International University Line*, *2006*, 0.

Cakmak, I. (2005). The role of potassium in alleviating detrimental effects of abiotic stresses in plants. *Journal of Plant Nutrition and Soil Science*, *168* (4), 521-530.

Carraretto, L., Formentin, E., Teardo, E., Checchetto, V., Tomizioli, M., Morosinotto, T., & Szabó, I. (2013). A thylakoid-located two-pore K+ channel controls photosynthetic light utilization in plants. *Science*, *342* (6154), 114-118.

Celedon, J. M., & Cline, K. (2013). Intra-plastid protein trafficking: how plant cells adapted prokaryotic mechanisms to the eukaryotic condition. *Biochimica et Biophysica Acta (BBA)-Molecular Cell Research*, *1833*(2), 341-351.

Chanroj S., Wang G., Venema K., Zhang M.W., Delwiche C.F, Sze H. (2012). Conserved and Diversified Gene Families of Cation/H+ Antiporters from Algae to Flowering Plants. *Frontiers in Plant Science,* 25 (3).

Chi, W., J. Mao, Q. Li, D. Ji, M. Zou, C. Lu and L. Zhang (2010). "Interaction of the pentatricopeptide-repeat protein DELAYED GREENING 1 with sigma factor SIG6 in the regulation of chloroplast gene expression in *Arabidopsis thaliana* cotyledons." *Plant Journal 64*(1): 14-25.

Chigri, F., Flosdorff, S., Pilz, S., Kölle, E., Dolze, E., Gietl, C., & Vothknecht, U. C. (2012). The *Arabidopsis thaliana* calmodulin-like proteins AtCML30 and AtCML3 are targeted to mitochondria and peroxisomes, respectively. *Plant Molecular Biology*, *78*(3), 211-222.

Choe, S. (2002). Potassium channel structures. *Nature Reviews Neuroscience, 3*, 115–121.

Ciais P, Reichstein M, Viovy N, Granier A, Ogee J, Allard V, Aubinet M, Buchmann N, Bernhofer Chr., Carrara A, Chevallier F, DeNoblet N, Friend A, Friedlingstein P, Grünwald T, Heinesch B, Keronen P, Knohl A, Krinner G, Loustau D, Manca G, Matteucci G, Miglietta F, Ourcival J, Papale D, Pilegaard K, Rambal S, Seufert G, F.Soussana J, J.Sanz M,.

D.Schulze E, Vesala T, (2005). Europe-wide reduction in primary productivity caused by the heat and drought in 2003. *Nature*, 437, 529–33.-

Cleverley, R., Barrett, J., Baslé, A., Bui, N., Hewitt, L., Solovyova, A., Xu, Z., Daniel, R., Dixon, N., Harry, E., Oakley, A., Vollmer, W. and Lewis, R. (2014). Structure and function of a spectrin-like regulator of bacterial cytokinesis. *Nature Communications*, 5, p.5421.

Clough S.J., Bent A.F. (1998). Floral dip: A simplified method for Agrobacterium-mediated transformation of *Arabidopsis thaliana*. *Plant Journal 16*, 735–743.

Cormack, B. P., Valdivia, R. H., & Falkow, S. (1996). FACS-optimized mutants of the green fluorescent protein (GFP). *Gene*, *173*(1), 33-38.

Cosentino, C., Fischer-Schliebs, E., Bertl, A., Thiel, G., & Homann, U. (2010). Na+/H+ antiporters are differentially regulated in response to NaCl stress in leaves and roots of Mesembryanthemum crystallinum. *New Phytologist*, *186* (3), 669-680.

Costa, J. (2004). Reacción en cadena de la polimerasa (PCR) a tiempo real. *Enfermedades Infecciosas y Microbiología Clínica*, *22*(5), 299-305.

Dalbey RE, von Heijne G (1992). Signal peptidases in prokaryotes and eukaryotes-a new protease family. *Trends in Biochemical Sciences*, 17, 474-478.

Darley, C., Van Wuytswinkel, O., Van Der Woude, K., Mager, W. And De Boer, A. (2000). *Arabidopsis thaliana* and Saccharomyces cerevisiae NHX1 genes encode amiloride sensitive electroneutral Na+/H+ exchangers. *Biochemistry Journal 351*(1), pp.241-249.

Del Sal, G., Manfioletti, G., & Schneider, C. (1988). A one-tube plasmid DNA mini-preparation suitable for sequencing. *Nucleic Acids Research*, *16* (20), 9878.

Demmig, B., & Gimmler, H. (1979). Effect of divalent cations on cation fluxes across the chloroplast envelope and on photosynthesis of intact chloroplasts.*Zeitschrift für Naturforschung C*, *34*(3-4), 233-241.

Demmig, B., & Gimmler, H. (1983). Properties of the isolated intact chloroplast at cytoplasmic K+ concentrations I Light-induced cation uptake into intact chloroplasts is driven by an electrical potential difference. *Plant Physiology*, *73*(1), 169-174.

Douce, R., Holtz, R. B., & Benson, A. A. (1973). Isolation and properties of the envelope of spinach chloroplasts. *Journal of Biological Chemistry*, *248* (20), 7215-7222.

Douglas, S. E. (1998). Plastid evolution: origins, diversity, trends. *Current Opinion in Genetics & Development*, *8*(6), 655-661.

Doyle, J. J. (1990). Isolation of plant DNA from fresh tissue. *Focus*, *12*, 13-15.

Dreyer, I., & Uozumi, N. (2011). Potassium channels in plant cells. *FEBS Journal, 278*(22), 4293-4303.

Enz, C., Steinkamp, T., & Wagner, R. (1993). Ion channels in the thylakoid membrane (a patch-clamp study). *Biochimica et Biophysica Acta (BBA)-Bioenergetics*, *1143*(1), 67-76.

Finazzi, G., Petroutsos, D., Tomizioli, M., Flori, S., Sautron, E., Villanova, V., Rolland, N. and Seigneurin-Berny, D. (2015). Ions channels/transporters and chloroplast regulation. *Cell Calcium*, 58(1), pp.86-97.

Flexas, J., Ribas-Carbó, M., Bota, J., Galmés, J., Henkle, M., Martínez-Cañellas,

S., & Medrano, H. (2006). Decreased Rubisco activity during water stress is not induced by decreased relative water content but related to conditions of low stomatal conductance and chloroplast CO2 concentration. *New Phytologist*, *172*(1), 73-82.

Foyer, C. H., & Shigeoka, S. (2011). Understanding oxidative stress and antioxidant functions to enhance photosynthesis. *Plant Physiology*, *155*(1), 93-100.

Fujisawa, M., Ito, M., & Krulwich, T. A. (2007). Three two-component transporters with channel-like properties have monovalent cation/proton antiport activity. *Proceedings of the National Academy of Sciences USA*, *104*(33), 13289-13294.

Fuks, B., & Homblé, F. (1999). Passive anion transport through the chloroplast inner envelope membrane measured by osmotic swelling of intact chloroplasts. Biochimica et Biophysica Acta (BBA) Biomembranes, *1416*(1), 361-369.

Furumoto, T., Yamaguchi, T., Ohshima-Ichie, Y., Nakamura, M., Tsuchida-Iwata, Y., Shimamura, M., Ohnishi, J., Hata, S., Gowik, U., Westhoff, P., Bräutigam, A., Weber, A. and Izui, K. (2011). A plastidial sodium-dependent pyruvate transporter. *Nature*, 478(7368), pp.274-274.

Fusco, C., Guidotti, E., & Zervos, A. S. (1999). In vivo construction of cDNA libraries for use in the yeast two-hybrid system. *Yeast*, *15*(8), 715-720.

Gajdanowicz, P., Michard, E., Sandmann, M., Rocha, M., Correa, L., Ramirez-Aguilar, S., Gomez-Porras, J., Gonzalez, W., Thibaud, J., van Dongen, J. and Dreyer, I. (2010). Potassium (K+) gradients serve as a mobile energy source in plant vascular tissues. *Proceedings of the National Academy of Sciences USA*, 108(2), pp.864-869.

Gietz, R. D., Schiestl, R. H., Willems, A. R., & Woods, R. A. (1995). Studies on the transformation of intact yeast cells by the LiAc/ss-DNA/PEG procedure. *Yeast*, *11*(4), 355-360.

Gietz, R. D., & Woods, R. A. (2002). Transformation of yeast by lithium acetate/single-stranded carrier DNA/polyethylene glycol method. *Methods in Enzymology*, *350*, 87-96.

Göhre, V., Ossenbühl, F., Crèvecoeur, M., Eichacker, L. A., & Rochaix, J. D. (2006). One of two alb3 proteins is essential for the assembly of the photosystems and for cell survival in Chlamydomonas. *The Plant Cell*, *18*(6), 1454-1466.

Goswami, P., Paulino, C., Hizlan, D., Vonck, J., Yildiz, Ö., & Kühlbrandt, W. (2011). Structure of the archaeal Na+/H+ antiporter NhaP1 and functional role of transmembrane helix 1. *The EMBO Journal*, *30*(2), 439-449.

Gutierrez, O. A., Campbell, M. R., & Glover, D. V. (2002). Starch Particle Volume in Single-and Double-Mutant Maize Endosperm Genotypes Involving the Soft Starch () Gene. *Crop Science*, *42*(2), 355-359.

Hageman J, Robinson C, Smeekens S, Weisbeek P (1986) A thylakoid processing protease is required for complete maturation of the lumen protein plastocyanin. *Nature* 324, 567-569.

Haro, R., Banuelos, M. A., Quintero, F. J., Rubio, F., & Rodríguez-Navarro, A. (1993). Genetic basis of sodium exclusion and sodium tolerance in yeast. A model for plants. *Physiologia Plantarum*, *89*(4), 868-874.

Haswell, E. S. & Meyerowitz, E. M. (2006). MscS-like Proteins Control Plastid

Size and Shape in *Arabidopsis thaliana*. *Current Biology* 16, (1), 1-11.
Heber, U., & Krause, G. H. (1972). Hydrogen and proton transfer across the chloroplast envelope. In *Photosynthesis, two centuries after its discovery by Joseph Priestley* (pp. 1023-1033). Springer Netherlands.
Heber, U., & Heldt, H. W. (1981). The chloroplast envelope: structure, function, and role in leaf metabolism. *Annual Review of Plant Physiology*, *32*(1), 139-168.
Hernández, J. A., Rubio, M., Olmos, E., Ros-Barceló, A., & Martínez-Gómez, P. (2004). Oxidative stress induced by long-term plum pox virus infection in peach (Prunus persica). *Physiologia Plantarum*, *122*(4), 486-495.
Heibert, T., Steinkamp, T., Hinnah, S., Schwarz, M., Flueggel, U. I., Weber, A., & Wagner, R. (1995). Ion channels in the chloroplast envelope membrane. *Biochemistry*, *34*(49), 15906-15917.
Heldt, H. W., Werdan, K., Milovancev, M., & Geller, G. (1973). Alkalization of the chloroplast stroma caused by light-dependent proton flux into the thylakoid space. *Biochimica et Biophysica Acta (BBA) Bioenergetics*, *314*(2), 224-241.
Huang, L., Berkelman, T., Franklin, A. E., & Hoffman, N. E. (1993). Characterization of a gene encoding a Ca (2+)-ATPase-like protein in the plastid envelope. *Proceedings of the National Academy of Sciences USA*, *90* (21), 10066-10070.
Höhner, R., Aboukila, A., Kunz, H. H., & Venema, K. (2016). Proton gradients and proton-dependent transport processes in the chloroplast. *Frontiers in Plant Science*, *7*, 218.
Hou, B., & Brüser, T. (2011). The Tat-dependent protein translocation pathway. *Biomolecular Concepts*, 2(6), 507-523.
Hunte, C., Screpanti, E., Venturi, M., Rimon, A., Padan, E., & Michel, H. (2005). Structure of a Na^+/H^+ antiporter and insights into mechanism of action and regulation by pH. *Nature*, *435*(7046), 1197-1202.
Hyman, S., & Jarvis, R. P. (2011). Studying *Arabidopsis thaliana* chloroplast structural organisation using transmission electron microscopy. *Chloroplast Research in Arabidopsis thaliana : Methods and Protocols, Volume I*, 113-132.
Jäger-Vottero, P., Dorne, A. J., Jordanov, J., Douce, R., & Joyard, J. (1997). Redox chains in chloroplast envelope membranes: spectroscopic evidence for the presence of electron carriers, including iron–sulfur centers. *Proceedings of the National Academy of Sciences USA*, *94*(4), 1597-1602.
Jarvis, P., & López-Juez, E. (2013). Biogenesis and homeostasis of chloroplasts and other plastids. *Nature Reviews Molecular Cell Biology*, *14*(12), 787-802.
Jarvis, P., & Robinson, C. (2004). Mechanisms of protein import and routing in chloroplasts. *Current Biology*, *14*(24), R1064-R1077.
Jeong, W. J., Park, Y. I., Suh, K., Raven, J. A., Yoo, O. J., & Liu, J. R. (2002). A large population of small chloroplasts in tobacco leaf cells allows more effective chloroplast movement than a few enlarged chloroplasts. *Plant Physiology*, *129*(1), 112-121.
Jiang, Y., Pico, A., Cadene, M., Chait, B. T., & MacKinnon, R. (2001). Structure of the RCK domain from the E. coli K+ channel and

demonstration of its presence in the human BK channel. *Neuron*, *29*(3), 593-601.
Kaiser, W. M., Stepper, W., & Urbach, W. (1981). Photosynthesis of isolated chloroplasts and protoplasts under osmotic stress. *Planta, 151*(4), 375-380.
Kalve, S., De Vos, D., & Beemster, G. T. (2014). Leaf development: a cellular perspective. *Frontiers in Plant Science*, *5*, 362.
Karim, S. and H. Aronsson (2014). "The puzzle of chloroplast vesicle transport – involvement of GTPases." *Frontiers in Plant Science* 5.
Karimi, M., De Meyer, B., & Hilson, P. (2005). Modular cloning in plant cells. *Trends in Plant Science*, *10*(3), 103-105.
Keegstra, K., & Froehlich, J. E. (1999). Protein import into chloroplasts. *Current Opinion in Plant Biology*, *2*(6), 471-476.
Keeling, P. J. (2004). Diversity and evolutionary history of plastids and their hosts. *American Journal of Botany*, *91*(10), 1481-1493.
Kelley, L. A., Mezulis, S., Yates, C. M., Wass, M. N., & Sternberg, M. J. (2015). The Phyre2 web portal for protein modeling, prediction and analysis. *Nature Protocols*, *10*(6), 845-858.
Kempin S.A., Liljegren S.J., Block L.M., Rounsley S.D., Lam E., Yanofsky M.F. (1997). Inactivation of the *Arabidopsis thaliana* AGL5 MADS-box gene by homologous recombination. *Nature* 389, 802–803.
Kessler, F., & Schnell, D. J. (2006). The function and diversity of plastid protein import pathways: a multilane GTPase highway into plastids. *Traffic*, *7* (3), 248-257.
Kikuchi, S., Hirohashi, T., & Nakai, M. (2006). Characterization of the preprotein translocon at the outer envelope membrane of chloroplasts by blue native PAGE. *Plant and Cell Physiology*, *47*(3), 363-371.
Kitao, M., & Lei, T. T. (2007). Circumvention of over-excitation of PSII by maintaining electron transport rate in leaves of four cotton genotypes developed under long-term drought. *Plant Biology*, *9*(01), 69-76.
Kochubey, S. M., Adamchuk, N. I., Kordyum, E. I., & Guikema, J. A. (2004). Microgravity affects the photosynthetic apparatus of Brassica rapa L. *Plant Biosystems- Plant Biology*, *138*(1), 1-9.
Kouranov A, Schnell DJ (1997) Analysis of the interactions of preproteins with the import machinery over the course of protein import into chloroplasts. *Journal of Cell Biology* 139, 1677-1685.
Kovacs-Bogdan, E., Soll, J., and Bolter, B. (2010). Protein import into chloroplasts: the Tic complex and its regulation. *Biochimica Biophysica Acta 1803*, 740–747.
Kramer, D.M., Cruz, J.A., and Kanazawa, A. (2003). Balancingthecentralrolesof the thylakoid proton gradient. *Trends Plant Sci*ences 8, 27–32.
Kronzucker HJ, Szczerba MW, Schulze LM, Britto DT. (2008) Non-reciprocal interac-tions between K+and Na+ions in barley (Hordeum vulgare L.). *Journal of Experimental Botany*, 59, 2793–801
Krulwich, T. A., Sachs, G., & Padan, Krulwich, T. A., Sachs, G., & Padan, E. (2011). Molecular aspects of bacterial pH sensing and homeostasis. *Nature Reviews Microbiology, 9*(5), 330-343.
Krysan P.J., Young J.C., Tax F., Sussman M.R. (1996). Identification of transferred DNA insertions within *Arabidopsis thaliana* genes involved in signal transduction and ion transport. *Proceeding National Academy*

of Sciences USA 93, 8145–8150.
Krysan, P. J., Young, J. C., & Sussman, M. R. (1999). T-DNA as an insertional mutagen in Arabidopsis thaliana. *The Plant Cell Online*, 11(12), 2283-2290.
Kunz, H. H., Gierth, M., Herdean, A., Satoh-Cruz, M., Kramer, D. M., Spetea, C., & Schroeder, J. I. (2014). Plastidial transporters KEA1,-2, and-3 are essential for chloroplast osmoregulation, integrity, and pH regulation in Arabidopsis thaliana. *Proceedings of the National Academy of Sciences USA*, *111*(20), 7480-7485.
Laloux, G. and C. Jacobs-Wagner (2014). "How do bacteria localize proteins to the cell pole?" *Journal of Cell Science 127*(1): 11-19.
Laemmli, U. K. (1970). Cleavage of structural proteins during the assembly of the head of bacteriophage T4. *Nature*, *227*, 680-685.
Land, A. D., Luo, Q., & Levin, P. A. (2014). Functional domain analysis of the cell division inhibitor EzrA. *PLOS One*, *9*(7).
Laufs, P., Autran, D., & Traas, J. (1999). A chromosomal paracentric inversion associated with T-DNA integration in Arabidopsis thaliana. *The Plant Journal*, *18*(2), 131-139.
Lawlor, D. W., & Cornic, G. (2002). Photosynthetic carbon assimilation and associated metabolism in relation to water deficits in higher plants. *Plant, Cell & Environment*, *25*(2), 275-294.
Lee, C., Kang, H., von Ballmoos, C., Newstead, S., Uzdavinys, P., Dotson, D., Iwata, S., Beckstein, O., Cameron, A. and Drew, D. (2013). A two-domain elevator mechanism for sodium/proton antiport. *Nature*, *501* (7468), pp.573-577.
Leech, R. M., Thomson, W. W., & Platt-Aloia, K. A. (1981). Observations on the mechanism of chloroplast division in higher plants. *New Phytologist*, *87*(1), 1-9.
Leigh, R. A., & Wyn Jones, R. G. (1984). A hypothesis relating critical potassium concentrations for growth to the distribution and functions of this ion in the plant cell. *New Phytologist*, *97*(1), 1-13.
Li, Z., Wakao, S., Fischer, B. B., & Niyogi, K. K. (2009). Sensing and responding to excess light. *Annual Review of Plant Biology*, *60*, 239-260.
Lin, X.; Kaul, S.; Rounsley, S.; Shea, T.P.; Benito, M.I.; Town, C.D.; Jufii, C.Y.; Mason, T.; Bowman, C.L. And Barnstead, M. (1999). Sequence analysis of chromosome 2 of the plant *Arabidopsis thaliana*. *Nature*, December, 402 (6763), 761-768.
Lu, Y., Chanroj, S., Zulkifli, L., Johnson, M. A., Uozumi, N., Cheung, A., & Sze, H. (2011). Pollen tubes lacking a pair of K+ transporters fail to target ovules in Arabidopsis thaliana. *The Plant Cell*, *23*(1), 81-93.
Maathuis, F. J. (2006). The role of monovalent cation transporters in plant responses to salinity. *Journal of Experimental Botany*, *57*(5), 1137-1147.
Mantoura, R. F. C., & Llewellyn, C. A. (1983). The rapid determination of algal chlorophyll and carotenoid pigments and their breakdown products in natural waters by reverse-phase high-performance liquid chromatography. *Analytica Chimica Acta*, *151*, 297-314.
Maresova, L., & Sychrova, H. (2005). Physiological characterization of Saccharomyces cerevisiae kha1 deletion mutants. *Molecular Microbiology*, *55*(2), 588-600.
Marmagne, A., Vinauger-Douard, M., Monachello, D., de Longevialle, A.,

Charon, C., Allot, M., Rappaport, F., Wollman, F., Barbier-Brygoo, H. and Ephritikhine, G. (2007). Two members of the *Arabidopsis thaliana* CLC (chloride channel) family, AtCLCe and AtCLCf, are associated with thylakoid and Golgi membranes, respectively. *Journal of Experimental Botany*, 58(12), pp.3385-3393.

Marschner, H. (1995). Functions of mineral nutrients: macronutrients. *Mineral nutrition of higher plants 2nd Edition. Academic Press, NY*, 299-312.

Martienssen, R. A. (1998). Functional genomics: probing plant gene function and expression with transposons. *Proceedings of the National Academy of Sciences USA*, *95*(5), 2021-2026.

Martin, W., & Herrmann, R. G. (1998). Gene transfer from organelles to the nucleus: how much, what happens, and why? *Plant Physiology*, *118*(1), 9-17.

Mäser, P., Thomine, S., Schroeder, J. I., Ward, J. M., Hirschi, K., Sze, H., ... & Harper, J. F. (2001). Phylogenetic relationships within cation transporter families of Arabidopsis thaliana. *Plant Physiology*, *126*(4), 1646-1667.

McAndrew, R. S., Froehlich, J. E., Vitha, S., Stokes, K. D., & Osteryoung, K. W. (2001). Colocalization of plastid division proteins in the chloroplast stromal compartment establishes a new functional relationship between FtsZ1 and FtsZ2 in higher plants. *Plant Physiology*, *127*(4), 1656-1666.

McFadden, G. (1999). Chloroplasts: ever decreasing circles. *Nature*, *400*(6740), 119-120.

McKinney, E. C., Ali, N., Traut, A., Feldmann, K. A., Belostotsky, D. A., McDowell, J. M., & Meagher, R. B. (1995). Sequence-based identification of T-DNA insertion mutations in Arabidopsis thaliana: actin mutants act2-1 and act4-1. *The Plant Journal*, *8*(4), 613-622.

Miyagishima, S. Y., Nozaki, H., Nishida, K., Nishida, K., Matsuzaki, M., & Kuroiwa, T. (2004). Two types of FtsZ proteins in mitochondria and red-lineage chloroplasts: the duplication of FtsZ is implicated in endosymbiosis. *Journal of Molecular Evolution*, *58*(3), 291-303.

Molas, J. (2002). Changes of chloroplast ultrastructure and total chlorophyll concentration in cabbage leaves caused by excess of organic Ni (II) complexes. *Environmental and Experimental Botany*, *47*(2), 115-126.

Müller, M., & Bernd Klösgen, R. (2005). The Tat pathway in bacteria and chloroplasts (review). *Molecular Membrane Biology*, *22*(1-2), 113-121.

Munné-Bosch, S., & Alegre, L. (2004). Die and let live: leaf senescence contributes to plant survival under drought stress. *Functional Plant Biology, 31*(3), 203-216.

Murata, Y., & Takahashi, M. (1999). An alternative electron transfer pathway mediated by chloroplast envelope. *Plant and Cell Physiology*, *40*(10), 1007-1013.

Nakanishi, H., Suzuki, K., Kabeya, Y., Okazaki, K., & Miyagishima, S. Y. (2009). Conservation and differences of the Min system in the chloroplast and bacterial division site placement. *Communicative & Integrative Biology, 2*(5), 400-402.

Natale, P., Brüser, T., & Driessen, A. J. (2008). Sec-and Tat-mediated protein secretion across the bacterial cytoplasmic membrane distinct translocases and mechanisms. *Biochimica et Biophysica Acta* (BBA)-*Biomembranes,* 1778 (9), 1735-1756.

Nacry, P., Camilleri, C., Courtial, B., Caboche, M., & Bouchez, D. (1998).

Major chromosomal rearrangements induced by T-DNA transformation in Arabidopsis thaliana. *Genetics*, *149*(2), 641-650.
Nagata, T., Iizumi, S., Satoh, K. and Kikuchi, S. (2008). Comparative molecular biological analysis of membrane transport genes in organisms. *Plant Molecular Biology*, 66(6), pp.565-585.
Neuhaus, H. E., & Wagner, R. (2000). Solute pores, ion channels, and metabolite transporters in the outer and inner envelope membranes of higher plant plastids. *Biochimica et Biophysica Acta (BBA) Biomembranes*, *1465*(1), 307-323.
Nickelsen, J., & Zerges, W. (2013). Thylakoid biogenesis has joined the new era of bacterial cell biology. *Frontiers in Plant Science*, *4*.
Nierzwicki-Bauer, S. A., D. L. Balkwill and S. E. Stevens, Jr. (1983). "Three-dimensional ultrastructure of a unicellular cyanobacterium." *Journal of Cell Biology 97*(3): 713-722.
Nobel, P. S. (1968). Light-Induced Chloroplast Shrinkage in vivo Detectable After Rapid Isolation of Chloroplasts From Pisum sativum. *Plant Physiology* 43 (5), 781-787.
Nobel, P. S. (1969). Light-induced changes in the ionic content of chloroplasts in Pisum sativum. *Biochimica Biophysica Acta 172* (1), 134-143.
Nobel, P. S., Chang, D. T., Wang, C. T., Smith, S. S., & Barcus, D. E. (1969). Initial ATP formation, NADP reduction, CO2 fixation, and chloroplast flattening upon illuminating pea leaves. *Plant Physiology*, *44*(5), 655-661.
Nordhues, A., Schottler, M., Unger, A., Geimer, S., Schonfelder, S., Schmollinger, S., Rutgers, M., Finazzi, G., Soppa, B., Sommer, F., Muhlhaus, T., Roach, T., Krieger-Liszkay, A., Lokstein, H., Crespo, J. and Schroda, M. (2012). Evidence for a Role of VIPP1 in the Structural Organization of the Photosynthetic Apparatus in Chlamydomonas. *The Plant Cell, 24*(2), pp.637-659.
Olsen, L. J., & Keegstra, K. (1992). The binding of precursor proteins to chloroplasts requires nucleoside triphosphates in the intermembrane space. *Journal of Biological Chemistry*, *267*(1), 433-439.
Osteryoung, K.W., and Vierling, E. (1995). Conserved cell and organelle division. *Nature* 376, 473-474.
Osteryoung, K. W., Stokes, K. D., Rutherford, S. M., Percival, A. L., & Lee, W. Y. (1998). Chloroplast division in higher plants requires members of two functionally divergent gene families with homology to bacterial ftsZ. *The Plant Cell*, *10*(12), 1991-2004.
Osteryoung, K. W. (2001). Organelle fission in eukaryotes. *Current Opinion in Microbiology*, *4*(6), 639-646.
Osteryoung, K. W., & McAndrew, R. S. (2001). The plastid division machine. *Annual Review of Plant Biology*, *52*(1), 315-333.
Osteryoung, K. W., & Weber, A. P. (2011). Plastid Biology: Focus on the Defining Organelle of Plants. *Plant Physiology*, *155*(4), 1475-1476.
Osteryoung, K. W., & Pyke, K. A. (2014). Division and dynamic morphology of plastids. *Annual Review of Plant Biology*, *65*, 443-472.
Palmer, T., & Berks, B. C. (2012). The twin-arginine translocation (Tat) protein export pathway. *Nature Reviews Microbiology*, *10*(7), 483-496.
Panou-Filotheou, H., Bosabalidis, A. M., & Karataglis, S. (2001). Effects of copper toxicity on leaves of oregano (Origanum vulgare subsp.

hirtum). *Annals of Botany, 88*(2), 207-214.
Parinov, S., Sevugan, M., Ye, D., Yang, W. C., Kumaran, M., & Sundaresan, V. (1999). Analysis of flanking sequences from dissociation insertion lines: a database for reverse genetics in Arabidopsis thaliana. *The Plant Cell*, *11*(12), 2263-2270.
Pater, S., Caspers, M., Kottenhagen, M., Meima, H., Ter Stege, R., & Vetten, N. (2006). Manipulation of starch granule size distribution in potato tubers by modulation of plastid division. *Plant Biotechnology Journal*, *4*(1), 123-134.
Peltier, J. (2002). Central Functions of the Lumenal and Peripheral Thylakoid Proteome of *Arabidopsis thaliana* Determined by Experimentation and Genome-Wide Prediction. *The Plant Cell*, *14*(1), pp.211-236.
Perry, S. E., & Keegstra, K. (1994). Envelope membrane proteins that interact with chloroplastic precursor proteins. *The Plant Cell*, *6*(1), 93-105.
Peters, J.S., and Berkowitz, G.A. (1998). Characterization of a chloroplast inner envelope P-ATPase proton pump. *Photosynthesis Research* 57, 323-333.
Peters, J. S. &Berkowitz, G. A. (1991). Studies on the System Regulating Proton Movement across the Chloroplast Envelope: Effects of ATPase Inhibitors, Mg, and an Amine Anesthetic on Stromal pH and Photosynthesis. *Plant Physiology* 95(4), 1229-1236.
Pevsner, J. (2015). *Bioinformatics and Functional Genomics*. John Wiley & Sons.
Pfeil, B. E., Schoefs, B. &Spetea, C. (2014). Function and evolution of channels and transporters in photosynthetic membranes. *Cell Molecular Life Science* 71 (6), 979-998.
Porra, R. J., Thompson, W. A., & Kriedemann, P. E. (1989). Determination of accurate extinction coefficients and simultaneous equations for assaying chlorophylls a and b extracted with four different solvents: verification of the concentration of chlorophyll standards by atomic absorption spectroscopy. *Biochimica et Biophysica Acta (BBA) Bioenergetics*, *975*(3), 384-394.
Possingham, J. V., & Lawrence, M. E. (1983). Controls to plastid division. *International Reviews. Cytol*, *84*(1), 13.
Pottosin, I., & Dobrovinskaya, O. (2014). Non-selective cation channels in plasma and vacuolar membranes and their contribution to K+ transport. *Journal of Plant Physiology*, *171*(9), 732-742.
Pottosin, I. I. (1992). Single channel recording in the chloroplast envelope. *FEBS letters*, *308*(1), 87-90.
Pottosin, II, J. Muniz and S. Shabala (2005). "Fast-activating channel controls cation fluxes across the native chloroplast envelope." *Journal of Membrane Biology 204*(3): 145-156.
Pyke, K. (1998). Plastid division: the origin of replication. *The Plant Cell*, *10*(12), 1971-1972.
Pyke, K. (1997). The genetic control of plastid division in higher plants. *American Journal of Botany*, *84*(8), 1017-1017.
Pyke, K. A., Marrison, J. L., & Leech, A. M. (1991). Temporal and spatial development of the cells of the expanding first leaf of *Arabidopsis thaliana* (L.) Heynh. *Journal of Experimental Botany*, *42*(11), 1407-1416.
Pyke, K.A. (2007). Plastid development and differentiation. In Topics in Current

Genetics: *Cell and Molecular Biology of Plastids, Bock, R. ed., (Berlin: Springer),* 1-28.
Pyke, K. A. (2009). Plastid division. *AoB plants*, *2010*, plq016.
Qi, Y., X. Liu, S. Liang, R. Wang, Y. Li, J. Zhao, J. Shao, L. A and F. Yu (2016). "A Putative Chloroplast Thylakoid Metalloprotease VIRESCENT3 Regulates Chloroplast Development in *Arabidopsis thaliana*." *Journal of Biological Chemistry 291*(7): 3319-3332.
Quesada, V., Ponce, M. R., & Micol, J. L. (2000). Genetic analysis of salt-tolerant mutants in *Arabidopsis thaliana*. *Genetics*, *154*(1), 421-436.
Rabe, M., C. Schwieger, H. R. Zope, F. Versluis and A. Kros (2014). "Membrane Interactions of Fusogenic Coiled-Coil Peptides: Implications for Lipopeptide Mediated Vesicle Fusion." *Langmuir 30*(26): 7724-7735.
Rast, A., Heinz, S., & Nickelsen, J. (2015). Biogenesis of thylakoid membranes. *Biochimica et Biophysica Acta (BBA) Bioenergetics*, *1847* (9), 821-830.
Richter, S., & Brüser, T. (2005). Targeting of unfolded PhoA to the TAT translocon of Escherichia coli. *Journal of Biological Chemistry*, *280*(52), 42723-42730.
Reguera, M., Bassil, E., Tajima, H., Wimmer, M., Chanoca, A., Otegui, M., Paris, N. and Blumwald, E. (2015). pH Regulation by NHX-Type Antiporters Is Required for Receptor-Mediated Protein Trafficking to the Vacuole in Arabidopsis thaliana. *The Plant Cell*, 27(4), pp.1200-1217.
Robinson, S. P. (1985). The involvement of stromal ATP in maintaining the pH gradient across the chloroplast envelope in the light. *Biochimica et Biophysica Acta (BBA)-Bioenergetics*, *806*(2), 187-194.
Rodríguez-Rosales, M. P., Gálvez, F. J., Huertas, R., Aranda, M. N., Baghour, M., Cagnac, O., & Venema, K. (2009). Plant NHX cation/proton antiporters. *Plant Signaling & Behavior*, *4*(4), 265-276.
Rolland, N., Dorne, A. J., Amoroso, G., Sültemeyer, D. F., Joyard, J., & Rochaix, J. D. (1997). Disruption of the plastid ycf10 open reading frame affects uptake of inorganic carbon in the chloroplast of Chlamydomonas. *The EMBO journal*, *16*(22), 6713-6726.
Roosild, T. P., Miller, S., Booth, I. R., & Choe, S. (2002). A mechanism of regulating transmembrane potassium flux through a ligand-mediated conformational switch. *Cell*, *109*(6), 781-791.
Rose, A., Schraegle, S. J., Stahlberg, E. A., & Meier, I. (2005). Coiled-coil protein composition of 22 proteomes–differences and common themes in subcellular infrastructure and traffic control. *BMC Evolutionary Biology*, *5*(1), 1.
Roston, R. L., Gao, J., Murcha, M. W., Whelan, J., & Benning, C. (2012).TGD1, -2, and-3 proteins involved in lipid trafficking form ATP-binding cassette (ABC) transporter with multiple substrate-binding proteins. *Journal of Biological Chemistry, 287*(25), 21406-21415.
Roux, M., Schwessinger, B., Albrecht, C., Chinchilla, D., Jones, A., Holton, N., Malinovsky, F., Tör, M., de Vries, S. and Zipfel, C. (2011). The *Arabidopsis thaliana* Leucine-Rich Repeat Receptor–Like Kinases BAK1/SERK3 and BKK1/SERK4 Are Required for Innate Immunity to Hemibiotrophic and Biotrophic Pathogens. *The Plant Cell*, 23(6), pp.2440-2455.
Saier, M. H. (2000). A functional-phylogenetic classification system for transmembrane solute transporters. *Microbiology and Molecular Biology*

Reviews, *64*(2), 354-411.
Sallas, L., Luomala, E. M., Utriainen, J., Kainulainen, P., & Holopainen, J. K. (2003). Contrasting effects of elevated carbon dioxide concentration and temperature on Rubisco activity, chlorophyll fluorescence, needle ultrastructure and secondary metabolites in conifer seedlings. *Tree Physiology, 23*(2), 97-108.
Sam, O., Ramírez, C., Coronado, M. J., Testillano, P. S., & Risueño, M. D. C. (2003). Changes in tomato leaves induced by NaCl stress: leaf organization and cell ultrastructure. *Biologia Plantarum, 47*(3), 361-366.
Sargent, F., Bogsch, E. G., Stanley, N. R., Wexler, M., Robinson, C., Berks, B. C., & Palmer, T. (1998). Overlapping functions of components of a bacterial Sec-independent protein export pathway. *The EMBO Journal*, *17*(13), 3640-3650.
Scherer, S., Hinrichs, I., & Böger, P. (1986). Effect of monochromatic light on proton efflux of the blue-green alga Anabaena variabilis. *Plant Physiology*, *81*(3), 939-941.
Schleiff, E., Soll, J., Küchler, M., Kühlbrandt, W., & Harrer, R. (2003). Characterization of the translocon of the outer envelope of chloroplasts. *The Journal of Cell Biology*, *160*(4), 541-551.
Schnell DJ, Blobel G, Keegstra K, Kessler F, Ko K, Soll J (1997). A consensus nomenclature for the protein-import components of the chloroplast envelope. *Trends in Cell Biology* 7, 303
Schroeder D. (1978).Structure and weathering of potassium containing minerals. In: *Proceding.11th Congress. International Potash Institute;* 5.
Schubert, M., Petersson, U. A., Haas, B. J., Funk, C., Schröder, W. P., & Kieselbach, T. (2002). Proteome map of the chloroplast lumen of *Arabidopsis thaliana*. *Journal of Biological Chemistry*, *277*(10), 8354-8365.
Shabala, S. (2003). Regulation of potassium transport in leaves: from molecular to tissue level. *Annals of Botany*, *92*(5), 627-634.
Sheng, P., Tan, J., Jin, M., Wu, F., Zhou, K., Ma, W., Heng, Y., Wang, J., Guo, X., Zhang, X., Cheng, Z., Liu, L., Wang, C., Liu, X. and Wan, J. (2014). Albino midrib 1, encoding a putative potassium efflux antiporter, affects chloroplast development and drought tolerance in rice. *Plant Cell Report 33* (9), pp.1581-1594.
Shingles, R., & McCarty, R. E. (1994). Direct measurement of ATP-dependent proton concentration changes and characterization of a K+-stimulated ATPase in pea chloroplast inner envelope vesicles. *Plant Physiology*, *106*(2), 731-737.
Shimoni, E., O. Rav-Hon, I. Ohad, V. Brumfeld and Z. Reich (2005). "Three-dimensional organization of higher-plant chloroplast thylakoid membranes revealed by electron tomography." *Plant Cell 17*(9): 2580-2586.
Singh-Gasson, S., Green, R. D., Yue, Y., Nelson, C., Blattner, F., Sussman, M. R., & Cerrina, F. (1999). Maskless fabrication of light-directed oligonucleotide microarrays using a digital micromirror array. *Nature Biotechnology*, *17*(10), 974-978.
Soll, J., & Schleiff, E. (2004). Protein import into chloroplasts. *Nature Reviews Molecular Cell Biology*, *5*(3), 198-208.
Song, C. P., Guo, Y., Qiu, Q., Lambert, G., Galbraith, D. W., Jagendorf, A., &

Zhu, J. K. (2004). A probable Na+ (K+)/H+ exchanger on the chloroplast envelope functions in pH homeostasis and chloroplast development in *Arabidopsis thaliana*. *Proceedings of the National Academy of Sciences USA, 101*(27), 10211-10216.

Sotomayor, M., Vásquez, V., Perozo, E., & Schulten, K. (2007). Ion conduction through MscS as determined by electrophysiology and simulation. *Biophysical Journal, 92*(3), 886-902.

Stathopoulos, C., Hendrixson, D. R., Thanassi, D. G., Hultgren, S. J., Geme III, J. W. S., & Curtiss III, R. (2000). Secretion of virulence determinants by the general secretory pathway in gram-negative pathogens: an evolving story. *Microbes and Infection*, *2*(9), 1061-1072.

Stokes, K. D., & Osteryoung, K. W. (2003). Early divergence of the FtsZ1 and FtsZ2 plastid division gene families in photosynthetic eukaryotes. *Gene*, *320*, 97-108.

Strahl, H., Ronneau, S., González, B., Klutsch, D., Schaffner-Barbero, C. and Hamoen, L. (2015). Transmembrane protein sorting driven by membrane curvature. *Nature Communications*, 6, p.8728.

Sze H, Padmanaban S, Cellier F, Honys D, Cheng NH, Bock KW, Conejero G, Li X, Twell D, Ward JM, Hirschi KD (2004). Expression patterns of a novel AtCHX gene family highlight potential roles in osmotic adjustment and K+ homeostasis in pollen development. *Plant Physiol*ogy 136(1): 2532-47

Tamura, K., Stecher, G., Peterson, D., Filipski, A. and Kumar, S. (2013). MEGA6: Molecular Evolutionary Genetics Analysis Version 6.0. *Molecular Biology and Evolution*, 30(12), pp.2725-2729.

Taubert, J. Hou, B., Risselada, H. J., Mehner, D., Lünsdorf, H., Grubmüller, H., & Brüser, T. (2015). TatBC-independent TatA/Tat substrate interactions contribute to transport efficiency. *PloS one*, *10*(3), e0119761.

Tisdale SL, Nelson WL, Beaton JD, Havlin JL. (1993) In: Soil fertility and fertilizers. *5th ed.Macmillan Publishing Company*. p. 634.

Tiller and Bock 2014, Vanhaeren H, Gonzalez N, Inze D (2014). *Arabidopsis thaliana* Book *Molecular Plant* 7, 1105-112013: e0181.

Tsonev, T., Velikova, V., Yildiz-Aktas, L., Gürel, A. and Edreva, A. (2011). Effect of water deficit and potassium fertilization on photosynthetic activity in cotton plants. *Plant Biosystems 145*(4), pp.841-847.

Tyler, B. (2006). Phytophthora Genome Sequences Uncover Evolutionary Origins and Mechanisms of Pathogenesis. *Science*, 313(5791), pp.1261-1266.

Vanhaeren, H., N. Gonzalez and D. Inze (2015). "A Journey Through a Leaf: Phenomics Analysis of Leaf Growth in *Arabidopsis thaliana*." *Arabidopsis thaliana* Book 13: e0181.

Viana, A. A., Li, M., & Schnell, D. J. (2010). Determinants for stop-transfer and post-import pathways for protein targeting to the chloroplast inner envelope membrane. *Journal of Biological Chemistry*, *285*(17), 12948-12960.

Vinothkumar, K. R., Smits, S. H., & Kühlbrandt, W. (2005). pH-induced structural change in a sodium/proton antiporter from Methanococcus jannaschii. *The EMBO Journal*, *24*(15), 2720-2729.

Vothknecht, U. C., & Westhoff, P. (2001). Biogenesis and origin of thylakoid membranes. *Biochimica et Biophysica Acta (BBA)-Molecular Cell*

Research, *1541*(1), 91-101.
Vothknecht, U. C., Otters, S., Hennig, R., & Schneider, D. (2012). Vipp1: a very important protein in plastids. *Journal of Experimental Botany, 63*(4), 1699-1712.
Wada, M., T. Kagawa and Y. Sato (2003). "Chloroplast movement." *Annual Review of Plant Biology* 54: 455-468.
Wang, X., Berkowitz, G. A., & Peters, J. S. (1993). K+-conducting ion channel of the chloroplast inner envelope: Functional reconstitution into liposomes. *Proceedings of the National Academy of Sciences USA*, *90*(11), 4981-4985.
Weigel, D., & Glazebrook, J. (2008). Genetic analysis of *Arabidopsis thaliana* mutants.*Cold Spring Harbor Protocols*, *2008*(3), pdb-top35.
Weigel, D., & Glazebrook, J. (2001) *Arabidopsis thaliana:* A Laboratory Manual. Cold Spring Harbor, NY: Cold Spring Harbor Laboratory Press.
Westphal, S., Soll, J., & Vothknecht, U. C. (2003). Evolution of chloroplast vesicle transport. *Plant and Cell Physiology*, *44*(2), 217-222.
Wickner, W., Driessen, A. J., & Haril, F. U. (1991). The enzymology of protein translocation across the Escherichia coli plasma membrane. *Annual Review of Biochemistry*, *60*(1), 101-124.
Wilson, K., Long, D., Swinburne, J., & Coupland, G. (1996). A Dissociation insertion causes a semidominant mutation that increases expression of TINY, an *Arabidopsis thaliana* gene related to APETALA2. *The Plant Cell*, *8*(4), 659-671.
Wilson, M. E., Jensen, G. S., & Haswell, E. S. (2011). Two mechanosensitive channel homologs influence division ring placement in *Arabidopsis thaliana* chloroplasts. *The Plant Cell*, *23*(8), 2939-2949.
Wilson, M. E., & Haswell, E. S. (2012). A role for mechanosensitive channels in chloroplast and bacterial fission. *Plant Signaling & Behavior*, *7*(2), 157-160.
Wisman, E., Hartmann, U., Sagasser, M., Baumann, E., Palme, K., Hahlbrock, K., Saedler, H. and Weisshaar, B. (1998). Knock-out mutants from an En-1 mutagenized *Arabidopsis thaliana* population generate phenylpropanoid biosynthesis phenotypes. *Proceedings of the National Academy of Sciences USA*, 95(21), pp.12432-12437.
Wodicka, L., Dong, H., Mittmann, M., Ho, M. H., & Lockhart, D. J. (1997). Genome-wide expression monitoring in Saccharomyces cerevisiae. *Nature Biotechnology*, *15*(13), 1359-1367.
Wu, W., & Berkowitz, G. A. (1992). K+ stimulation of ATPase activity associated with the chloroplast inner envelope. *Plant Physiology*, *99*(2), 553-560.
Wu, W., Peters, J., & Berkowitz, G. A. (1991). Surface charge-mediated effects of Mg2+ on K+ flux across the chloroplast envelope are associated with regulation of stromal pH and photosynthesis. *Plant Physiology, 97*(2), 580-587.
Wu, F. H., Shen, S. C., Lee, L. Y., Lee, S. H., Chan, M. T., & Lin, C. S. (2009). Tape-*Arabidopsis thaliana* Sandwich-a simpler *Arabidopsis thaliana* protoplast isolation method. *Plant Methods*, *5*(1), 1.
Yang, J., Yan, R., Roy, A., Xu, D., Poisson, J., & Zhang, Y. (2015). The I-TASSER Suite: protein structure and function prediction. *Nature Methods, 12*(1), 7-8.

Young, M. E., Keegstra, K., & Froehlich, J. E. (1999). GTP promotes the formation of early-import intermediates but is not required during the translocation step of protein import into chloroplasts. *Plant Physiology*, *121* (1), 237-244.
Zhu, J. K., Liu, J., & Xiong, L. (1998). Genetic analysis of salt tolerance in Arabidopsis thaliana: evidence for a critical role of potassium nutrition. *The Plant Cell*, *10* (7), 1181-1191.
Zhu, J. K. (2003). Regulation of ion homeostasis under salt stress. *Current Opinion in Plant Biology*, *6*(5), 441-445.